TECHNICAL REPORT 1862
February 2002

Thermal and Nuclear Aspects of the Pd/D_20 System

Volume 1: A Decade of Research at Navy Laboratories

S. Szpak
P. A. Mosier–Boss
Editors

SSC San Diego
San Diego, CA 92152-5001

SSC SAN DIEGO
San Diego, California 92152-5001

P. A. Miller, CAPT, USN
Commanding Officer

R. C. Kolb
Executive Director

ADMINISTRATIVE INFORMATION

The work described in this report was performed for the Office of Naval Research through the collaboration of Space and Naval Warfare Systems Center, San Diego (SSC San Diego); the Naval Air Warfare Center, Weapons Division, China Lake; and the Naval Research Laboratory (NRL).

Contributing authors (in alphabetical order)

Dr. Pamela A. Mosier–Boss
Code D363
Spawar Systems Center San Diego
San Diego, CA 92152–5000
(619) 553–1603; FAX (619) 553–1269

Dr. Scott R. Chubb
Code 7252
Naval Research Laboratory
Washington, DC 20375–5343
(202) 767–5270; FAX (202) 767–3303

Professor Martin Fleischmann, F.R.S.
Bury Lodge, Duck Street
Tisbury, Salisbury, Wilts SP3 6LJ
United Kingdom
(+44) 1747 870384; FAX (+44) 1747 870845

Dr. M. Ashraf Imam
Code 6320
Naval Research Laboratory
Washington, DC 20375–5343
(202) 767–2185; FAX (202) 767–2623

Dr. Melvin H. Miles
Department of Chemistry
Middle Tennessee State University
Murfreeboro, TN 37132
(615) 904–8558

Dr. Stanislaw Szpak
3498 Conrad Ave
San Diego, CA 92117
(858) 272–9401

FOREWORD

Twelve years have passed since the announcement on 23 March 1989 by Professors Fleischmann and Pons that the generation of excess enthalpy occurs in electrochemical cells when palladium electrodes, immersed in D_2O + LiOH electrolyte, are negatively polarized. The announcement, which came to be known as "Cold Fusion," caused frenzied excitement. In both the scientific and news communities, fax machines were used to pass along fragments of rumor and "facts." (Yes, this was before wide spread use of the internet. One can only imagine what would happen now.) Companies and individuals rushed to file patents on yet to be proven ideas in hopes of winning the grand prize. Unfortunately, the phenomenon described by Fleischmann and Pons was far from being understood and even factors necessary for repeatability of the experiments were unknown. Over the next few months, the scientific community became divided into the "believers" and the "skeptics." The "believers" reported the results of their work with enthusiasm that at times overstated the significance of their results. On the other hand, many "skeptics" rejected the anomalous behavior of the polarized Pd/D system as a matter of conviction, i.e., without analyzing the presented material and always asking "where are the neutrons?" Funding for research quickly dried up as anything related to "Cold Fusion" was portrayed as a hoax and not worthy of funding. The term "Cold Fusion" took on a new definition much as the Ford Edsel had done years earlier.

By the Second International Conference on Cold Fusion, held at Villa Olmo, Como, Italy, in June/July 1991, the attitude toward Cold Fusion was beginning to take on a more scientific basis. The number of flash-in-the-pan "believers" had diminished, and the "skeptics" were beginning to be faced with having to explain the anomalous phenomenon, which by this time had been observed by many credible scientists throughout the world. Shortly after this conference, the Office of Naval Research (ONR) proposed a collaborative effort involving the Naval Command, Control and Ocean Surveillance Center, RDT&E Division, which subsequently has become the Space and Naval Warfare Systems Center, San

Diego (SSC San Diego); the Naval Air Warfare Center, Weapons Division, China Lake; and the Naval Research Laboratory (NRL). The effort's basic premise was to investigate the anomalous effects associated with the prolonged charging of the Pd/D system and "to contribute in collegial fashion to a coordinated tri-laboratory experiment."

Each laboratory took a different area of research. At San Diego, our goal was to understand the conditions that initiate the excess heat generation (the Fleischmann–Pons effect) and the search for evidence that indicates their nuclear origin. To eliminate the long incubation times (often weeks), Drs. Stan Szpak and Pam Boss decided to prepare the palladium electrodes by the co-deposition technique. Initially, they concentrated on tritium production and the monitoring of emanating radiation. More recently, they extended their effort to monitoring surface temperature via IR imaging technique and showed the existence of discrete heat sources randomly distributed in time and space. This discovery may prove to be a significant contribution to the understanding of the phenomenon.

At China Lake, Dr. Miles and his collaborators showed that a correlation exists between the rate of the excess enthalpy generation and the quantity of helium in the gas stream. Such a correlation is the direct evidence of the nuclear origin of the Fleischmann–Pons effect.

The research at NRL was directed toward the metallurgy of palladium and its alloys and the theoretical aspects of the Fleischmann–Pons effect. In particular, Dr. Imam prepared Pd/B alloys that Dr. Miles used in calorimetric experiments. It was shown that these alloys yielded reproducible excess enthalpy generation with minimal incubation times (approximately 1 day). The theoretical work of Dr. Chubb contributed much to our understanding of the Fleischmann–Pons effect.

Although funding for Cold Fusion ended several years ago, progress in understanding the phenomenon continues at a much slower pace, mostly through the unpaid efforts of dedicated inquisitive scientists. In preparation of this report the authors spent countless hours outside of their normal duties to jointly review their past and current contributions, including the "hidden" agenda that Professor Fleischmann pursued for several years in the 1980s when he was partially funded by ONR. Special thanks are extended to all scientists who have worked under these conditions, including those who contributed to this report and especially to Professor Fleischmann.

As I write this Foreword, California is experiencing rolling blackouts due to power shortages. Conventional engineering, planned ahead, could have prevented these blackouts, but it has been politically expedient to ignore the inevitable. We do not know if Cold Fusion will be the answer to future energy needs, but we do know the existence of Cold Fusion phenomenon through repeated observations by scientists throughout the world. It is time that this phenomenon be inves-

tigated so that we can reap whatever benefits accrue from additional scientific understanding. It is time for government funding organizations to invest in this research.

Dr. Frank E. Gordon
Head, Navigation and Applied Sciences Department
Space and Naval Warfare Systems Center, San Diego

TABLE OF CONTENTS

CHAPTER 1: THE EMERGENCE OF COLD FUSION

S. Szpak and P. A. Mosier–Boss

1.0 Introduction.

In this chapter, we address briefly the events proceeding and following the 23 March 1989 announcement that nuclear reactions could be induced at room temperatures and atmospheric pressure when electrochemically generated deuterium is compressed into the Pd lattice. In particular, we discuss the events that led Fleischmann to this conclusion, his philosophy of research and the characteristic of the Pd/^{n}H (n = 1,2) system that prompted him to initiate research into host lattice assisted nuclear reactions. An extensive discussion of these topics can be found in the recently published paper by Fleischmann entitled: *Reflections on the Sociology of Science and Social Responsibility in Science, in Relationship to Cold Fusion* [1].

The announcement by Fleischmann and Pons that nuclear events can and do occur in the Pd/D system when deuterium is electrochemically compressed in the Pd lattice was a totally new and controversial concept, incompatible with the standard teachings of nuclear physics. A question that naturally arises is what prompted Fleischmann to undertake this kind of research. Was it the short note published in *Nature* by Oliphant et al. in 1934 [2] who demonstrated that nuclear reaction can occur in condensed matter, or was it something else? In what follows, we seek the answer in Fleischmann and his collaborators numerous publications/presentations that appeared after the 23 March 1989 press conference.

In a lecture given at the First International Conference on Cold Fusion (ICCF–1), Fleischmann [3] said the following: *"Our interest in nucleation phenomena and our knowledge of the prediction of the formation of metallic hydrogen (and*

deuterium) at extreme compressions in United States and Soviet work during the mid 70s was, in fact, a key element in the initiation of this research project." Toward the end of his lecture, he remarked: *"We, for our part, would not have started this investigation if we have accepted the view that nuclear reactions in host lattices could not be affected by coherent processes."* These quotes suggest that his interest in the Pd/^{n}H system extended over a period of years prior to the 23 March announcement and that his research was concerned with fundamental aspects of solid state chemistry and physics.

2.0 Chronology of events.

A brief chronology of events is as follows. Early in 1947, Fleischmann realized that the Pd/H system is *"the most extraordinary example of an electrolyte"*, i.e., exhibiting behavior that could not be satisfactorily explained in terms of the Debye-Huckel theory. In the 1960s, he was convinced that the correct approach to the behavior of ions in solution must be in terms of quantum electrodynamics (QED). In the late 60s, he concluded that *"the measurements and interpretation of fluctuations in small systems was one possible route for probing the applicability of QED, especially the applicability to the behavior of condensed matter"* [1, p. 27]. Facing opposition in scientific circles to this approach, Fleischmann decided to follow an "hidden agenda". The underlying goal of such research was to illustrate the need to apply QED reasoning when examining the behavior of condensed matter as well as demonstrating that such effects can be probed using electrochemical procedures (methods), since these methods have the required accuracy and sensitivity to probe such effects (e.g., the ability to measure small signals for small systems, an increase in sensitivity by using modulation methods, etc.). While at the University of Southampton (1967–1980), he and his collaborators studied the effects of the various parameters on the behavior of the Pd/^{n}H system that could not be predicted using classical and quantum mechanics.

Concerning the emergence of cold fusion, we have to ask (i) how did cold fusion fit with Fleischmann's research plans and (ii) why did Fleischmann and Pons select to investigate the electrochemical compression of deuterium into a host lattice? The answer to the first is to demonstrate that the QED paradigm is the correct one. The answer to the second is a conclusion that, to probe the Pd/H system, energy balance rather than momentum will be consistent with the "hidden agenda." Experiments were conducted to probe the effects of (i) space, (ii) time, (iii) length, (iv) dimensionality, (v) number, and (vi) structure. The missing factor was (vii) energy and experiments on this were started at the University of Utah. As such, cold fusion was, and is simply, a part of a wider program aimed at showing that electrochemical measurements could be used to probe the applicability of the QED paradigm.

In 1983, collaborative projects with Professor S. Pons (University of Utah) were initiated and aimed at answering two questions [1, p. 31]:

(i) *"would the putative reactions of D^+ compressed into host lattices be different from the reactions in a dilute plasma (or reactions of highly excited D in solids)?"* (i.e., could nuclear reactions be generated within a host lattice?
(ii) *"could such changes in the reactions be observed?"*

To answer these queries, two methods of charging the metal lattices were considered: (i) Compression of D^+ using applied electric fields (electro-diffusion) and (ii) compression using electrochemical charging. Of these, the latter provides the easiest and efficient way to raise the potential energy of an extended quantum system [1, p. 31]. Initially, calorimetric studies were selected to assess the magnitude of excess heat generation by nuclear events. Furthermore, the isoperibolic calorimetry was the preferred method to explore the behavior of the charged Pd/D system because it is the low cost and "catch all" method. By 1988, measured rates of excess enthalpy generation were shown to be consistent with those obtained for nuclear reactions. In 1986, an uncontrolled heat release due to system being driven into the "positive feedback" was observed. With the passage of time, other techniques were used to investigate the behavior of the Pd/D system and theories have been formulated to understand the dynamics of such systems. In spite of the enormous potential for practical applications, the dissemination of relevant information is limited to a very few journals. To comprehend the scale of activities following the 23 March 1989 press conference, one should review the material published in the *Proceedings of the International Conference on Cold Fusion, ICCF 1–8.*

3.0 The Pd/^{n}H system.

What was it about the Pd/D system that prompted Martin Fleischmann to begin this research? It appears that the starting point was the work of Coehn [6], done in the late 1920s and early 1930s, on the electro-diffusion of hydrogen in Pd wires. Coehn found that the absorbed hydrogen (deuterium) is present as a charged species, i.e., it exists in its nuclear – not atomic state and that the Nernst–Einstein relation, $u_{D^+} = FD_{D^+}/RT$, is obeyed. But, the existence of D^+ while in the Pd lattice in the presence of high concentration of s – electrons should lead to the formation of D_2 as dictated by the law of mass action. Furthermore, the application of the Born–Haber cycle to the dissolution of protons into the lattice is *ca* 12 eV. Such a large magnitude of the "solvation energy" implies that the proton sits in deep energy wells while high mobility puts it in shallow holes. Thus, to quote: *"How can it be that the protons (deuterons) are so tightly bound yet they are virtually unbound in their movement through the lattice?"* [5]. Thus, Coehn's observation, when coupled with the quasi-thermodynamic analysis of the electrochemical potential, as defined by Lange [6] ($\overline{\mu}_{D^+} = \mu_{D^+} + e\phi$), posed a number of questions, among them: What is the nature of the species at high D/Pd atomic ratios? What are the dynamics of D^+ under these conditions? These questions, combined with experimental evidence (e.g., heat after death, electro-diffusion), led Fleischmann to consider the possibility that nuclear events can occur in the host lattice.

The characteristics of the Pd/^{n}H system that sets it aside from other metal hydride systems include (i) high concentrations of ionized hydrogen (deuterium), (ii) its (their) high mobility, (iii) high H/D separation factor at equilibrium, (iv) large diffusion coefficients with inverse isotopic effect, and (v) high electrochemical potential of dissolved hydrogen (deuterium). Each of these characteristics is associated with a certain action (activity). In particular:
(i) A high concentration of ionized species within the lattice indicates that electrostatic fields within the unit cell force the transition from the atomic to nuclear state. The high solvation energy implies that deep electrostatic potential holes are present.
(ii) The high hydrogen and deuterium mobility, accelerated by electric fields indicates that ^{n}H, in their nuclear states, are immersed in a dense plasma of d–electrons; if so, then why does highly compressed atomic hydrogen not form?
(iii) The high H/D separation factor is consistent with a model based on delocalized classical oscillators having a high affinity for Pd. High affinities and high separation factors imply highly delocalized wave functions and shallow potential holes.
(iv) Large diffusion coefficients (D = 10^{-7} cm^{2}s^{-1}) where $D_D^+ > D_H^+ > D_T^+$ indicate the presence of shallow holes while the inverse isotope effect implies that deuterium has a configuration space different from that of hydrogen and tritium.
(v) High chemical/electrochemical potentials, *via* their galvanic potential ϕ, tend to promote the formation of large proton clusters.

4.0 The announcement and establishment response

It is known [1] that Fleischmann opposed the disclosure of the results of this research in March 1989; at the earliest, he preferred autumn of 1990. The reasons for his opposition were (i) a premature disclosure would force him to work in a rather narrow set of topics while his interests were in exploring the implications of quantum field effects in natural sciences, and (ii) the expected attitude of industry, where the option of clean production of low grade heat would be contrary to their short and medium-term interests.

Indeed, the research results of Fleischmann and his collaborators were questioned because they did not fit into the accepted views of the $D^+ + D^+$ fusion path. Instead of proceeding along the usual route of scientific inquiry, the critics disregarded the experimental results of many scientists consistent with the manifestations of nuclear activities in the Pd/D system. Fleischmann's view (in 1989) that the establishment would seek to stop the research, by ridicule, disinformation, cutting of funding, and prevention of publications was confirmed. Moreover, many researchers decided that it would be in their interest to report negative conclusions. This can be done by selecting bad data, by using inadequate or flawed experiment design, or by not providing the raw data to prevent further evaluation of the results. To illustrate, in this report, frequent references are made to non–authorized changes in procedures or interpretation employed

even by collaborating laboratories (cf. Chapter 4).

5.0 Fleischmann's philosophy of research

The answer to theorists that the Pd host lattice assisted nuclear processes are not possible is obvious: experimental evidence carries more weight than theoretical speculations. In 1991, Fleischmann [7], in his address to the Royal Institute of Chemistry, stated: *"It is the qualitative demonstrations which are unambiguous; the quantitative analyses of the experimental results can be subject to debate but, if these quantitative analyses stand in opposition to the qualitative demonstration, then these methods of analysis must be judged to be incorrect"*. It is quite remarkable that a similar view was expressed several decades earlier (1943) by the noted theoretical physicist, Max Born [8], in his address to the Durham Philosophical Society, viz., *"My advice to those who wish to learn the art of scientific prophecy is not to rely on abstract reason, but to decipher the secret language of Nature from Nature's documents, the facts of experience"*.

6.0 Summary of events.

To reiterate, as early as 1960, Fleischmann concluded that the behavior of H^+ and D^+ electrochemically compressed into Pd-host lattices could only be understood in terms of quantum field theory. This conclusion led Fleischmann, in 1983, to two questions: (i) would the nuclear reactions of D^+ compressed into host lattices be different to the reactions in a dilute plasma? and (ii) would such effects be observed? The expected answers: Yes to the first and No to the second. In the intervening years (1986, 1987), Fleischmann collected enough evidence, e.g., heat after death, compression by electro-diffusion, to change the answer to (ii) from No to Yes. Finally, in March 1989, events forced Fleischmann and Pons to present their evidence of nuclear activities in Pd/D system.

7.0 References

1. Martin Fleischmann, Accountability in Research, **8**, 19 (2000)
2. M. L. Oliphant, P. Harteck and Lord Rutherford, Nature, **133**, 413 (1934)
3. M. Fleischmann, *An overview of cold fusion phenomena* ICCF 1
4. A. Coehn, Z. Elektrochem., **35**, 676 (1929)
5. C. Bartomoleo, M. Fleischmann, G. Larramona, S. Pons, J. Roulette, H. Sugiura and G. Preparata, Trans. Fusion Technol., **26** 23 (1994)
6. E. Lange, Z. Elektrochem., **55**, 76 (1951)
7. M. Fleischmann, *The present state of research in cold fusion*, ICCF 2, p. 475
8. M. Born, *Experiment and theory in physics*, Dover publ., New York, 1953.
26,23 (1994)

CHAPTER 2: EVENTS IN A POLARIZED Pd+D ELECTRODES PREPARED BY THE CO-DEPOSITION TECHNIQUE.

S. Szpak and P.A. Mosier–Boss

1.0 Introduction.

This chapter reviews our research activities of the polarized Pd/D_2O system. In contrast to the pioneering work of Fleischmann and his collaborators, we consider only events at, and/or, within Pd electrodes prepared by the co-deposition technique developed in this laboratory. Our effort proceeded along two paths: (i) investigation of thermal and nuclear events in the Pd host lattice [1–8] and (ii) examination of the role of the interphase region [9–13]. These paths were undertaken to assess the intensity of events and to provide some information on the factors controlling the initiation and maintenance of excess enthalpy generation, i.e., the "performance envelope."

The scope is limited to a brief description of the experimental work followed by conclusions. A full description of the experimental techniques as well as a thorough discussion is provided in cited references.

2.0 Co-deposition technique.

It is well known that the structure of electrodeposited metal is controlled by a number of factors, among them (i) current density (cell current), (ii) concentration of metal ions (or its complexes), (iii) additives, and (iv) the structure of the substrate. One of the methods to examine the details of a deposit is the use of scanning tunneling microscope. Recently, Naohara et al. [14] reported that during the electroreduction of $PdCl_4^{2-}$ complex, "the Pd deposition proceeds in a layer-by-layer growth mode." If the electroreduction of the palladium complex takes place in the presence of evolving hydrogen/deuterium, the absorbed H/D

accumulates in the regions separated by the lattice defects where the β–Pd/D is formed, transforming the smooth Pd surface into a modular–like structure [15].

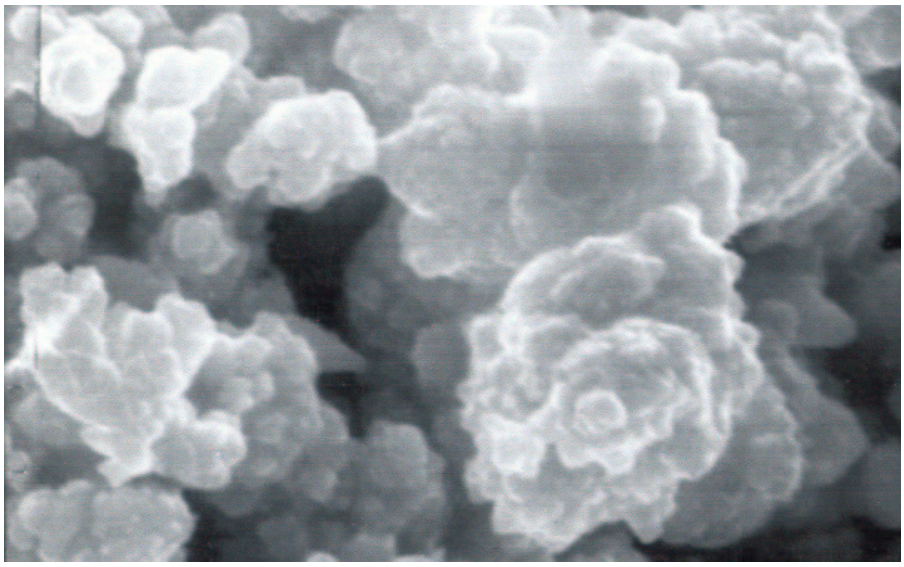

Fig. 1 SEM photograph of co–deposited Pd.

The Pd+D co-deposition is a process where palladium and deuterium are simultaneously deposited on a non-hydrogen absorbing metallic substrate, e.g., Cu or Au, at sufficiently high negative potentials from electrolytes containing palladium salts dissolved in heavy water [1]. The surface morphology and bulk structure are controlled by the solution composition and cell current. As a rule, at cell currents close to the $Pd^{2+} + 2\ e^- \rightarrow Pd$ limiting current density, "cauliflower–like" Pd films are produced. An SEM photograph, Fig. 1, shows the typical structure of an electrode prepared by co-deposition. The individual spherical globules are of submicron size. Characteristic features of the co-deposited films are (i) an almost instantaneous saturation of the Pd lattice [2] with D/Pd atomic ratios > 1.0, (ii) high surface to volume ratio, and (iii) reproducible bulk structure.

3.0 Thermal events.

The objective of this research was, and still is, directed towards determining the conditions maximizing excess enthalpy production. At the present time, a sustained low grade heat source can be maintained for considerable periods of time [3]. We considered two types of measurements, viz. excess enthalpy and surface temperature distribution.

3.1 Excess enthalpy.

The excess enthalpy/power production was assessed in two types of calorimeter designs: (i) for short duration experiments, a calorimeter with an adiabatic enclosure was employed, (ii) for long term experiments, a Fleischmann-Pons type cell was used [3]. It is noteworthy that calorimeters with adiabatic enclosures offer additional information, viz. information on the effect of electrolyte temperature on the process effectiveness. Examples of excess enthalpy plotted against enthalpy input for short time experiments are shown in Fig. 2a and that for long time experiments in Fig. 2b.

Several points can be made: long charging times are eliminated and the rate of excess enthalpy production is both cell current and temperature dependent with occasional bursts, points A, B,.., Fig. 2a and, most importantly, electrodes prepared by co-deposition yield reproducibly higher excess power than the commonly used solid electrodes, Fig. 2b.

One of the features of the Pd/D electrodes prepared by the co-deposition process is the generation of excess enthalpy at relatively low current densities (cell currents). This feature suggests that a new class of Pd/D electrodes should be considered, among them, the fluidized bed electrode [16]. The behavior of copper fluidized bed electrodes has been investigated in great detail. These electrodes can be employed in a variety of configurations, depending on the location of the current feeder electrodes and the direction of current and fluid flow. It is noteworthy that such electrodes have very good heat and mass transfer characteristics.

3.2 Temperature distribution.

The electrode surface temperature distribution can be monitored by infrared imaging. Using this technique, the presence of discrete reaction sites randomly distributed in time and space, Fig. 3a and steep temperature gradients, Fig. 3b, are observed. These features are characteristic of the co-deposition process. The steep temperature gradients, seen in the images, indicate that the heat sources are located in the immediate vicinity of the electrode/electrolyte contact surface [3, 4]. The average surface temperatures are ca 6^{o}C above that of the solution. It is noted that the infrared imaging requires very close placement of the negative electrode to the cell wall to minimize attenuation.

The display of "hot spots" and their interpretation using simplifying assumptions may define a number of new experiments which, in turn, could throw new light on the "cold fusion" mechanism(s). Employing the most drastic assumptions, it is concluded that the nuclear activities occur within the 1μm layer adjacent to the electrode/electrolyte contact surface. It is noted that this conclusion is in an agreement with the findings reported by Bockris et al. [17].

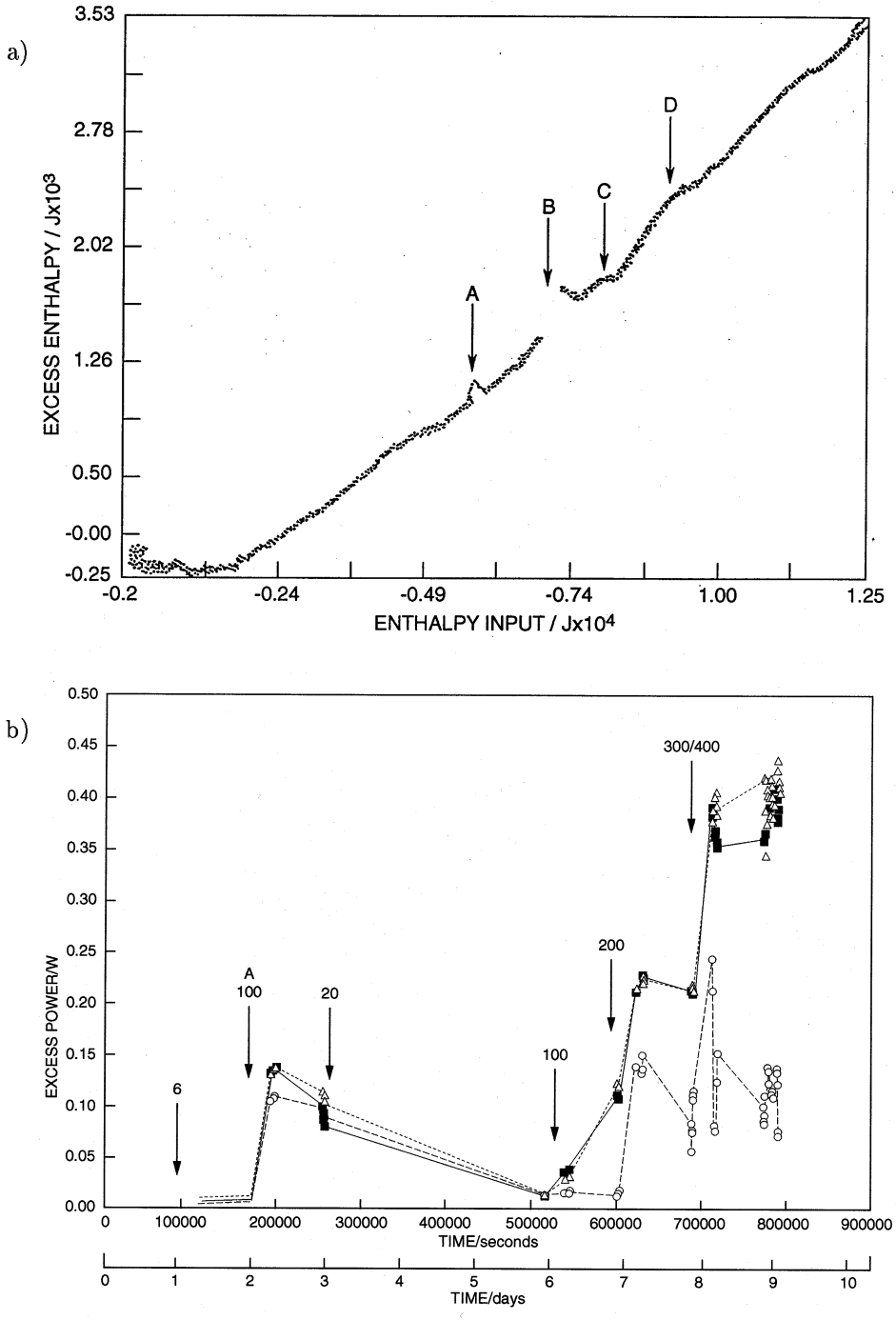

Fig. 2. Excess enthalpy generation in (a) short time and (b) long time experiments.

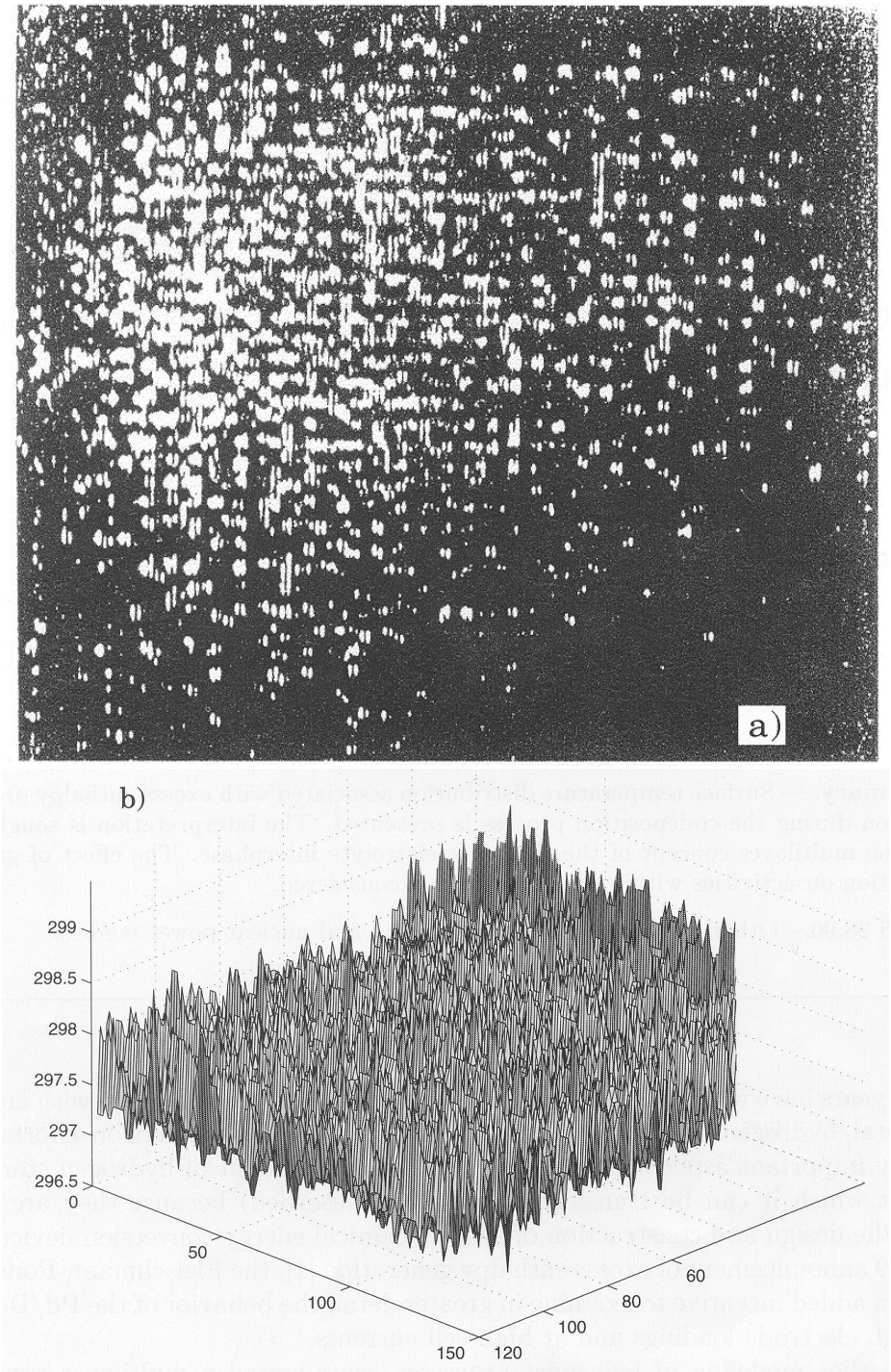

Fig. 3. Surface temperature by infrared imaging; (a) perpendicular, (b) parallel view.

4.0 Nuclear events.

For the excess enthalpy generation to be of nuclear origin, there must be a resulting nuclear "ash" present. Cells for the simultaneous measurements of excess enthalpy and nuclear ash are difficult to construct and operate. Of possible nuclear events, we focused our efforts on measuring X-ray emanation and tritium production.

4.1 Emanating radiation.

Early in the investigation [1], we constructed a cell in which photographic film was placed in close proximity to a working electrode made of Ni screen onto which the Pd+D was co-deposited. After 24 hours exposure to the cathodically polarized electrode, the photographic film was developed producing the image shown in Fig. 4a. To obtain spectral data, Fig. 4b, of the X-ray emissions required the use of background radiation shielding, the appropriate selection of detector(s) and cell design. Because of the very low intensity of the electromagnetic radiation, both the photographic film [1] and the detector [6] must be placed as close as possible to the radiation source.

To summarize, we offer the following conclusions:
(i) Reliable monitoring of emanating radiation requires adequate shielding, proper cell design, and the placement of the suitable detector.
(ii) Cathodically polarized Pd/D system emits X-rays with a broad energy distribution with an occasional emergence of recognizable peaks (e.g., at 21 keV).
(iii) The emission of X-rays appears to be sporadic and of limited duration.
(iv) The surface morphology influences radiation emission, eg, co-deposited electrodes exhibit shorter initiation time than smooth surfaces. Also, the addition of Be^{2+} ions and urea activate the X-ray emission.

4.2 Tritium production.

Tritium production is determined by (i) comparing the computed and measured concentrations of tritium, (ii) observation of the non-equilibrium distribution of tritium between the solution and gas phases and (iii) mass balance. Selected examples of tritium production and its distribution are shown in Figs. 5a and 5b. It is clear that tritium release occurs via two paths, one favoring the electrolyte phase, Fig. 5a, the other the gas phase, Fig. 5b. [8]. The presence of tritium in the bulk metal was observed only upon addition of small amounts of Al^{3+} ions to the electrolyte prior to electrolysis [7].

The sporadic as well as low production rates, 10^3 to 10^4 atoms/second averaged over a 24-hour period [7], demand a very carefully designed system and sampling procedure, Figs. 6a and 6b. Figure 6a shows the design of the calibrated cell (a) and recombiner (b) containing a suitable catalyst. Due to the sporadic occurrence of nuclear events, low rates of tritium production and errors in tritium

a)

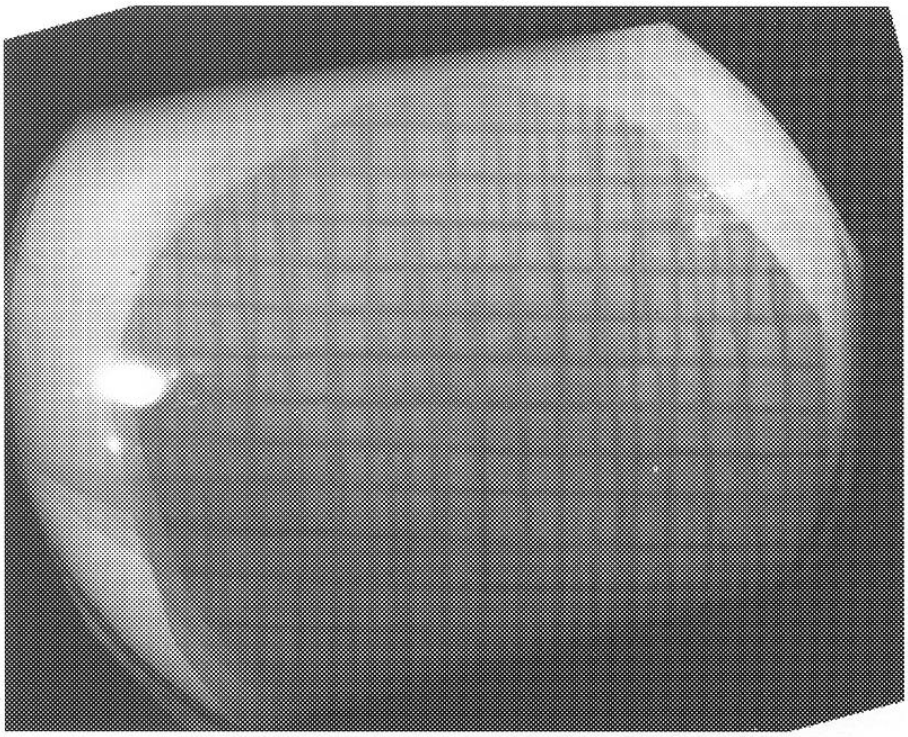

b)

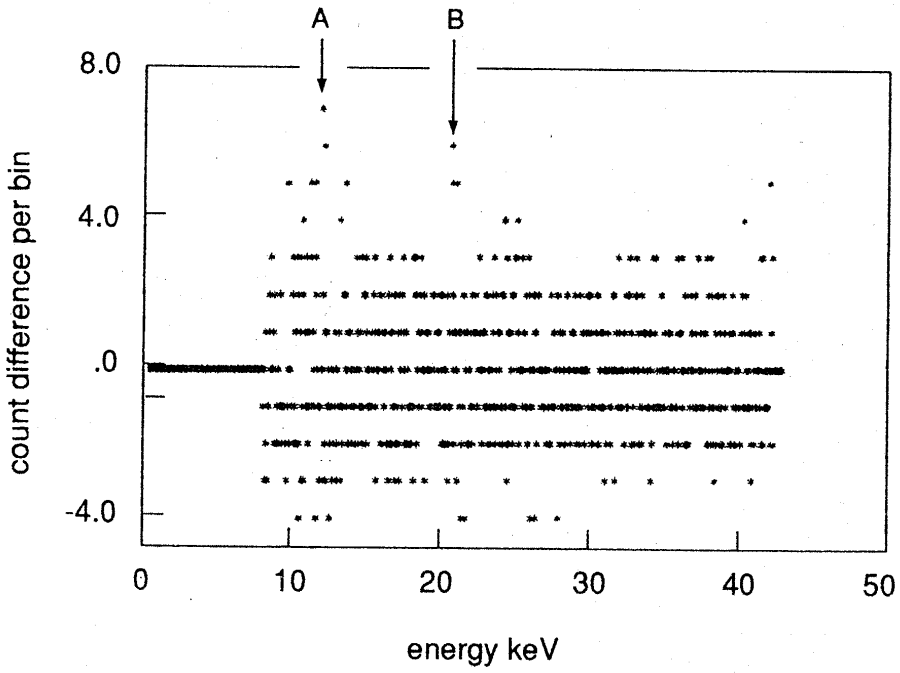

Fig. 4. Emanating radiation, a) recorded on film, b) spectral data.

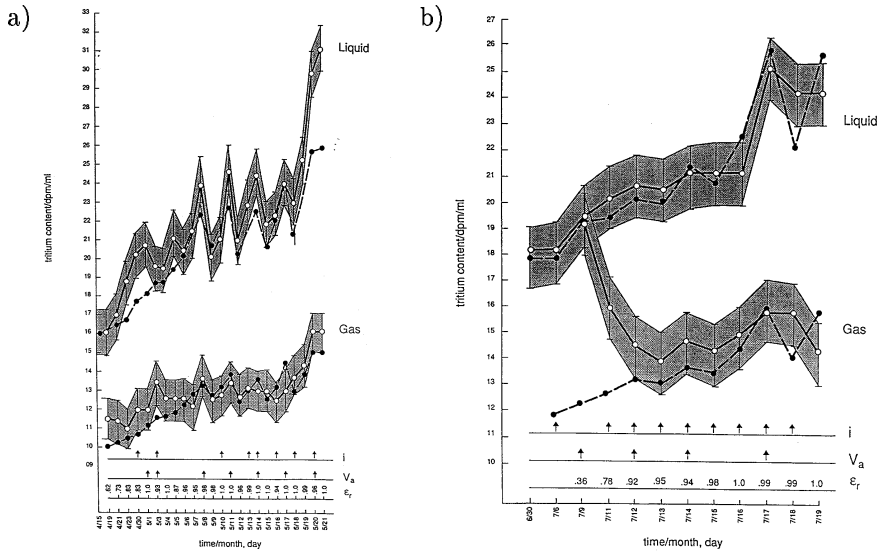

Fig. 5. Tritium production and release paths.

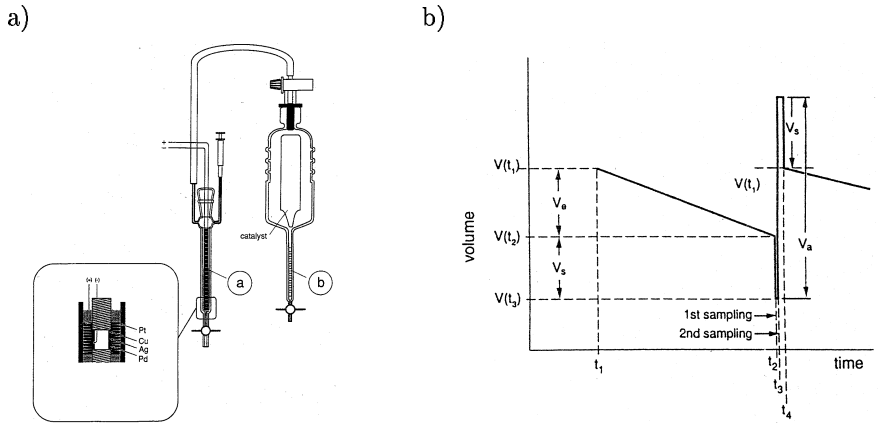

Fig. 6. Apparatus for tritium measurements, a) cell design, b) sampling schedule.

analysis, short sampling times are necessary because averaging over long time periods may obscure its detection.

To reiterate, we note:
(i) Closed cells (i.e., cells with recombining catalyst) are considered superior to close system arrangements (cf. Fig. 6a) for the detection of tritium production in electrolytic cells. But, a closed cell, by design, represents an integrating system, i.e., a system incapable of detecting time dependent tritium production rates. In contrast, a closed system arrangement, such as used in our laboratory, provides information on the rate and frequency of the "burst-like" tritium production.
(ii) The evidence for tritium production as well as its production rate is calculated from the difference between the computed and observed concentration of tritium, the non-equilibrium distribution and the total mass balance.
(iii) The production of tritium takes place within the interphase region. The surface morphology affects the distribution of tritium between the gas and electrolyte phases.

5.0 The interphase region.

Even a cursory examination of the thermal and nuclear activities indicate the importance of the region separating the homogeneous electrolyte and bulk metal phases. In an attempt to determine the factors affecting the "performance envelope," we undertook an exploration of the interphase structure and processes therein. In particular, we discuss the structure of the interphase, the driving forces on loading/unloading, and development of thermal instabilities.

5.1 Structure of the interphase.

The layer separating the electrolyte and bulk metal homogeneous phases contains particles that interact with particles in neighboring phases. If the number of interacting particles is large compared to the total number of particles, then this layer is defined as non-autonomous. Evidently, the Pd/D_2O interphase layer has a non-autonomous character. The complex structure of the Pd/D_2O interphase and the operating forces acting during loading and/or unloading can be best visualized by considering the sequence of events taking place [4]. These events are as follows:

$$(b) \leftrightarrow (\lambda_s) \leftrightarrow (\lambda_m) \leftrightarrow (m) \tag{1}$$

where (b) is the homogeneous solution phase, (λ_s) and (λ_m) are the solution and metal sides of the non-autonomous interphase and (m) denotes the bulk metal, Fig. 7. The solution side comprises of two layers: the reaction layer (r) and the absorption layer (a) while the metal side consists of the absorption (ab) and ionization (io) layers. Thus, for a Pd electrode in contact with an electrolyte containing dissolved D_2 in D_2O acidified with DCl or D_2SO_4, the distribution of components is as follows: Pd, e^- and D^+ in the metallic phase, Pd, D, D^+ and e^- in the interphase, and D_2, D^+, Cl^-/SO_4^{2-} in the electrolyte phase. Evidently,

not all phases contain the same components.

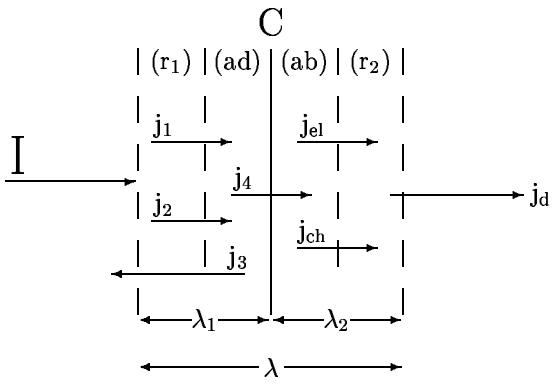

Fig. 7. Structure of the interphase.

5.2 Driving forces.

The dynamics of the interphase during loading/unloading is driven by forces arising from chemical potential gradients. The use of the chemical potential difference as the driving force for the transport of species between two phases is subject to the application of the Gibbs–Duhem equation which states that local equilibrium must be assumed. But transport across the interphase as well as other processes put the system in a non-equilibrium state. A non-equilibrium system in local equilibrium can be modeled by segmenting the system in individual layers, each in mechanical and thermal equilibrium with a stopped transport/reaction, i.e., where the Gibbs–Duhem equation is valid. By reassembling the system and assuming local equilibria, the non-homogeneous nature of the system is restored [4].

Chemical/electrochemical potentials in a system containing charged particles in thermal and mechanical equilibrium is given by $\mu_i = \frac{\partial \Delta G}{\partial n_i}|_{p,T,n_i \neq n_j}$. When this system is placed in an external electric field, ψ, the potential energy of charged particles becomes a function of position, the system becomes non-electroneutral and its chemical potential becomes $\mu_i = \frac{\partial \Delta G}{\partial n_i}|_{p,T,n_i \neq n_j,\psi}$. Thus, any change in p, T, n_j and ψ has a direct effect on the dynamics of the electrode/electrolyte interphase.

5.3 Development of thermal instabilities.

Even small changes in system variables are expected to have an effect on the dynamics of the interphase. To demonstrate, a single grain when viewed under a microscope equipped with Nomarski optics shows preferred sites for deuterium

to enter, Fig. 8. The associated volume changes within the λ_m layer produces motion in the λ_s layer which can be displayed by interference fringes. Obviously, at high current densities, the formation, growth and detachment of evolving deuterium bubbles would have a profound effect on the overall processes in both the solution and the metal side of the interphase.

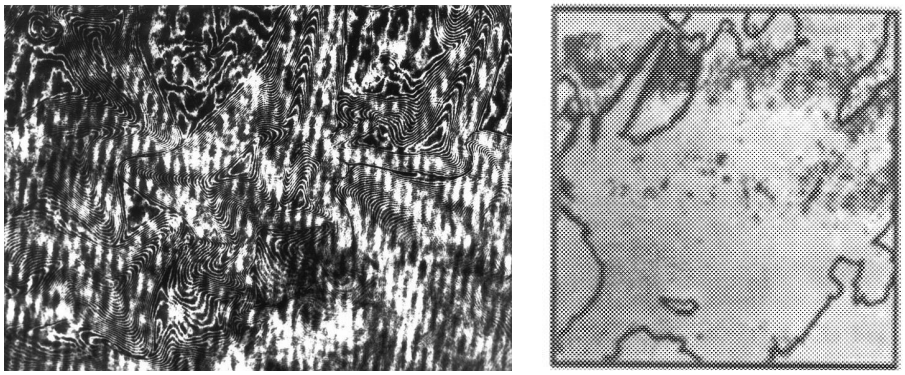

Fig. 8. Effect of D absorption. Left, changes in electrode (by Nomarski optics), right, in electrolyte (recorded by interferometer).

The nature of the driving forces and the experimental evidence suggest that excess enthalpy generation can be expressed as a function of externally applied field, ψ, (overpotential, η), surface coverage, θ, concentration of absorbed deuterium, c_D and concentration of reactive states, c_s, i.e., $\Delta H = \Phi(p, T, \psi, \theta, c_D, c_s)$. The time/space dependent location of short duration of discrete reaction sites further suggests that derivatives of these variables are involved. Such functional dependence and the highly nonlinear behavior leads to the development of thermal instabilities which, in extreme, can lead to electrode melting [5].

6.0 Concluding remarks.

The Pd electrodes prepared by the co-deposition technique show (i) excellent reproducibility, (ii) an increase in the excess enthalpy production with the increase in cell current and electrolyte temperature, and (iii) the heat sources are located in close proximity to the electrode/electrolyte contact surface.

The search for the evidence of the Pd lattice assisted nuclear events requires well designed cells and a strict adherence to experimental protocols. Thus, X-ray detection necessitates shielding and placement of the detector in close proximity to the Pd electrode while tritium production must be based on a complete mass balance. Short sampling times are required to detect low rates of production.

Note: To our knowledge, electrodes prepared by co–deposition technique were employed by Hodko and Bockris [18] and Miles [10]. In both cases, remarkable reproducibility was demonstrated.

7.0 References

1. S. Szpak, P. A. Mosier–Boss and J. J. Smith, J. Electroanal. Chem., **302**,255 (1991)
2. S. Szpak, P. A. Mosier–Boss and J. J. Smith, J. Electroanal. Chem., **379**, 121 (1994)
3. S. Szpak, P. A. Mosier–Boss and M. H. Miles, Fusion Technology, **36**, 234 (1999)
4. P. A. Mosier–Boss and S. Szpak, Ill Nuovo Ciminto, **112 A**, 577 (1999)
5. S. Szpak and P. A. Mosier-Boss, Physics Letters A, **221**, 141 (1996)
6. S. Szpak, P. A. Mosier–Boss and J. J. Smith, Physics Letters A, **210**, 382 (1996)
7. S. Szpak, P. A. Mosier–Boss, R. D. Boss and J. J. Smith, Fusion Technology, **33**, 38 (1998)
8. S. Szpak and P. A. Mosier–Boss, Fusion Technology, **34**, 273 (1998)
9. S. Szpak, C. J. Gabriel and J. J. Smith, J. Electroanal. Chem., **337**,273 (1991)
10. S. Szpak, P. A. Mosier–Boss and S. R. Scharber, ibid., **337**,147 (1992)
11. S. Szpak, P. A. Mosier–Boss, C. J. Gabriel and S. R. Scharber, ibid., **365**, 275 (1994)
12. S. Szpak, P. A. Mosier–Boss and J. J. Smith, ibid., **379**,121 (1994)
13. S. Szpak, P. A. Mosier–Boss, S. R. Scharber and J. J. Smith, ibid., **380**, 1 (1995)
14. H. Naohara, S. Ye and K. Uosaki, J. Phys. Chem., **102B**, 4366 (1998)
15. T. Ohmori, K. Sakamaki, K. Hashimoto and A. Fujishima, Chem. Letters (The Chemical Society of Japan), p. 93 (1991)
16. M. Fleischmann, private communication to F. Gordon, 15 Nov. 00
17. J. O'M. Bockris, R. Sundarasen and Z. Minevski, Extended Abstracts, Electrochemical Society 185th Meeting, San Francisco, CA, May 1994
18. D. Hodko and J. O'M. Bockris, J. Electroanal. Chem., **353**, 33 (1993)
19. M. H. Miles private communication, 1999

CHAPTER 3: EXCESS HEAT AND HELIUM PRODUCTION IN PALLADIUM AND PALLADIUM ALLOYS.

Melvin H. Miles

1.0 Introduction.

The research effort at the Naval Air Warfare Center, Weapons Division, China Lake, proceeded along three main paths: (i) the development of accurate calorimetric methods for detecting excess heat generation, (ii) sampling of the electrolysis gases for determining helium production, and (iii) monitoring the electrolysis cells for radiation effects. The review of our research is presented in two parts. The first part covers research activities at China Lake during 1989 to 1995 that became part of an official U.S. Navy program titled *Anomalous Effects in Deuterated Systems*, funded by the ONR in 1992. The second part reviews experiments conducted by the author at the New Hydrogen Energy Laboratory (NHE), Sapporo, Japan, during October 1997 to March 1998. The research at NHE focused on producing the following: (i) excess heat in China Lake type cells using palladium and palladium particles, (ii) excess heat using palladium alloys in the Fleischmann–Pons Dewar type cells, and (iii) excess heat using the co-deposition method in the Fleischmann–Pons cells.

2.0 Excess Heat Production.

The main signature for fusion in the Pd/D_2O system reported by Fleischmann and Pons is excess heat production. Their announcement in 1989 excited the world because it offered the possibility of unlimited, almost free, non-polluting energy. If cold fusion can be rendered reliable and scaled-up, then it will likely be one of the important scientific discoveries of the 20th century. Unfortunately, the Department of Energy (DOE) panel, in their report on Cold Fusion, published in November 1989, stated that the China Lake studies along with those of California

Institute of Technology (Caltech), Massachusetts Institute of Technology (MIT), and Harwell showed no excess heat production.

Indeed, the initial calorimetric measurements at China Lake showed no measurable excess heat generation, and this was reported at the Santa Fe, New Mexico meeting, 22–25 May 1989 and later published [1]. However, early in the research, we recognized that two factors play a decisive role in the initiation and monitoring of the excess heat production, viz., the metallurgy of the Pd and its alloys and a correct calorimeter design.

2.1 China Lake Isoperibolic Calorimeter.

Various designs were investigated consisting mostly of open, isoperibolic systems. It was found that the decreasing level of the electrolyte, as D_2O was electrolyzed to D_2 and O_2 gases, was identified as a major error in the calorimetry [1]. To minimize this problem, the electrochemical cell was placed into a secondary compartment filled with H_2O, and the temperature was measured within the secondary compartment inside the calorimeter, Fig. 1. With this design, the electrochemical cell served basically as an electrical heater for the secondary compartment. These experiments showed that the ratio of Heat Out/Heat In was 1.00 $\pm$0.04 [1].

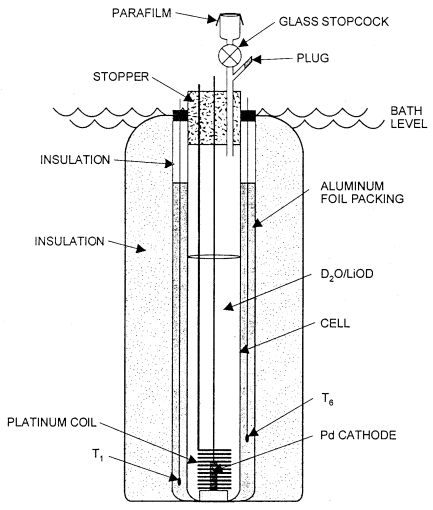

Fig. 1 Basic features of the China Lake isoperibolic calorimeter.

2.2 Johnson–Matthey Palladium.

All the early China Lake studies that showed no excess heat production used cathodes prepared from palladium wire (Wesgo) of unknown origin. It was later

found that the Wesgo palladium shows very poor loading characteristics. After a few months, a large diameter (d = 0.63 cm) palladium rod was received from Johnson–Matthey. Two segments from this rod were studied in two similar calorimetric cells in experiments that started in September 1989. After about 10 days of electrolysis, both experiments showed excess heat production that was well outside the calorimetric error [3]. We later turned these experiments off for a few weeks and then re-started the electrolysis. Once again, excess heat was measured[3].

These results were presented at the First International Conference on Cold Fusion (ICCF–1) in Salt Lake City, Utah, 28–31 March 1990 [4]. It is noteworthy that both our results and the Fleischmann and Pons results indicate that days of electrolysis are necessary before any excess heat appears and that rather large current densities (exceeding 100 mA/cm^2) are required.

The same two initial samples of the Johnson–Matthey palladium rod were later used, cf. 4.1, in the experiments that yielded helium-4 in the electrolysis gas [5]. The Johnson–Matthey palladium proved to be reliable for producing excess heat in our experiments. These experiments demonstrated the importance of the metallurgical aspects of the palladium.

2.3 Naval Research Laboratory Materials Program.

In 1992, our research activities merged with those of NRL in a program funded by ONR. It was realized, by this time, that the properties of the palladium were a critical experimental parameter. Consequently, a major program was undertaken to produce palladium materials that yielded excess heat and to identify the critical parameters of such material.

In 1994, Imam [6] produced three compositions of a new palladium–boron alloy material with nominal concentrations of 0.75, 0.50, and 0.25 weight percent boron. Analyses showed that the three alloy compositions actually contained 0.62, 0.38, and 0.18 weight percent boron. Two distinct phases of the same cubic structure were found in all three compositions of the alloy.

Unlike previous NRL materials, these new Pd-B alloys produced excess heat in almost every experiment [7]. The only Pd-B sample that failed to produce the excess heat was one that had a large, folded-over metal region due to the swaging of this rod that acted as a long crack [7]. Although we had achieved a major Navy goal for this program, i.e., production of palladium materials that reproducibly yielded excess heat, the ONR sponsored program was terminated a few months after the report of excess heat for the Pd-B alloys, and no further research was conducted at China Lake after June 1995. This same palladium-boron material produced significant excess heat in an experiment in Japan using the Fleischmann–Pons Dewar type calorimetry (cf. 5.3).

The question naturally arises regarding why the Pd-B alloys proved so successful

in producing excess heat. Possible explanations include the fact that the added boron significantly increases the hardness of the palladium and the presence of boron also greatly retards the rate at which deuterium escapes from the palladium metal [7]. There are also proposals of fusion reactions that involve boron.

The most likely explanation for the beneficial effect of the added boron is that it minimizes the activity of oxygen in the palladium by converting it to B_2O_3. This B_2O_3 floats to the surface and is removed during the molten phase of the Pd–B preparation. This explains the lower boron concentrations in the final material. The Johnson–Matthey process that produced good materials for excess heat generation reportedly used a cracked ammonia atmosphere, i.e., N_2 and H_2. Here again, oxygen would be removed from the palladium by its reaction with hydrogen to produce water. Perhaps this is the key for reproducible excess heat effects: palladium that is relatively free of oxygen. The co-deposition method developed by Szpak and Mosier–Boss would also produce palladium that is free of oxygen contamination. One can speculate that the deuterium in the lattice reacts with the oxygen impurity to form D_2O and that this breaks up the palladium–deuterium lattice structure.

3.0 Radiation Measurements at China Lake.

We realized our lack of expertise in radiation measurements and never planned on this becoming any official part of our research program at China Lake. However, radiation monitoring was required by the safety personnel; hence, we purchased some equipment including Geiger–Mueller (GM), sodium iodide (NaI) and neutron detectors, as well as Scalar Ratemeters for monitoring any possible harmful radiation.

3.1 Dental Film Exposure.

The excess heat measurements for the two Johnson–Matthey palladium cathodes at China Lake led to further experiments using these same two electrodes. These experiments were designed to test for excess heat, X-rays by dental film exposure, neutrons by gold activation, radiation by GM detectors, and helium-4 by the sampling of the electrolysis gases [5]. Evidence was found for everything except for neutrons [5, 8]. Exposure of the dental film X–rays was observed [5]. The film positioned the closest to the palladium cathode (Cell A) showed the greatest exposure [5].

3.2 Measurements Using GM and NaI Detectors.

Anomalously high radiation counts were observed using several different GM detectors as well as NaI detectors during electrolysis experiments with palladium cathodes in heavy water [7]. These high radiation counts were often observed in co-deposition experiments where palladium metal is deposited from a D_2O solution onto a copper cathode in the presence of evolving deuterium gas. The

radiation counts reached values as high as 73 σ above normal background counts. The radiation would appear within a few hours in the co-deposition experiments. In contrast, the appearance of radiation required days of electrolysis for the palladium rods [9]. The emission of low intensity X-rays from similar Pd/D systems was reported by Szpak et al. [10].

3.3 Neutron Measurements.

Neutron emissions from these experiments are very low and difficult to detect. Our measurements were strictly for safety concerns. We used a Ludlum Model 15 neutron survey meter that was placed close to the water bath containing the electrochemical cells. We used only an audio detection signal and never recorded any neutron counts versus time for either the experiments or the background. Our one experiment using neutron activation of indium and gold foils mounted at the surface of the electrochemical cells shows that any neutron production would have to be less than 10^5 per second [5].

4.0 Helium Measurements.

Two major theories had predicted that helium-4 would be the main fusion product in the Pd/D system prior to our experimental measurements and had also predicted that the helium-4 would be present in the electrolysis gases. The first, by Preparata [11], was based on Quantum Electrodynamics (QED) while the second, by Chubb and Chubb [12], was based on Ion Band States. It is noted that the first solid evidence for helium production was reported by us. Following our initial measurements of helium-4 production in the Pd/D system, a number of other laboratories have verified this result. Very strong evidence for helium-4 production is found in the recent work of Arata et al. [13] and McKubre et al. [14].

4.1 Samples Collected in Glass Flasks.

Our initial report of helium-4 production during excess heat events in D_2O electrolysis experiments was published in March 1991 [15]. In these experiments, the flow of the electrolysis gases was directed through a 500 mL glass flask and then through an oil bubbler to the outside atmosphere. A positive pressure was maintained within the system to minimize any atmospheric contamination. These experiments began 3 October 1990 and ended 25 December 1990. The system was thoroughly flushed with boil-off N_2 gas whenever a glass flask was replaced or when D_2O was added. The collected electrolysis gas samples were sent to the University of Texas for helium analysis. Based on these experiments, helium-4 is the major product when excess heat occurs [15].

A major criticism of these results was the possibility of atmospheric helium-4 contamination, especially due to the known diffusion of helium through glass. It was precisely because of these concerns that we conducted control experiments performed using H_2O+LiOH in place of D_2O + LiOD. These control studies

gave no evidence of helium-4 production [5, 7, 8, 15]. Our first D_2O + LiOD electrolysis gas sample (10/17/90–A) also served as a control since there was no significant excess heat and no helium-4 detected [5, 7, 11, 16]. Our controls, therefore, covered time periods both before and after the excess heat experiments; this refutes arguments by critics that we were simply getting better at keeping out helium-4 [16].

4.2 Samples Collected in Metal Flasks.

These helium-4 experiments were repeated using metal flasks for collecting electrolysis gas samples to rule out the possibility of helium diffusion through glass. All experimental conditions were intentionally kept the same except for the use of the metal flasks. The helium-4 measurements for the metal flask samples were performed at the U.S. Bureau of Mines, Amarillo, Texas, laboratory that specialized in these measurements. The end result was the same as before. The electrolysis gas samples collected in metal flasks during excess heat production also contained excess helium-4 [7, 17]. Furthermore, the rate of helium production could now be established at 10^{11} to 10^{12} atoms per second per watt of excess power [12, 17]. This is the correct magnitude for typical deuteron fusion reactions that yield helium-4 as a product.

4.3 Summary of Helium Measurements.

A total of thirty-three experiments were conducted that involved the measurement of helium-4 in the electrolysis gas. In experiments producing excess heat, 18 out of 21 also produced helium-4. Two experiments using a Pd–Ce cathode produced excess heat, but no helium-4 was detected [7]. The explanation is that the helium-4 remains trapped in this alloy. The third experiment involved a flawed excess heat measurement due to an unusually low D_2O level in the cell [7]. For all 12 experiments where no excess heat was produced, there was no evidence for helium-4 production [7]. The probability of finding the correct relationship between excess heat and helium-4 in 30 out of 33 experiments is about one in a million [7]. The probability of also observing the correct magnitude of helium–4 production (10^{11} to 10^{12} atoms per second per watt of excess power) in each experiment due to random errors is a very unlikely situation.

5.0 Research at NHE.

No further research in the Pd/D system was done at China Lake after the ONR funding ended in June 1995. However, a New Energy Development Organization (NEDO) appointment became available to work at the New Hydrogen Energy (NHE) laboratory in Sapporo, Japan, from late October 1997 until the end of March 1998. Numerous calorimetric data were collected. Much of this data still awaits extensive analysis.

5.1 China Lake Calorimetry at NHE.

The final two cold fusion experiments at China Lake in 1995 involved tests of 1.0 mm diameter Johnson–Matthey palladium wire. One experiment produced 200 mW of excess power while the other did not [7]. These same two cells, electrodes, and calorimeters were used again at NHE in Japan. The only major change was the use of aluminum foil rather than water in the secondary compartment surrounding the cells. This change made the calorimetric system much more sensitive to the detection of excess power (± 5 mW versus ± 20 mW). Once again, the palladium wire that produced excess heat in China Lake produced significant excess heat at NHE in Japan. The other palladium wire also performed as before and produced no measurable excess heat effects. These results have been recently published [18].

5.2 Cells Using Platinum and Palladium particles.

These experiments in China Lake cells were designed to give dynamic electrolysis conditions by using small palladium and platinum particles. These particles were actually miniature cylindrical rods with the dimensions of 0.6 to 0.65 mm diameter and 0.65 to 0.70 mm length. The China Lake calorimetry was used to test platinum particles in Cell A as a control while palladium particles were investigated in Cell B [19]. Figure 2 shows the electrochemical power along with the output power for the cell containing palladium particles.

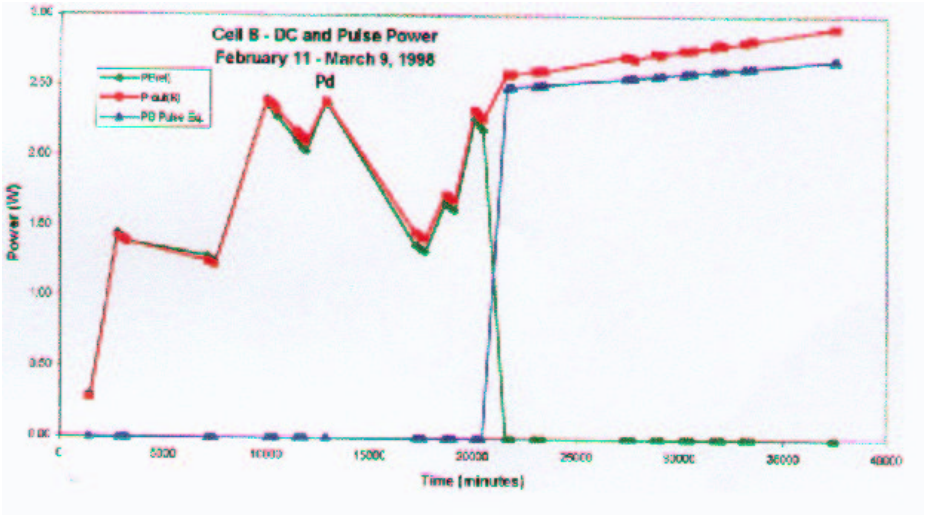

Figure 2. The electrochemical power and output power for the palladium particles in Cell B.

After about a week of electrolysis, the output power began to exceed the input power to the cell. This excess power was nearly 100 mW for direct current

electrolysis. The electrochemical input power was switched to pulse power at 20490 minutes. This involved a peak voltage of nearly 100 V, a peak current of 6 A, a pulse width of 1.0 μs, a pulse frequency of 5 kHz, and an average electrolysis current of 0.012 A [19]. As shown in Fig. 2, larger amounts of excess power exceeding 200 mW were observed. The cell containing platinum particles gave no excess power for either direct current or pulse electrolysis [19].

The small metal particles jostle about during electrolysis; hence, new surface areas are continually exposed to the metal/electrolyte interface where electrolysis occurs. This experiment was designed to give a fluidized bed electrolysis effect, but the metal particles were too heavy. The many tiny palladium particles make these experiments less sensitive to the variables that produce excess heat in one palladium rod, but not in another similar rod.

5.3 Palladium Alloy Cathodes in Fleischmann–Pons Type Cells.

The three Dewar-type electrochemical cells used at NHE were silvered in their top portions so that heat transfer is confined almost exclusively to radiation across the unsilvered part. The palladium cathodes selected for the first calorimetric studies in these cells were Pd-Ce-B, Pd-B (0.5 weight % boron), and Pd-Ce. These experiments require accurate determination of the radiative heat transfer coefficient and the water equivalent of the cell. The approximate methods used for the analysis are discussed elsewhere [20]. These approximate methods show no measurable excess power for the Pd-Ce-B cell and significant excess power for the Pd–B and Pd–Ce cells [19, 20]. Figure 3 presents the excess power for the Pd–B experiment using the Fleischmann–Pons calorimetry.

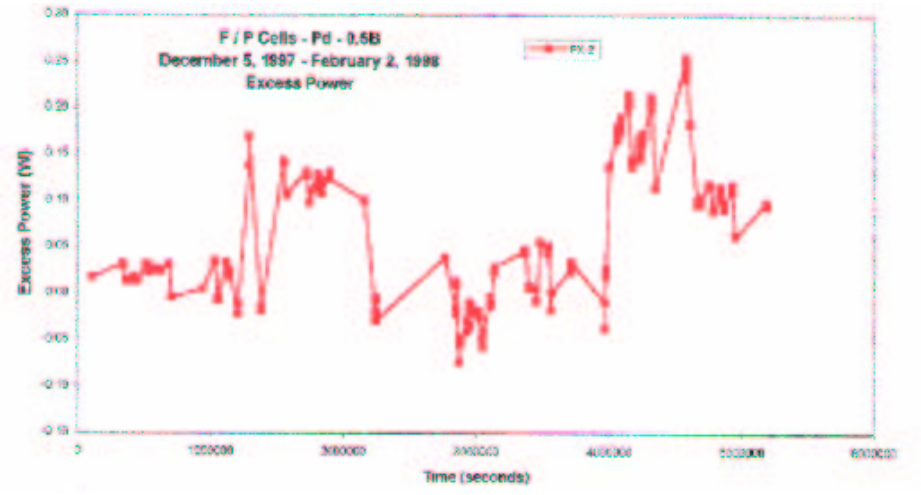

Fig. 3. Excess power measurements for the Pd-0.5B cathode in Cell A-2.

The data set from this Pd–B experiment has been examined in detail by Fleischmann

and his results are presented elsewhere in this report. This independent evaluation of the raw data by Fleischmann shows the same general trends as Fig. 3, but the excess power is significantly higher. Comparisons of these two methods show that the radiative heat transfer coefficient used for Fig. 3 is 4.64% too small (8.112×10^{-10} W/K^4 versus 8.5065×10^{-10} W/K^4). The NHE method used for this experiment as well as for other experiments [21] is found to be completely invalid [21]. An interesting feature of this Pd–B study is the early onset of the excess heat effect.

Excess power measurements for the Pd–Ce cathode in the Fleischmann–Pons type cell is presented in Figure 4.

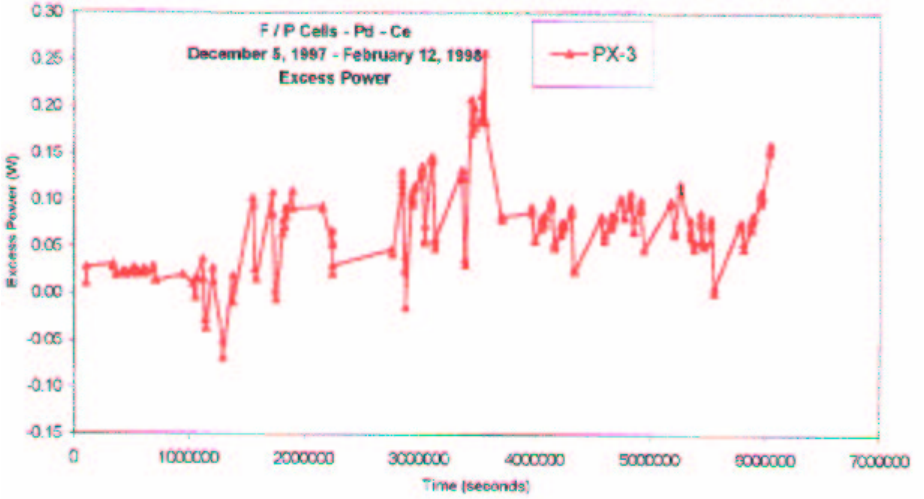

Figure 4. Excess power measurements for the Pd-Ce cathode in Cell A-3.

This Pd–Ce material was obtained from Fleischmann and gave significant excess heat in a previous study at China Lake [7]. The radiative heat transfer coefficient used for the results shown in Fig. 4 was 8.000×10^{-10} W/K^4. An independent evaluation of the raw data for this experiment by Fleischmann is in progress.

5.4 Co-Deposition Experiments in Fleischmann–Pons Type Cells.

The method of depositing palladium from solution onto a copper cathode in the presence of evolving deuterium gas was first reported by Szpak et al. [22]. For the experiments at NHE, a modified plating solution was used consisting of 0.025 M $PdCl_2$, 0.15 M ND_4Cl, and 0.15 M ND_4OD in D_2O [19]. No lithium salts were used. The mixing of these chemicals produced an orange solution and the formation of a precipitate. This precipitate was likely $Pd(OD)_2$ due to the rather high initial pH of the solution (pH=9 to 10).

Three co-deposition experiments were conducted at NHE using the Fleischmann–Pons calorimetric cells. The initial current was 0.006 A in each cell. The deposition of palladium onto the copper cathode was visible within a few minutes, and the copper was completely covered by a dark palladium deposit within 30 minutes. After 24 hours, the plating solution was nearly clear and gassing was readily visible at the Pd/Cu cathode. The current was then increased to 0.100 A in each cell. On the second day, the solution had turned to a pale yellow color. The current was then increased to 0.200 A, but a chlorine odor developed in the room; hence, the current had to be reduced to 0.020 A for the weekend. The following week, the cell currents were increased to 0.100 A, then 0.200 A, and finally to 0.400 A without any further problems with the chlorine odor.

The excess power for these three co-deposition cells is shown in Figure 5.

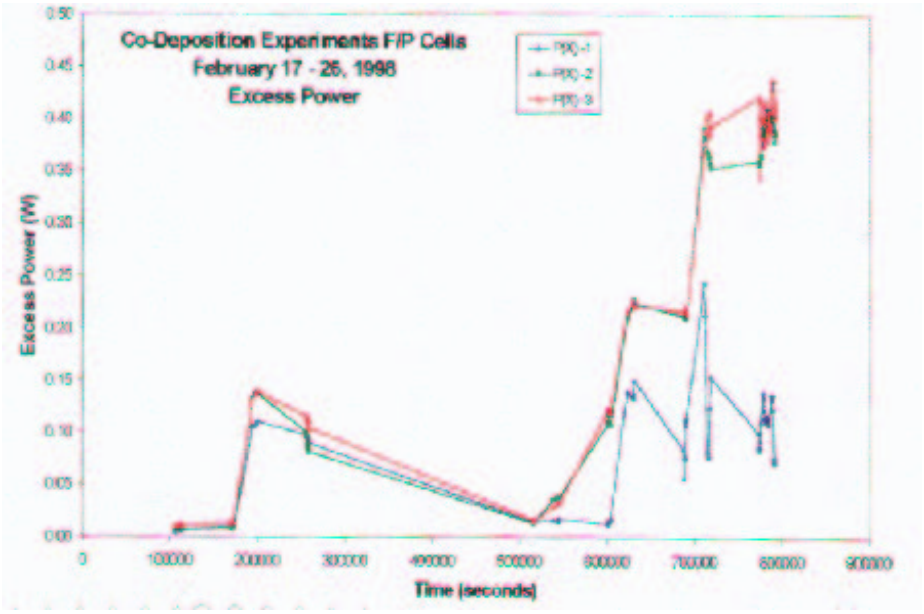

Figure 5. Excess power measurements in co-deposition experiments.

Excess power is generated in each cell. During the last 2 days of this experiment, about 400 mW of excess power was present in both Cells A-1 and A-3 while about 100 mW of excess power was present in Cell A-2. These results have been included in a refereed publication [23]. The raw data sets for these experiments still await complete analysis. Based on other independent analysis for these Fleischmann–Pons cells, even larger excess heat effects are likely. The co-deposition results for Cell A-2 were evaluated by Fleischmann, and results reported at the March 2001 meeting of the American Physical Society [24]. There is clear evidence for positive feedback effects in this experiment [24].

6.0 Concluding Remarks.

This new field of anomalous effects in the Pd/D system has endured a difficult 12-year survival struggle. Many scientists who have persisted with this research have seen their careers placed in jeopardy. Nevertheless, no scientific publications have clearly disproved any claims of excess heat, helium production, radiation, or tritium. In contrast, similar results for this research have been reported by many laboratories around the world. Unfortunately, this new field was dismissed from the scientific table in 1989 by ridicule rather than by the proper application of the scientific method. A recent book has clearly documented this struggle [25]. In the end, the scientific truth about this field will prevail.

7.0 References.

1. D. E. Stilwell, K. H. Park, and M. H. Miles, J. Fusion Energy, **9** (1990) 333.
2. *"Cold Fusion Research.* A Report of the Energy Research Advisory Board to the United States Department of Energy", John Huizenga and Norman Ramsey, co-chairmen, November 1989, p. 12.
3. M. H. Miles, K. H. Park, and D. E. Stilwell, J. Electroanal. Chem. **296**, 241 (1990).
4. M. H. Miles, K. H. Park, and D. E. Stilwell, Proc. of the First Annual Conference on Cold Fusion, (ICCF – 1), 1990, Salt Lake City, Utah, pp. 328-334.
5. M. H. Miles, R. A. Hollins, B. F. Bush, J. J. Lagowski, and R. E. Miles, J. Electroanal. Chem., **346**, 99 (1993) .
6. D. D. Dominguez, P. L. Hagans, and M. A. Imam, Technical Report – NRL/MR/6170-96-7803, Jan. 1996.
7. M. H. Miles, B. F. Bush, and K. B. Johnson, Technical Report – NAWCW-PNS TP 8302., Sept. 1996.
8. M. H. Miles, B. F. Bush, and J. J. Lagowski, Fusion Technol., **25**, 478 (1994).
9. M. H. Miles and B. F. Bush, Proc. of ICCF-7, 1998, Vancouver, Canada, p. 236.
10. S. Szpak, P. A. Mosier-Boss, and J. J. Smith, Physics Letters , **A 210**, 382 (1996).
11. G. Preparata, Proc. of the First Annual Conference on Cold Fusion, 1990, Salt Lake City, Utah, p. 91.
12. T. A. Chubb and S. R. Chubb, Fusion Technol., **20**, 93 (1991).
13. Y. Arata and Y. C. Zhang, Proc. of ICCF-8, 2000, Lerici, Italy (pp. 11–16).
14. M. McKubre, F. Tanzella, P. Tripodi, and P. Hagelstein, Proc. of ICCF-8, 2000, Lerici, Italy (pp. 3–10).
15. B. F. Bush, J. J. Lagowski, M. H. Miles, and G. S. Ostrom, J. Electroanal. Chem., **304**, 271 (1991).
16. M. H. Miles, J. Phys. Chem. B, **102** , 3642 (1998) .
17. M. H. Miles, K. B. Johnson, and M. A. Imam, Proceedings of ICCF-6, 1996, Lake Toya, Hokkaido, Japan, p. 20.
18. M. H. Miles, J. Electroanal. Chem., **482**, 56 (2000).
19. M. H. Miles, NEDO Final Report, NHE Laboratory, Sapporo, Japan, 1998.

20. M. H. Miles, Proc. of ICCF-8, 2000, Lerici, Italy, (pp. 97–104).
21. T. Saito, M. Sumi, N. Asami, and H. Ikegami, Proc. of ICCF-5, 1995, Monte-Carlo, Monaco, p. 105.
22. S. Szpak, P. A. Mosier-Boss, and J. J. Smith, J. Electroanal. Chem., **302**, 255 (1991).
23. S. Szpak, P. A. Mosier-Boss, and M. H. Miles, Fusion Technol., **36**, 234 (1999).
24. M. H. Miles, S. Szpak, P. A. Mosier-Boss and M. Fleischmann, Proc. of the American Physical Society, March 18-22, 2001, Seattle, WA.
25. C. Beaudette, *Excess Heat, Why Cold Fusion Research Prevailed*, Oak Grove Press, LLC, South Bristol, Maine, 2000.

CHAPTER 4: ANALYSIS OF EXPERIMENT MC–21: A CASE STUDY.

S. Szpak, P. A. Mosier–Boss, M. H. Miles, M.A. Imam, and M. Fleischmann

PART I: DEVELOPMENT OF DIAGNOSTIC CRITERIA.

I/1.0 Introduction.

In the text, frequent reference is made to the "ICARUS methodology" and "experiment MC-21". The term ICARUS is an acronym for Isoperibolic Calorimetry: Acquisition, Research and Utilities System. It is a document specifying cell design, operating equipment, experimental protocol, and data analysis. Experiment Mc–21 identifies an experimental run conducted by M.H. Miles at the New Hydrogen Energy (NHE) laboratories in Sapporo, Japan, while on leave from the NWC China Lake.

This chapter contains two parts. the first deals with the development of diagnostic criteria for the assessment of excess enthalpy generation based on the modelling of the isoperibolic calorimeters used and leading to the definition of a number of versions of the heat transfer coefficient. These heat transfer coefficients define the behavior of the calorimetric systems. The second part contains the application of these criteria to a specific run, e.g., that of experiment Mc–21.

I/2.0 Symbols used.

$C_{p,g}$ – heat capacitance of the D_2O vapor. [J(gMole)$^{-1}$K^{-1}]
$C_{p,l}$ – heat capacitance of liquid D_2O. [J(gMole)$^{-1}$K^{-1}]
$E_c(t)$ – cell voltage at time t. [V]
$E_{th,b}$ – thermoneutral potential at the bath temperature.[V]
F – Faraday constant. [coulombs (gMole)$^{-1}$]
$H(t-t_i)$ $i = 1, 2$ – Heavyside unity shift function. [$H(t-t_i) = 0$ for $t < t_i$; $H(t-t_i) = 1$ for $t > t_i$].

ΔH_{ev} – rate of evaporative cooling. [W]
$\Delta H_{net}(t)$ – rate of net enthalpy input at the time t. [W]
I – cell current. [A]
$k_{i,j,l}$ – heat transfer coefficient. [WK^{-4}].
L – latent heat of evaporation. [$J(gMole)^{-1}$
M– number of mole of D_2O at $t = 0$.
P – vapor pressure at the cell temperature. [bar]
P^* – atmospheric pressure. [bar]
P_{D_2} – pressure of deuterium. [bar]
$Q_f(t)$ – generation of excess enthalpy in the cell at time t. [W]
t – time. [s]
$\Delta\theta$ –temperature difference between the cell and the water bath. [K]
θ_b – bath temperature. [K]
μ –chemical potential. [J]
$\overline{\mu}$ – electrochemical potential. [J]
τ – time. [s]
ϕ – Galvani potential. [V]
Φ – proportionality constant relating conductive heat transfer to the radiative

I/3.0 Calorimetry: the governing equation.

At low to intermediate cell temperatures (i.e., $30°C < \theta < 80°C$), the behavior of the calorimeters, shown in Fig. 1, is modelled adequately by the differential equation:

$$\left[C_{p,l}M\frac{d\Delta\theta}{dt}\right] = [(E_c - E_{th})I] + [Q_f(t)] + [\Delta QH(t-t_1) - \Delta QH(t-t_2)] -$$

$$\left[\frac{3I}{4F}\left[\frac{P(t)}{P^* - P(t)}\right][(C_{p,g} - C_{p,l})\Delta\theta(t) + L_l]\right] - \left[k'_R[(\theta_b + \Delta\theta(t))^4 - \theta_b^4]\right] \quad (2)$$

where terms in square brackets indicate that the time rate of change in the enthalpy content of the calorimeter equals the sum of the rate of enthalpy input due to electrolysis, rate of excess enthalpy generation, the calibration pulse less the rate of enthalpy removal in the gas stream, and the rate of heat transfer to the water bath, given in Eq. (1) by the rate of radiative transfer alone.

In arriving at Eq. (1), we have made a number of approximations,[1] the major one being the representation of the heat transfer term

$$-k_R^0\theta_b^3[1-\gamma t]\left[\frac{(\theta_b + \Delta\theta(t))^4}{\theta_b^3} + 4\Phi\Delta\theta(t)\right] \quad (3)$$

by the purely radiative term with an appropriate increase of the radiative heat transfer coefficient to k'_R. As we have shown elsewhere [1], this leads to a small

[1]Extensive discussion can be found in e.g., ref. [1].

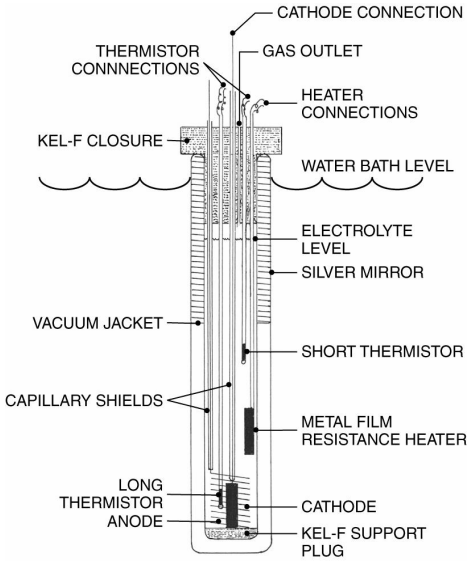

Fig.1. Silvered Dewar calorimeter.

underestimate of the heat output and, therefore, to a small underestimate of Q_f.[2] At the first level of approximation, we can neglect the residual small time dependence of the heat transfer coefficient.

With the calorimeters supplied with the ICARUS systems, the conductive contribution to heat transfer was very small. In fact, if this term was "lumped" into the radiative term by allowing for a small increase in the radiative heat transfer coefficient:

$$\text{radiative heat transfer} = (k_R'^{,0})[1 - \gamma t][(\theta_b + \Delta\theta)^4 - \theta_b^4] \qquad (4)$$

then the values of the "pseudo-radiative" heat transfer coefficient derived $(k_R'^{,0})[1 - \gamma t]$, were close to those calculated from the Stefan-Boltzmann coefficient and the radiative surface area.[3] [4]

[2]We have sought throughout to ensure that all approximations should lead to underestimates of Q_f.

[3]Typical values: 0.72×10^{-9} WK^{-4} $< (k_R'^{,0})[1 - \gamma t] < 0.76 \times 10^{-9}$ WK^{-4}. However, for the cell used in the experiment Mc–21, this "pseudo-radiative" heat transfer coefficient is 0.85×10^{-9} WK^{-4} so that the conductive contribution was evidently increased. We have to assume that this increase in the heat transfer coefficient must have been due to a "softening" of the vacuum in the Dewar calorimeters.

[4]An increase in the "pseudo-radiative" heat transfer coefficient can normally only be observed if the cells are "overfilled" with D_2O during the periodic replenishment of the cells. This "overfilling" of the cells leads to the approach of the electrolyte level to the base of the Kel-F plug sealing the cells thereby increasing the conductive losses through the top of the cell. This effect (which leads to a 4 to 5 % increase in the "pseudo-radiative" heat transfer coefficient) can be observed in the results for day 61 of experiment Mc 21.

If the time dependence of the heat transfer coefficient is not included explicitly in Eq. (3), then

$$\text{radiative heat transfer} = (k'_R)[(\theta_b + \Delta\theta)]^4 - \theta_b^4] \tag{5}$$

where the radiative heat transfer coefficient (k'_R) now shows a weak time–dependence.

I/4.0 Excess enthalpy generation.

Whether or not a particular cell generated excess enthalpy is determined by energy balance. We, therefore, need to examine all the terms in Eq. (1).

I/4.1 Enthalpy removal by gas stream.

In calculating the rate of enthalpy removal by the gas stream, Eq. (5),

$$(3I/4F)[P/(P^* - P)][(C_{p,g} - C_{p,l})\Delta\theta + L] \tag{6}$$

we have always assumed that the partial pressure of D_2O in this gas stream can be calculated using the Clausius–Clapeyron equation with the latent heat of evaporation, L, being that at the boiling point. Evaporative cooling only becomes an important term at temperatures close to the boiling point (at $ca\Delta\theta > 70°C$) where these two assumptions are justified. At low to intermediate temperatures, $\Delta H_{ev}(t)$ is a minor correction term so that errors due to the two assumptions introduce second order small quantities. In particular, the errors introduced by neglect of the temperature dependence of the latent enthalpy of evaporation are $< 0.1\%$ under all conditions of operation of the cells. It is also important to bear in mind that such errors are further reduced for all evaluations of the "true" heat transfer coefficients, as these evaluations are based on differences in temperature induced by the calibration pulses (or on differences in temperature induced by "topping" up of the cells or perturbations of the current density; such methods of calibration are not considered in this report).

The parameters required for this calculation were contained in data files of the ICARUS-1 and ICARUS-2 software and were identical for both systems[5]. The Handbooks [2, 2A] contained specific instructions that some of these parameters would need to be changed (here, θ_b and P^*; see below) as well as instructions as to how such changes in the parameter listing were to be carried out.[6]

[5]The values installed in the programs as supplied were:
$C_{p,l}$ = 84.349 J Mol−1 K^{-1}
$C_{p,g}$ = 44.500 J $Mol^{-1}K^{-1}$
θ_b = 374.570 K^{-1}
F = 96484.56 C $Mole^{-1}$
R = 8.3 14410 J $Mole^{-1}K^{-1}$
L = 41,672.600 J $Mole^{-1}$
P = 1.003 Ats

[6]However, it appears that values of the rates of evaporative enthalpy loss close to those given

The first of these changes is the adjustment of the boiling point to the value which applies to the ambient atmospheric pressure.[7] The values of P^* that have been used in the present interpretation have been obtained from the Sapporo Airport. Furthermore, it has been assumed that the pressure in the cell is the same as the ambient pressure, although it may well be that the pressure in the cell was somewhat higher than this value.

The second change is that it is necessary to take note of the fact that the boiling point corresponds to that of the electrolyte solution in the cell. It has been assumed that this correction is given by that for an ideal solution $\Delta\theta_{bp} = (R/L)(\theta_{bp}^2 ln x_1)$ where x_1 is the mole fraction of the D_2O in the electrolyte. It will be evident that this correction becomes especially important on day 68 when the cell contents are driven to dryness. In that case, the boiling point must be adjusted at each measurement interval as the D_2O content of the cell decreases. The values of the boiling points appropriate for the interpretation of the experimental data for day 68 are discussed further in vol. II/5.0

I/4.2 Rate of reflux.

The third change again applies specifically to day 68, namely, an allowance for the effect of reflux in the cell. In order to evaluate the effects of reflux, we need to take note of the fact that the vapor space in the cell is filled predominantly by D_2O as the cell is driven to dryness. Thus, even at the start of day 68, the mole fraction of D_2O in the vapor space was *ca* 0.85 for this experiment. In consequence, heat transfer from the vapor phase to the walls of the Dewar (to provide the enthalpy input required by radiation across the vacuum gap) was dominantly from the D_2O content of the vapor. We also need to take note of the fact that the contribution to the heat capacitance of the vapor phase in the vicinity of the boiling point due to the D_2O content of this phase is

$$-d(LP/P^*)/d\Delta\theta = L^2/R\theta_{bp}^2 e^{[-L\Delta\theta/R\theta_{bp}^2]} \tag{7}$$

where $\Delta\theta$ is the temperature displacement from the boiling point. This heat capacitance is *ca* 67 times larger than that of equivalent gas space filled with oxygen and hydrogen and, therefore, *ca* 380 times larger than the heat capacitance due to these gases for the actual working conditions at the start of day 68.

in the NHE. Analyses may be calculated for low to intermediate temperatures using the parameter listing supplied with the instruments, i.e., the changes required were not made. (It also appears that the latent enthalpy of evaporation was not corrected for changes in temperature.) The consequent errors are sufficiently small that they do not invalidate the analyses. However, the values of the rates of evaporative enthalpy loss contained in the $(k'_R)_{11}$-spreadsheets of the NHE analyses for temperatures close to the boiling point cannot be calculated with any values of the parameters close to those contained in the listing supplied with the instruments. This matter has not been investigated further as it is in any event necessary to make three further changes if experiment cycles close to the boiling point are to be evaluated.

[7]It should be noted that the ICARUS-2 system was supplied with the means for the continuous recording of the barometric pressure, but this facility was evidently disabled following the installation of the system.

This marked increase in the heat capacitance of the part of the cell filled with gas and D_2O vapor has two consequences. In the first place, the heat transfer across the vacuum gap must be maintained at the same value as that which applies to the liquid phase.[8] Secondly, the radiative output across the section of the Dewar Cells filled with vapor must be balanced by the condensation of an amount of vapor sufficient to supply the radiative enthalpy.

A first approximation for the rate of reflux in the cell is

$$\text{rate of reflux} = (k'_R)_{12} f_1(\theta) \Sigma \Delta M / L \Delta t M^0 \tag{8}$$

where ΔM is amount of D_2O evaporated in each measurement interval, Δt. Equation (7) represents an upper limit for this extent of reflux since we are neglecting the heat transfer to the walls by the deuterium and oxygen in the gas space as well as the effects of the reheating of this gas space by the liquid in the lower section of the calorimeter.[9]

It will be evident that analyses based on the use of Eqs. (5–7) can only be approximations. Two of the most obvious deficiencies are the use of dilute solution theory in the interpretation and the neglect of hydrostatic pressure on the boiling points used in the Clausius–Clapeyron equation. It follows, therefore, that a part of the analyses of the raw data for the episodes of cells being driven to dryness should be based on assumptions which are independent of the use of Eqs (5–7). These matters are considered further in vol. II/5.0.

I/5.0 Heat Transfer Coefficients: Definition and evaluation.

The heat transfer coefficients will be described by the suffices used previously, i.e. $(k'_R)_{i,j,l}$ where $i = 1, 2, 3$ denotes differential, backward integration and forward integration, j is defined at appropriate points below and $l = 1, 2$ denotes lower bound and true coefficients, respectively. The simplest starting point is to assume that there is no excess enthalpy generation in the system i.e., $Q_f(t) = 0$ in Eq. (1) and to evaluate a lower bound heat transfer coefficient (i.e., a coefficient which assumes that the rate of excess enthalpy generation is zero) at a time just

[8]Independent calibrations show that the heat transfer coefficient for cells filled with air are about 0.75 of the values of these coefficients for cells filled with liquid [3, 4]. It follows therefore that the marked increase in the heat capacitance of the cells filled with D_2O vapor at temperatures close to the boiling point must lead to the maintenance of the heat transfer coefficient at the value which applies to cells filled with liquid.

[9]The group at the NHE laboratories attempted to determine the values of ΔM directly by adding a condensation section to the cells. It was difficult to see how anybody could convince themselves that such measurements could give meaningful results. One would at best have derived information about the reflux ratio, a quantity which does not give any useful information about the rate of excess enthalpy generation. The only useable information is the detection of the time at which the cells are driven to dryness. However, this time can be determined directly from raw data by noting the fall in the cell current or by direct visual observation.

before the end of the calibration pulse, $t = t_2$:

$$(k'_R)_1 = \frac{[E_c(t) - E_{th,b}]I - \Delta H_{ev}(t) - C_pM(d\Delta\theta/dt)}{f_1(\theta)} \tag{9}$$

where $f_1(\theta) = [\theta_b + \Delta\theta(t)]^4 - \theta^4$ is the temperature function.

This, Eq. (9), was the first heat transfer coefficient used in our investigations; hence, the designation $(k'_R)_1$. It should be noted that this designation should really be changed so as to be consistent with the definition (8), but this will not be done principally because the definition (10) was subsequently extended to any part of the measurement cycle, the coefficient being designated $(k'_R)_{11}$.[10]

Having obtained $(k'_R)_{11}$, it is frequently desirable to establish the 11-point averages $(\overline{k'_R})_{11}$ so as to decrease the noise.[11] Such averaging gives *ca* 26 independent values for measurement cycles lasting 1 day, or better *ca* 52 values for the recommended 2-day cycles. In turn, it is useful to evaluate the 6-point averages of $(\overline{k'_R})_{11}$ which have been designated as $(\overline{\overline{k'_R}})_{11}$. It is not useful to extend this averaging beyond 6 points, because any such extension makes the systematic errors (due to the residual decrease of $(k'_R)_{11}$ with time) larger than the random errors.

I/5.1 Determination of C_pM.

It is apparent from Eq. (10) that we need accurate values of C_pM to make $(k'_R)_{11}$ generally useful.[12] A first approach to the determination of the value of C_pM for any given cell is to rearrange Eq. (8) to the straight line form

$$y = mx + c \tag{10}$$

i.e.,

$$\frac{[E_c(t) - E_{th,b}]I - \Delta H_{ev}(t)}{f_1(\theta)} = \frac{C_pM(d\Delta\theta/dt)}{f_1(\theta)} + (k'_R)_{1,j,1} \tag{11}$$

and to derive then approximate values of C_pM from the slopes of the plots in regions where the temperature is varying relatively rapidly with time. We can distinguish four such plots designated by the relevant derived heat transfer coefficients $(k'^{,0}_R)_{151}$, $(k'^{,0}_R)_{161}$ $(k'^{,0}_R)_{171}$, and $(k'^{,0}_R)_{181}$ according to whether the

[10] We should perhaps change this designation of $(k'_R)_{101}$ to denote $i = 1$, differential; $j = 0$, any part of the measurement cycle; $l = 1$, lower bound; but the description $(k'_R)_{11}$ will be retained as it has been used extensively in earlier reports and papers.

[11] Other averages can be made but the use of the 11-point average has been found to be especially useful.

[12] It is apparent that the group at NHE retained the value of C_pM specified in the parameter listing rather than to determine the correct value and to substitute this corrected value in the listing.

fitting of Eq. (10) is carried out at times somewhat above the origin, at times somewhat above t_1 (the time of application of the calibration pulse), at times somewhat above t_2 (the time of cessation of the calibration pulse), or by the combination of the last two time regions, see Fig. 2.[13]

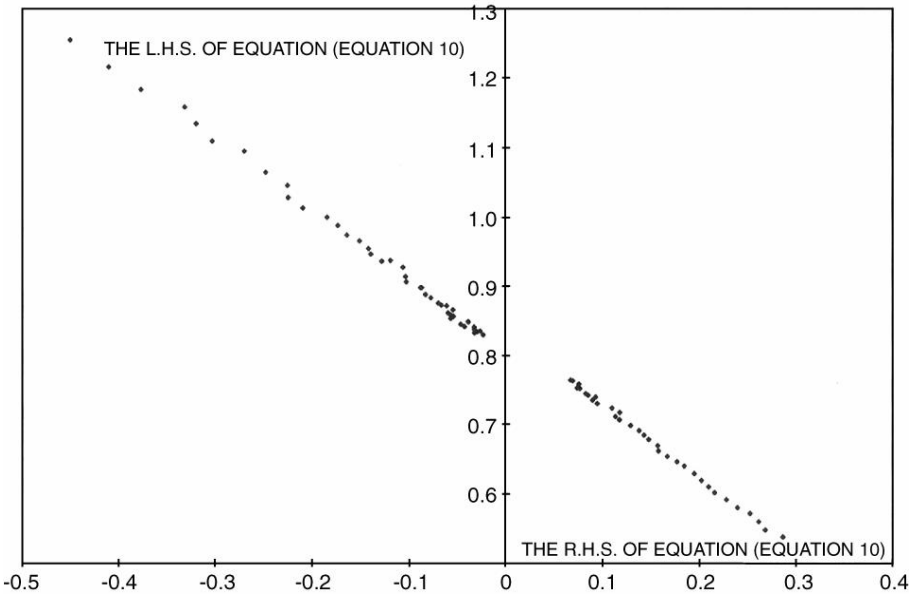

Fig. 2. Evaluation of $(k'_R)_{181}$ and C_pM according to Eq. (10).

It should be noted that $(k'^{,0}_R)_{151}$ cannot be evaluated systematically for experiment Mc–21 because of the irregular schedule of the addition of D_2O (see vol. II/1.3). Evaluations of $(k'^{,0}_R)_{161}$, $(k'^{,0}_R)_{171}$ and $(k'^{,0}_R)_{181}$ for the important data set for day 3 are markedly degraded due to the early onset of positive feedback, see vol. II/1.3. The procedure based on Eq. (10) has limited precision because of the need to differentiate the inherently noisy experimental data. It is therefore necessary to carry out the fitting procedures over extended regions of the abscissae, $(d\Delta\theta/dt)/f_1(\theta)$, so that the data are inevitably affected by the onset of the positive feedback detected for the operation of the cell on that day.

In this connection, it should also be noted that separate investigations have shown that $(d\Delta\theta/dt)$ is best estimated by using the second order central differences (i.e., the chords of the curves). More accurate values could be derived in principle by using higher order differences. However, in practice, the repeated differentiation of the experimental data (implicit when using higher order differences) leads to an increase in noise if we use differences higher than the second

[13]However, there is a measure of ambiguity about the interpretation of the values of $(k'^{,0}_R)_{1,j,1}$ derived, which is discussed in vol. II of this report.

order.[14]

In the absence of sufficiently precise determinations of C_pM, the evaluations must necessarily be restricted to regions of time where the contribution of the term $C_pM(d\Delta\theta/dt)/f_1(\theta)$ is adequately small. In that case, it is adequate to use a "guesstimate" of C_pM. This matter (including the evaluation of a "guesstimate" of C_pM) is considered further in vol. II/2.0. It is next necessary to evaluate a true differential heat transfer coefficient. The simplest procedure, giving $(k'_R)_2$ near the end of the calibration period at time t = t_2, is obtained by including the calibration pulse,[15] ΔQ:

$$(k'_R)_2 = \frac{\Delta Q + [E_c(\Delta\theta_2, t_2) - E_c(\Delta\theta_1, t_2]I}{f_2(\theta)}$$

$$- \frac{\Delta H_{ev}(\Delta\theta_2, t_2) + \Delta H_{ev}(\theta_1, t_2) - C_pM[(d\Delta\theta/dt)_{\Delta\theta_2,t_2} - (d\Delta\theta/dt)_{\Delta\theta_1,t_2}]}{f_2(\theta)} \tag{12}$$

where we now have

$$f_2(\theta) = [\theta_b + (\Delta\theta_2, t_2)]^4 - [\theta_b + (\Delta\theta_1, t_2)]^4 \tag{13}$$

In order to carry out such evaluations, it is useful to construct A.4- or A.3-sized plots of the raw data and then to obtain appropriate averages by using a transparent ruler. This type of analysis used to be a generally accepted approach but then fell into disrepute. However, the methodology is now again accepted giving so-called robust estimates.

I/5.2 Precision and accuracy – differential coefficients.

It may be noted that the errors in $(k'_R)_2$ are measures of the accuracy of the true heat transfer coefficient as the estimates are made in terms of the known Joule enthalpy input to the calibration heater. Errors in $(k'_R)_1$ or $(k'_R)_{11}$ are measures of the precision of the lower bound heat transfer coefficients as there is no independent calibration and there may be excess enthalpy generation in the system. It is important that $(k'_R)_{11}$ and $(k'_R)_2$ are the least precise and least accurate coefficients which can be obtained from the raw data. Statements that the errors are larger than this (e.g., see [5]) simply show that mistakes have been made in the data analysis procedures and/or the execution of the experiments.

We have always insisted that the construction and evaluation of plots of the raw data is an essential prerequisite of the more elaborate data evaluation

[14] Objections have often been raised to the procedures which we have adopted based on the fact that we have not "binned the data," i.e., we have not signal averaged before the data analysis. However, "binning of the data" must always be approached with great caution: one should only "bin data" or "bin coefficients" if these data or coefficients are to be expected to be constant over the averaging interval. This is not the case for $(k'_R)_{11}$ unless the effects of the term $C_pM(d\Delta\theta/dt)$ have been taken into account. Once this is done we can, of course, bin the coefficients as we have done in deriving $\overline{(k'_R)}_{11}$ and $\overline{\overline{(k'_R)}}_{11}$ [as well as $(k'_R)_{181}$].

[15] $(k'_R)_2$ was the second heat transfer coefficient used in our investigations.

procedures. For one thing, it shows whether the noise levels in the experiments were sufficiently low to justify more detailed evaluations and also points to malfunctions in the experiments. It also shows immediately whether the $\theta - t$ and $E_c - t$ transients have relaxed sufficiently to permit the evaluation of $(k'_R)_1$ and $(k'_R)_2$. Furthermore, it gives immediate indications of the presence (or absence) of positive feedback. As has been pointed out repeatedly all calibration procedures require that the rate of excess enthalpy generation, $Q_f(t)$, be constant during the calibration periods. These matters are considered further in the main text, vol. II/2.0 and vol. II/3.0.

Having obtained the true heat transfer coefficient at a single point (usually near the end of the calibration pulse, $t = t_2$) it is important to ask: what is the true heat transfer coefficient, $(k'_R)_{12}$, at any other time? We can make such an evaluation within the duration $t_1 < t < t_2$ of the calibration pulse simply by using Eq. (11) giving $(k'_R)_{12}$ rather than $(k'_R)_2$. Note also that Eq. (11) can be rearranged to the straight line form

$$\frac{\Delta Q + [E_c(\Delta\theta_2, t) - E_c(\Delta\theta_1, t)]I - \Delta H_{ev}(\Delta\theta_2, t) + \Delta H_{ev}(\Delta\theta_1, t)}{f_2(\theta)}$$

$$= \frac{C_p M[(d\Delta\theta)/dt)_{\Delta\theta_2,t} - (d\Delta\theta/dt)_{\Delta\theta_1,t}]}{f_2(\theta)} + (k_R^{\prime,0})_{162} \qquad (14)$$

which is applicable at times close to and above t_1. It is evident, therefore, that such plots can also be used to obtain estimates of $C_p M$, but the accuracy of such values is inevitably much lower than the precision of those obtained by the application of the corresponding expression for the lower bound heat transfer coefficient, $(k'_R)_{161}$, Eq. (10). Nevertheless, Eq. (11) is useful because it allows the removal of the effects of the water equivalent, $C_p M$, on the true heat transfer coefficient, $(k_R^{\prime,0})_{162}$, simply by extrapolating to zero value of the abscissa. However, the time corresponding to this point will not be accessible experimentally for calibrations carried out with a calibration pulse of 6-hour duration for polarizations carried out at low cell currents (although this time is probably close to $t = t_2$).[16]

In the regions in which there is no application of a heater pulse, i.e., for $0 < t < t_1$ and $t_2 < t < T$, the true heat transfer coefficient can only be obtained from the heating and cooling curves, i.e. the driving force is the change in the enthalpy content of the calorimeters rather that ΔQ. It is now sensible to cast Eq. (11) in the form

[16] A similar comment applies to the determination of $(k'^{,0_R})_{161}$: the time at which $(d\Delta\theta/dt = 0)$ will usually be accessible to experiments in which $t_1 = 9$ hours. However, no such point can be defined for $(k'^{,0_R})_{171}$ so that this determination is mathematically questionable. This is therefore equally true for $(k'^{,0_R})_{181}$, although these extrapolations are certainly sound from an operational point of view.

$$\frac{C_p M[(d\Delta\theta/dt)_{\Delta\theta_2,t} - (d\Delta\theta/dt)_{\Delta\theta_1,t}]}{f_2(\theta)} =$$

$$-(k_R^{\prime,0})_{152} + \frac{[E_c(\Delta\theta_2,t) - E_c(\Delta\theta_1,t)]I - \Delta H_{ev}(\Delta\theta_2,t) + \Delta H_{ev}(\Delta\theta_1,t)}{f_2(\theta)} \quad (15)$$

(same for $(k_R^{\prime,0})_{172}$.)

If the system is functioning correctly, then it will be found that the L.H.S. of Eq. (14) is essentially constant (although this constancy can only be probed over a short time range). The second term on the R.H.S. of Eq. (14) will be much smaller than the term on the L.H.S., i.e. it is in the nature of a correction term to give point-by-point values of $(k_R^{\prime,0})_{152}$ or $(k_R^{\prime,0})_{172}$. It will be evident that the accuracy of these versions of the true heat transfer coefficient is limited by the accuracy of the estimates of $C_p M$. This particular part of the methodology is therefore only useful to serve as a check on the operation of the cells and methods of data evaluation. Furthermore, it is not possible to apply Eq. (14) systematically to the time region $0 < t < t_1$ for experiment Mc–21 in view of the irregular schedule of addition of D_2O to the cell.[17]

The assumption underlying this part of the account presented in this report is that we can only determine $(k'_R)_{12}$ within the duration of the calibration pulse $t_1 < t < t_2$, Fig. 3, and, at a lower accuracy, $(k_R^{\prime,0})_{152}$ and $(k_R^{\prime,0})_{172}$ in regions adjacent to the origin and for times adjacent and above t_2 respectively. However, this conclusion is incorrect. We need to make the additional assumption that the rate of any excess enthalpy generation is constant during any particular calibration period in order to determine $(k'_R)_{12}$.

This means that we can only obtain a single value of this heat transfer coefficient per calibration period and, consequently, a single value of $[(k'_R)_{12} - (k'_R)_{11}]$. Two important points follow from this conclusion. In the first place, the precision of $(k'_R)_{12}$ must be very nearly equal to the precision of $(k'_R)_{11}$. Secondly, and related to the first point, we see that if we extend the assumption that the rate of excess enthalpy production is constant during the period $t_1 < t < t_2$ to saying that it is constant for the whole measurement cycle, $0 < t < T$, then it is immediately possible to derive $(k'_R)_{12}$ over the whole of this cycle. Thus, if the difference between the true and lower bound heat transfer coefficients can be established at any one time [say, $\Delta(k'_R)_t$ at time t_2], then $[k'_R(t)]_{12}$ at any other time t will be given by

$$[k'_R(t)]_{12} = [k'_R)(t)]_{11} + \Delta(k'_R)_{t_2} \frac{f_1(\theta)_{t_2}}{f_1(\theta)_{t_1}} \quad (16)$$

The ratio $f_1(\theta)_{t_2}/f_1(\theta)_2$ is of order unity, which implies that the shift $(k'_R)_{l2} - (k'_R)_{11}$ is always close to that at the calibration point.

[17] As has been noted previously (cf vol. II), we have been unable to combine data in the regions just above t_1 and t_2 to give a simple equation leading to $(k_R^{\prime,0})_{182}$.

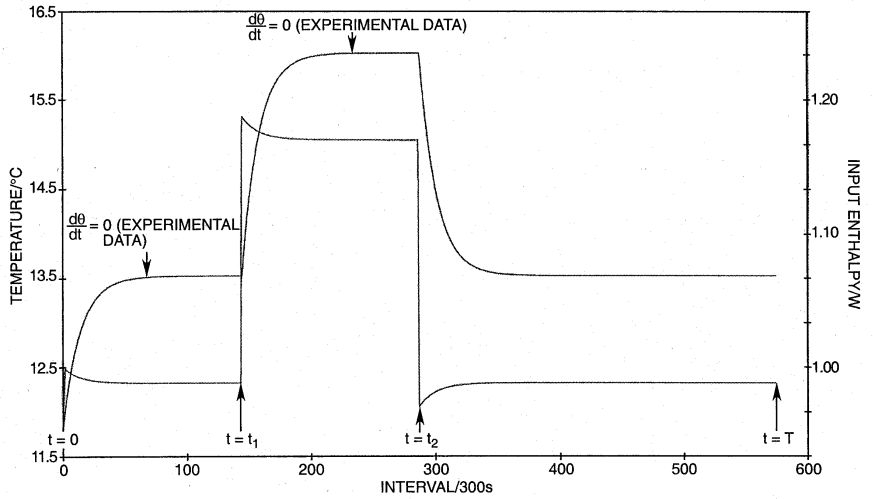

Fig. 3. Schematic of methodology used in calorimeter calibrating.

Equation (15) shows that the precision of $(k'_R)_{12}$ is very nearly equal to the precision of $(k'_R)_{11}$.[18] It follows that changes in the rates of excess enthalpy production can be established at the same level of precision as that of $(k'_R)_{11}$. The same comments apply to the precision of the true heat transfer coefficient, $(k'_R)_{22}$ relative to that of the lower bound heat transfer coefficient, $(k'_R)_{21}$, which is discussed below. In consequence, the changes in the rates of excess enthalpy production can be established with relative errors $< 0.01\%$, and these errors determine the level of significance with which such changes can be discussed. Of course, the accuracy of the true heat transfer coefficients remains determined by the errors of differences such as that of $[(k'_R)_{12} - (k'_R)_{11}]$.

It is important here to stress once again that any attempt to calculate the variation of rates of excess enthalpy generation within the measurement cycles must also pay due regard to the fact that it is not possible to calibrate the systems if the rate of excess enthalpy generation varies with time. It is also important that this comment applies equally to any calorimetric system which we might wish to use. If the rate of excess enthalpy generation does, in fact, vary with time, then $\Delta(k'_R)$ must be derived from separate experiments. This is the situation which applies to experiment Mc–21 as is discussed in vol. II/2.0 and vol. II/3.0. The comments made in this part of vol. I/5.0 should be read in conjunction with vol. II of this report.

The discussion of the accuracy of true heat transfer coefficients versus the pre-

[18]The validity of Eq. 15 was established at the time of construction of the ICARUS-2 system.

cision of the lower bound heat transfer coefficients prompted our search for methods that would increase both the precision and accuracy. The reason for the limited precision of $(k'_R)_{11}$ and accuracy of $(k'_R)_{12}$ is mainly due to the need to differentiate noisy experimental data sets in order to derive $C_pM(d\Delta\theta/dt)$.

I/5.3 Precision and accuracy – integral coefficients.

If we wish to avoid the numerical differentiation of the experimental data sets, then we can rely instead on the numerical integrations of these data and compare these to the integrals of the differential equation representing the model of the calorimeters. For the backward integrals starting from the end of the measurement cycles at $t = T$, we obtain

$$(k'_R)_{21} = \frac{\int_T^t \Delta H_{net}(\tau)d\tau}{\int_T^t f_1(\theta)d\tau} - \frac{C_pM[\Delta\theta(t) - \Delta\theta(T)]}{\int_T^t f_1(\theta)d\tau} \tag{17}$$

while the corresponding equation for forward integration from the start of the measurement cycle is

$$(k'_R)_{31} = \frac{\int_0^t \Delta H_{net}(\tau)d\tau}{\int_0^t f_1(\theta)d\tau} - \frac{C_pM[\Delta\theta(t) - \Delta\theta(0)]}{f_1(\theta)d\tau} \tag{18}$$

Here, the suffices 21 and 31 denote respectively backward integration, lower bound and forward integration, lower bound. $(k'_R)_{21}$ and $(k'_R)_{31}$ are the corresponding integral heat transfer coefficients defined at time t. We have to take note of the fact that care is needed when integrating the terms $f_1(\theta)$ and net enthalpy input, $\Delta H_{net}(\tau)$, around the discontinuities at $t = t_1$ and $t = t_2$ (also the times $t = 0$ and $t = T$ if the range of the integrations is extended).[19] It may be noted that the only straightforward way in which we can integrate around the discontinuities at $t = t_1$ and $t = t_2$ is by means of the trapezium rule and this is the method which has been used in the recalculations presented in this report. If the times of application and cessation of the heater calibration pulses correspond exactly to t_1 and t_2 respectively, then we can carry out the integrations around the discontinuities by inserting extra data points at these times. It appears that the data sets in experiment Mc–21 satisfy this criterion although this is not generally true for all experiments carried out with the ICARUS-2 system; lack of synchronization of the calibration pulses with t_1 and t_2 appeared to be generally true for measurements with the ICARUS–1 systems. In that case, it is necessary to determine these times separately (this can be done adequately from the $\theta - t$ plots) so as to establish the integration intervals and it is then

[19] At different times, the trapezium rule, Simpson's rule or the mid-point rule have been used to carry out the integrations. Of these rules, only the mid-point rule is strictly speaking correct in that it agrees with the mathematical definition of an integral. It is quite generally assumed that integrations carried out using the trapezium or Simpson's rule will converge onto the correct algebraic result if the integration interval is made adequately small, but this does not necessarily follow. This is a matter which needs to be investigated for each particular case.

necessary to insert four additional data points.[20]

The adequacy (or inadequacy) of the particular integration procedures coupled to the adequacy of the chosen integration interval is revealed more clearly when we come to the use of Eqs. (16) and (17) to determine C_pM and to carry out extrapolations to remove the effects of the second term on the R.H.S. of these equations on the corresponding heat transfer coefficients. The procedure set out in the handbook for the ICARUS-1 System [2, 2A] restricted the integrations to the time region of the application of the heater calibration pulse. For backward integration, we obtain

$$\frac{\int_{t_2}^{t} \Delta H_{net}(\tau)d\tau}{\int_{t_2}^{t} f_1(\theta)d\tau} = \frac{C_pM[\Delta\theta(t) - \Delta\theta(t_2)]}{\int_{t_2}^{t} f_1(\theta)d\tau} + (k_R^{\prime,0})_{261} \tag{19}$$

while for forward integration, we obtain

$$\frac{\int_{t_1}^{t} \Delta H_{net}(\tau)d\tau}{\int_{t_1}^{t} f_1(\theta)d\tau} = \frac{C_pM[\Delta\theta(t) - \Delta\theta(t_2)]}{\int_{t_1}^{t} f_1(\theta)d\tau} + (k_R^{\prime,0})_{361}. \tag{20}$$

Equation (18) can be used to derive accurate values of C_pM while there is some minor degradation when using forward integration, Eq. (19). The application of Eq. (18) to the data sets was the target methodology of the ICARUS systems (e.g., see [2, 2A]) and the derived lower bound heat transfer coefficient, $(k_R^{\prime,0})_{261}$, was described as $(k_R')_{21}$ in the Handbook and the associated correspondence. We have since then used the more extended description, $(k_R^{\prime,0})_{261}$, to denote the fact that with $j = 6$, we are carrying out the evaluation in the time region $t_1 < t < t_2$. The same types of evaluation may be used to derive $(k_R^{\prime,0})_{251}$, $(k_R^{\prime,0})_{271}$, and $(k_R^{\prime,0})_{281}$ as well as $(k_R^{\prime,0})_{351}$, $(k_R^{\prime,0})_{371}$ and $(k_R^{\prime,0})_{381}$. It is only necessary to start the integrations from the appropriate times which also give the starting values of θ for the R.H.S. of the relevant equations. Of these sets of estimates, that leading to $(k_R^{\prime,0})_{281}$ is especially useful and this particular fit also gives good estimates of C_pM. However, it should be noted that it is necessary to use care in applying these procedures to the data for day 3 of experiment Mc–21 because of the early onset of positive feedback, see vol. II/2.0.

In order to obtain the true heat transfer coefficients it is necessary to combine the integrals of the enthalpy inputs in Eqs. (18) and (19) with thermal balances made at one or a series of points. This can be done in a number of ways and it is important that this part of the evaluation [2, 2A] was changed in the

[20]The evaluations of $(k_R')_{21}$ and $(k_R')_{22}$ (see below) and of $(k_R')_{31}$ and $(k_R')_{32}$ (see also below) were to have been carried out using $(k_R')_{21}$ and $(k_R')_{31}$ spreadsheets produced by the software. As we have never had access to these spreadsheets (if, in fact, they were ever produced), we cannot now establish whether the integrations around the discontinuities were carried out correctly, although we believe that they must have been in error. In any event, all the integrations used in the evaluations described in this report have been carried out using the raw data.

summer of 1994 following the receipt of the first two sets of data collected by NHE. Attention will be confined here to the procedure originally suggested in the Handbook for the ICARUS-1 system [2, 2A].[21] We make a thermal balance just before the application of the calibration pulse and, if the system has relaxed adequately and if $d\theta/dt = 0$, then if we consider $(k'_R)_{32}$,

$$0 = \Delta H_{net}(t_1)[t - t_1] + Q_f[t - t_1] - (k'_R)_{32}[(\theta_b + \Delta\theta(t_1))^4 - \theta_b^4][t - t_1] \quad (21)$$

combination with Eq. (14) eliminates the unknown rate of excess enthalpy generation. We obtain

$$(k'_R)_{32} = \frac{\int_{t_1}^{t} \Delta H_{net}(\tau)d\tau - \Delta H_{net}(t_1)(t - t_1)}{\int_{t_1}^{t} f_2(\theta)d\tau} - \frac{C_pM[\Delta\theta(t) - \Delta\theta(t_1)]}{\int_{t_1}^{t} f_2(\theta)d\tau}. \quad (22)$$

The corresponding equation for $(k'_R)_{22}$ follows from Eq. (21) on replacing t_1 by t_2. (see Eq. (22) below).[22]

It is convenient also to rewrite the derived equation for $(k'_R)_{22}$ in the "straight line form"

$$\frac{\int_{t_2}^{t} \Delta H_{net}(\tau)d\tau - \Delta H_{net}(t_2)(t - t_2)}{\int_{t_2}^{t} f_2(\theta)d\tau} = \frac{C_pM[\Delta\theta(t) - \Delta\theta(t_2)]}{\int_{t_2}^{t} f_2(\theta)d\tau} + (k'^{,0}_R)_{262} \quad (23)$$

$(k'_R)_{22}$ and $(k'^{,0}_R)_{262}$ were the versions of the true heat transfer coefficient that we used in our investigations prior to the construction of the ICARUS–1 system. As we did not wish to discuss the differences between $(k'_R)_{32}$, $(k'^{,0}_R)_{362}$, $(k'_R)_{22}$ and $(k'^{,0}_R)_{262}$, and, as we expected $(k'_R)_{32}$ to converge onto $(k'_R)_{22}$ for the specified 2-day measurement cycles (within the error limits specified for the ICARUS-1 system) we also labelled $(k'_R)_{32}$ as $(k'_R)_{22}$ [23].

It should be noted that the extrapolation (21) automatically removes the effect of the term $C_pM[\theta(t) - \theta(t_2)]/\int_{t_2}^{t} f_2(\theta)d\tau$ on the true heat transfer coefficient. This application of Eq. (21) (and of $(k'_R)_{22}$ evaluated close to the mid-point $t = t_2$) was one of the major objectives for our methodology because C_pM is the least accurate parameter in the analysis.

While it is also possible to write Eq. (21) in the form (22) to give $(k'^{,0}_R)_{362}$, this method of analysis is not useful as the range of the extrapolation required is

[21] It is in any event necessary to change the methodology of the evaluation in view of the early onset of "positive feedback"(II/3.0).

[22] We note again that the group at NHE did not follow the instruction in the ICARUS-1 Handbook [2, 2A] to use measurement cycles of 2-day duration and, for the reduced time scales of 1-day cycles in particular, it is necessary to include the term $C_pM(d\Delta\theta/dt)$ in the thermal balances, Eq. (18). However, the group at NHE continued to use the original form of the equation. It also appears that NHE did not follow the instruction [2, 2A] to evaluate $(k'_R)_{32}$ at times close to t_2. This matter is discussed further in vol. II/3.0.

[23] We retained the designation 22 as a flag to indicate the backward integration methodology was the primary objective for accurate evaluations

too long [2, 2A] (see also vol. II). For this reason, it was recommended in the ICARUS-1 Handbook [2, 2A] that $(k'_R)_{32}$ should be evaluated at times close to $t = t_2$ using values of C_pM determined from applications of Eq. (19). However, in view of the errors in the determination of C_pM, these values of $(k'_R)_{32}$ are inevitably less accurate than those of $(k'_R)_{22}$ or $(k'_R)_{262}$ (see also vol. II/3.0).[24]

We should observe furthermore that Eq. (21) is soundly based (in a mathematical sense) in that the extrapolation to $[\Delta\theta(t) - \Delta\theta(t_2)] = 0$ gives the value of $(k'^{,0}_R)_{262}$ at a well defined time, $t = t_2$. This is equally true of all of the coefficients based on forward or backward integration; however, the starting points for these integrations will usually be chosen to be $t = 0$, $t = t_1$ or $t = T$ and the definition of the heat transfer coefficients at these points is not generally useful. The exception here is the lower bound heat transfer coefficient, $(k'^{,0}_R)_{261}$ which is also defined at time $t = t_2$. We observe also that $(k'^{,0}_R)_{261}$ and $(k'^{,0}_R)_{262}$ are the most precise and accurate values of the lower bound and true heat transfer coefficients which can be derived with the methodology as presently developed. Furthermore, $(k'^{,0}_R)_{261} = (k'_R)_{11}$ at $t = t_2$ and $(k'^{,0}_R)_{262} = (k'_R)_{12}$ at $t = t_2$, so that the best value of $\Delta(k'_R)_t$ that can be obtained for use in Eq. (15) is

$$\Delta(k'_R)_t = (k'_R)_{12} - (k'_R)_{11} = (k'^{,0}_R)_{252} - (k'^{,0}_R)_{251} \tag{24}$$

This sound basis of the heat transfer coefficients derived by forward and backward integration should be contrasted with the corresponding position for the differential heat transfer coefficients which has been discussed above.

I/6.0 Time dependence of the heat transfer coefficients.

In the final part of this section, we need to consider somewhat further the time dependence of the various forms of the heat transfer coefficient (compare [6]). We observe first of all that we are interpreting here the systematic variations of typically 0.4% of the differential or 0.2% of the integral coefficients. The only reason why we are able to investigate systematic variations of such small quantities is the very high precision of the methods of data evaluation. We observe secondly, that as the differential coefficients are evaluated at local times, they will show the weak time dependence:

$$(k'_R) = (k'^{,0}_R)[1 - \gamma t] \tag{25}$$

(c.f. Eqs. (3) and (5)). In the definition of the integral heat transfer coefficients given in this section (k'_R) has been regarded as being constant whereas the investigation of the differential heat transfer coefficients shows that we should really include the time dependence, Eq. (24), i.e., we must use Eq. (3) in the integrations. Integration of this equation gives

$$(k'^{,0}_R)\left[\int f_1(\theta)d\tau - \gamma t \int f_1(\theta)d\tau + \gamma \int\int f_1(\theta)d\tau d\tau\right]. \tag{26}$$

[24] We note here also that care must be taken in carrying out the required linear regression fitting procedures as is illustrated in vol. II/3.0.

If we now regard $f_1(\theta)$ as being constant throughout the measurement cycle (which is a rough approximation for the case of the lower bound heat transfer coefficients), then the integral becomes

$$(k'^{,0}_R) f_1(\theta) t[1 - \gamma t/2]. \tag{27}$$

It follows that the heat transfer coefficients given by Eqs (16) and (17) are given by

$$(k'_R)_{21} = (k'^{,0}_R)_{21}[1 + \gamma(T - t)/2] \tag{28}$$

and

$$(k'_R)_{31} = (k'^{,0}_R)_{31}[1 - \gamma t/2] \tag{29}$$

within the limits of this approximation. $(k'^{,0}_R)_{21}$ and $(k'^{,0}_R)_{31}$ are respectively the values of $(k'_R)_{21}$ at $t = T$ and of $(k'_R)_{31}$ at $t = 0$. It follows that the slopes of the plots of $(k'_R)_{21}$ and $(k'_R)_{31}$ versus time are roughly one half of the plot of $(k'_R)_{11}$ versus time.

Equation (24) also shows the way in which we can test whether the characteristics of the Dewar cells can be described by a single, time–independent heat transfer coefficient. Thus, evaluation of $(k'_R)_{21}$ according to Eq. (16) gives us the heat transfer coefficient

$$(k'_R)_{21} = (k'^{,0}_R)_{21} \left[1 - \gamma t + \gamma \frac{\int_T^t \int_T^t f_1(\theta) d\tau d\tau}{\int_T^t f_1(\theta) d\tau} \right] \tag{30}$$

so that the time independent heat transfer coefficient, $(k'^{,0}_R)_{21}$ is readily determined. The fact that heat transfer from the cells can be represented by such a single time independent heat transfer coefficient has been demonstrated several times (e.g. see Fig. 51 of vol. II). Indeed, such representations are the basis of our statement that the integral lower bound heat transfer coefficients can be determined with a precision given by relative errors of less than 0.01%.[25]

The variations of $(k'_R)_{11}$, $(k'_R)_{21}$ and $(k'_R)_{31}$ with time show that this time dependence of the heat transfer coefficients must be taken into account in evaluation of the rates of excess enthalpy generation aiming at the highest achievable accuracy. If this is not done, then the values of the heat transfer coefficients at the mid-points, $t = t_2$, should be used. In that case, the values of the rates of excess enthalpy generation calculated will be slightly too small for $t < t_2$ and slightly too large for $t > t_2$. However, the total excess enthalpy calculated for a complete measurement cycle will be approximately correct.[26] We must also note that the differential heat transfer coefficient, $(k'_R)_{12}$, must be used in the evaluations of the rates of excess enthalpy generation and the integral heat transfer coefficients

[25] Vol. II contains extensive discussions of the errors of the various heat transfer coefficients and the cause of these errors.

[26] This will explain both our strategies for determining the heat transfer coefficients (which give the values at $t = t_2$ as well as giving a further reason for choosing 2-day measurement cycles with t_2 corresponding to the end of day 1.)

in the evaluation of the excess enthalpy (including the total excess enthalpy for complete measurement cycles). In particular, the use of $(k'_R)_{22}$ in the evaluation of the rates of excess enthalpy generation will underestimate these quantities.

I/7.0 Remarks concerning ICARUS-1 data evaluation procedures and experimental protocols.

The modelling of the ICARUS-1 type calorimeters, Fig. 1, has been investigated repeatedly by means of the evaluation of data sets for appropriate blank experiments (using in the main Pt-cathodes polarized in D_2O–based electrolytes). The objective here has been the definition of the appropriate instrument function, which can be accurately defined by Eq. (1).

The next step in this initial phase of the work has been to define a set of heat transfer coefficients that characterize the behavior of the calorimeters and to investigate their precision and accuracy leading up to their use in evaluating the raw data sets of the experimental measurement cycles. The raw data used in these investigations have been both those for the appropriate blank experiments and those generated by simulations of the cell behavior. An illustration of this phase of the investigation has been given in vol. II (see also e.g., [3, 4, 6]).

The outcome of these investigations has been the demonstration that it is useful to determine first of all the time dependence of the differential lower bound heat transfer coefficient, $(k'_R)_{11}$, as well as of the derived means, $(\overline{k'_R})_{11}$ and $(\overline{\overline{k'_R}})_{11}$. However, these coefficients have a limited precision because their evaluation requires the differentiation of the inherently noisy experimental data. Precise and accurate evaluations are therefore best based on the integral lower bound heat transfer coefficient, $(k'_R)_{21}$, and the integral true heat transfer coefficient, $(k'_R)_{22}$, as well as on the values $(k'_R)_{251}$ and $(k'_R)_{252}$ derived in the extrapolation procedures. These extrapolation procedures lead both to the elimination of the effects of the water equivalent, C_pM, on their values as well as to reasonably accurate determinations of C_pM. The differences $(k'_R)_{22} - (k'_R)_{11}$ or $(k'_R)_{252} - (k'_R)_{251}$ between the "true" and lower bound heat transfer coefficients can then be used to define the differential true heat transfer coefficient, $(k'_R)_{12}$.

It has been found that the precision and accuracy of the integral heat transfer coefficients is so high, that it is possible to investigate their systematic variations with time (typically the systematic variations of just 0.4% of their numerical values). Furthermore, it is possible to reduce such data to a single, time independent heat transfer coefficient, e.g., of $(k'^{,0}_R)_{21}$ with relative errors below 0.01 %. This result is hardly surprising. The physics of the calorimeters are quite simple (they are ideal well-stirred tanks) and the errors are mainly those set by the temperature measurements. It is also relatively straightforward to specify the changes which would need to be made to reduce the errors further – say to 0.001% – if that should ever prove to be necessary or desirable.

Although the precision and accuracy of the heat transfer coefficients based on the forward integration procedures, $(k'_R)_{31}$ and $(k'_R)_{32}$, was known to be lower than those based on the backward integrations, $(k'_R)_{21}$ and $(k'_R)_{22}$, the ICARUS-1 methodology was nevertheless based on such forward integrations [2, 2A] because such forward integration was easier to implement and to combine with the evaluations of the data sets. It was anticipated that the extension of the measurement cycles from 1 to 2 days and, in particular of the calibration periods from 6 to 12 hours, would allow the determination of $(k'_R)_{31}$ and $(k'_R)_{32}$ with the required and specified precisions and accuracies [2, 2A]. These changes in the measurement cycles were also expected to facilitate other parts of the investigation such as the determination of the true heat transfer coefficient $(k'_R)_2$. The production of plots of the raw data and the inspection of these plots leading to the graphical evaluation of $(k'_R)_1$ and $(k'_R)_2$ were to be the first step in the data processing. Unfortunately, the protocols laid down in the Handbook for the ICARUS-1 system [2, 2A] were not followed in the experiments carried out by the Group at NHE. Furthermore, following the receipt of the first set of data for experiments carried out in the Sapporo Laboratories, it became clear that there were timing errors in the ICARUS-1 system. These timing errors did not affect the determination of $(k'_R)_{21}$ and $(k'_R)_{22}$. It was therefore recommended that the protocol set down in the Handbook [2] be strictly adhered to, that the preliminary evaluations should be based on $(k'_R)_1$, $(k'_R)_2$, and $(k'_R)_{11}$, and that the final evaluation should be based on $(k'_R)_{21}$, $(k'_R)_{22}$, $(k'_R)_{251}$, and $(k'_R)_{262}$. It is evident that these instructions were ignored.

The development of the various aspects of the data analysis described in vol. I/7.0 is illustrated in part by the analysis of Experiment Mc–21 described in vol. II/3.0. Inevitably, this illustration is incomplete because of the very early development of positive feedback in this experiment.

PART II: APPLICATION OF DIAGNOSTIC CRITERIA.

In part II, we illustrate how the use of a faulty methodology (i.e., the non–standard ICARUS methodology), used by the New Hydrogen Energy (NHE) group, led to an incorrect evaluation of data. An experiment, designated here as Mc–21, provides the required data for the correct/incorrect application of diagnostic criteria developed in part I.

II/1.0 Preliminary descriptions and evaluations.

II/1.1 Experimental set-up.

The cell used in the experiment was of the ICARUS-1 type with the 99.5%Pd + 0.5%B electrode in the form of a rod (4.7 x 20.1 mm), Fig. 1. The electrolyte was 0.1 M $LiOD/D_2O$. The cell was inserted into water thermostats whose temperature was independently controlled by Techne TE–8A stirrer/heater/regulator units. The water thermostats were in turn maintained in a room whose temperature was controlled to within $\pm 2^0$ of that of the thermostats.[27]

The experiment was carried out using an ICARUS-2 type electrochemical polarization, control, and data acquisition system. The electrochemical system consisted of an Hi-Tek DT2101 potentiostat wired up as a galvanostat. These potentiostats/galvanostats are capable of delivering currents of ± 1A at output voltages up to *ca* ± 100V. A separate potentiostat/galvanostat was used to deliver constant currents to the resistive heater used to calibrate the cell. The system was controlled by a 486 data acquisition computer which also controlled an Hewlett Packard 44705A multiplexer and data acquisition system. This data acquisition system was on an IEEE-GPIB bus so that it would be anticipated that there would not have been any timing errors introduced into the measurements.

[27]There are misleading statements about this aspect of the experiment design. This design follows the common strategy of using two thermal impedances in series, a strategy which is required for experiments aiming at high accuracy.

II/1.2 Experimental protocols.

The protocol used for the experiment Mc–21 was as follows:
(i) the electrode was first of all polarized for two days without any application of calibration pulses;
(ii) on the third day (and on all subsequent days including days 68 and 69 when the cell had reached dryness) calibration pulses were applied;
(iii) changes of current density were made frequently. These changes of current density are shown in Fig. 4;
(iv) the cell was topped up with D_2O whenever this was judged to be necessary at the start time of all the measurement cycles; the cell was then left to equilibrate for 9 hours followed by the application of calibration pulses of 6 hour duration; the cell was then again left to equilibrate for a further 9 hours before reaching the next day of the experimental sequence;
(v) as is evident from **(iv)**, the duration of the measurement cycles was 24 hours;

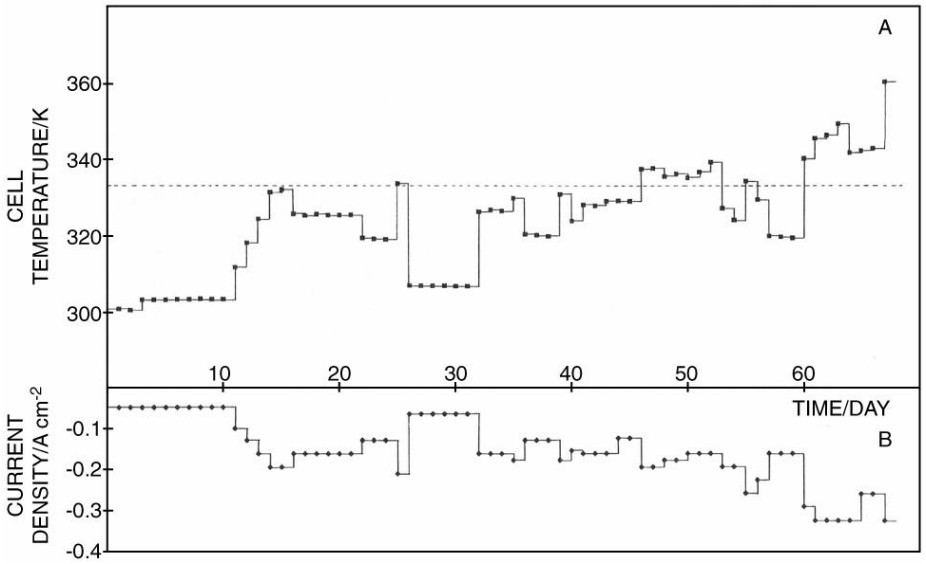

Fig. 4. Cell temperature (A) and current density profiles (B). The dotted lines delineate the regions for the expected onset of positive feedback (A) and excess enthalpy generation (B).

This protocol differs substantially from that specified for the operation of the ICARUS-1 and -2 systems, which was as follows [2, 2A]:
(ia) the electrodes were to be polarized for 4 days (i.e., two measurement cycles, see **(va)** below) without any application of calibration pulses;
(iia) on the 5th day (i.e., for the third measurement cycle) and for 9 further measurement cycles, calibration pulses were to be applied as specified in **(iva)** below; this was to be followed by two further measurement cycles without the

application of calibration pulses and, in turn, by 10 further cycles with calibration pulses. A total experiment duration of 48 days was therefore specified for the initial phase of the work.
(iiia) the initial experiments were to be carried out at a single low current density, typically < 250 mAcm^{-2}; in later experiments a single, low, current density was to be applied for various initial durations followed by a raising of the current density to values typically > 1 Acm^{-2}; this protocol was in broad accord with that used in previous investigations [7, 8]; changes of current density were to be made at the beginning of measurement cycles.
(iva) cells were to be topped up at the start of each measurement cycle; the cells were then to be left to equilibrate for 12 hours and calibration pulses of 12 hour duration were then to be applied; the cells were then again to be left to equilibrate for a further 24 hours so as to reach the start of the next measurement cycle.
(va) as is evident from **(iva)**, the duration of the measurement cycles was to be 48 hours.

We now consider further the major differences between the operation of experiment Mc–21 and the conditions used in previously reported investigations e.g, [1, 7, 8]. Apart from the frequent changes of current density, Fig. 4, we can see that these current densities were mostly in the vicinity of the threshold value required for the onset of the phenomenon of excess enthalpy generation [1]. Furthermore, the cell temperatures were mostly below the level required for the onset of positive feedback, Fig. 4 [9, 10, 11], and which leads to a marked increase in the rates of excess enthalpy generation.[28] The conditions in the cell therefore remained in the vicinity of the region of onset of positive feedback and, under these conditions, we would not expect to see a marked build up in the rate of excess enthalpy generation.

Consideration of Fig. 4 also allows us to decide on the measurement cycles likely to provide examples of "Heat after Death" (objective **(v)** of this investigation). As was pointed out in the original investigation [3, 4] it would be expected that this phenomenon would be observable under several distinct conditions which include
(i) Cell full: cell operated at intermediate temperatures; cell current then reduced in stages
(ii) Cell empty: cell allowed to boil dry; cell then maintained at the rail voltage of the galvanostat
(iii) Cell empty: cell allowed to boil dry; cell disconnected from the galvanostat.

Consideration of the hard copy of the data sets shows that condition **(ii)** applies to part of day 68 of the sequence measurement cycles (see II/7.0) while condition

[28] It has been argued that this phenomenon is linked to the need to achieve high levels of loading of the cathode by D^+, which is probably associated with a change from exo– to endothermic absorption. An alternative explanation is that these phenomena are linked to the formation of a new phase, the γ–phase.

(iii) applies to part of day 69 of this sequence (see II/8.0). Consideration of Fig. 4 shows that condition **(i)** is likely to apply to several of the measurement cycles. The effects would be expected to be most marked for parts of days 25 and 26 (reduction of the cell current from above to below the threshold for excess enthalpy generation; reduction in cell temperature from above the level for the onset of positive feedback to below this level). Attention is confined in this report to this particular day (see II/9.0) although it is evident that there are several further regions of time which might well give examples of "Heat-after-Death" following scenario **(i)**.

II/1.3 Further differences.

In this section we should also consider a further difference between the protocols for experiment Mc–21 and those used in earlier studies, namely, the schedules of addition of D_2O to make up the losses due to electrolysis. The volume of the electrolyte in a cell in an hypothetical experiment carried out first at a cell current of 200 mA for 29 days followed by a cell current of 500 mA and with a daily schedule of additions falls by some 1.21 cm^3 between the two time regions. We can estimate that this would cause a decrease of the mean value of $(k'_R)_{12}$ by *ca* 0.15% or of $(k'_R)_{22}$ by *ca* 0.075%. Such small changes are close to the error limits quoted for the instrumentation and can normally be neglected. However, the magnitude of the changes are above the error limits which can actually be achieved (e.g., see vol. II and I/3.0) and should be taken into account in evaluations carried out at the maximum achievable precision and accuracy.

Figure 5 shows the effects of the schedule of additions as actually used in experiment Mc–21. The exact values of D_2O added were recorded throughout this experiment. It can be seen that the expected changes in $(k'_R)_{12}$ lie between –0.15% and +0.3%, changes which should certainly again be taken into account.

The schedule of additions leads to an important conclusion. We find that by day 67, the total volume of D_2O added was 262.5 ml whereas the total volume electrolyzed was 253.3 ml. It is evident that the volume of D_2O is 3.6% larger then the volume electrolyzed; therefore, there could not have been any recombination of the deuterium and oxygen produced by electrolysis. This is in agreement with earlier measurements [1] and numerous measurements by other authors.

The horizontal lines in Fig. 5 delineate the volumes of D_2O below and above which we would expect the electrolyte level to fall below the base of the silvering in the upper part of the cell, Fig. 1, or to approach the base of the Kel F plug at the top of the cell. It can be seen that the electrolyte level remained within the space defined by this silvered portion throughout the measurement cycles. However, we can see that at long times the electrolyte level must have approached the base of the Kel F plug at the start of several of the measurement cycles following the topping up of the cells. In the work at IMRA-Europe, it was established that such overfilling of the cells leads to an anomalous increase of the pseudo-radiative heat transfer coefficient by 4 to 5% of the values which apply

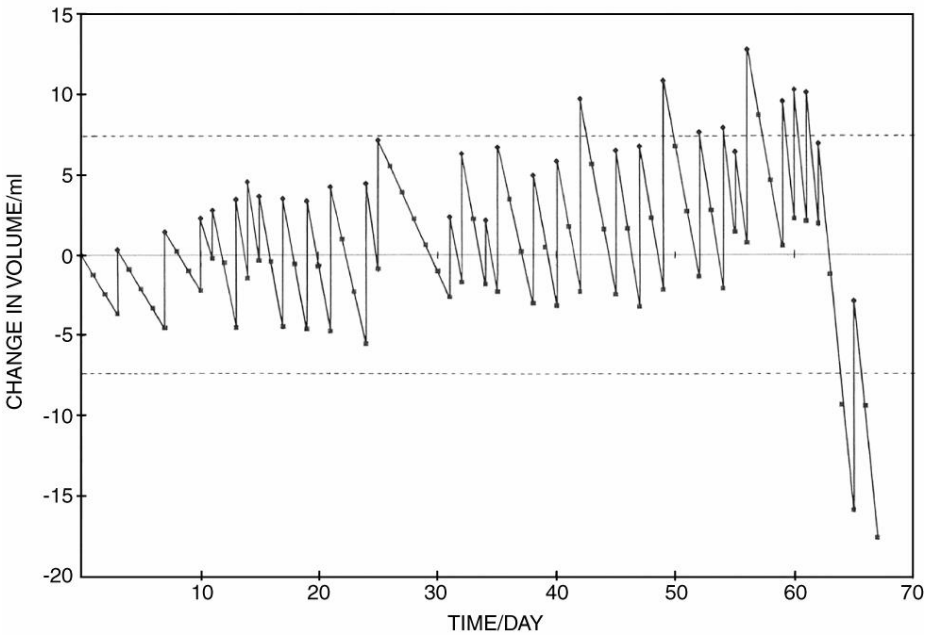

Fig. 5. The changes in the volume of electrolyte. The polarizations were carried out at the current densities shown in Fig. 4.

at the mean level. This increase in (k'_R) is almost certainly due to an increase in the conductive contribution through the Kel F plug to the overall heat transfer from the cell[29](cf. Eq. 4).

II/1.4 Temperature/potential–time profiles.

We also make a number of preliminary assessments of the form of the temperature-time and cell potential-time series for day 3, i.e., the third measurement cycle of the experiment Mc–21, Figs. 6–8. The data for this day are of special importance because the group at NHE have quoted a value of the true heat transfer coefficient as given by their method of evaluation for this day. This value of the true heat transfer coefficient was then used in the evaluation of all the measurement cycles.[30]

[29]This type of behavior applies to day 61, which is a measurement cycle for which we can get important confirmatory evidence of the true heat transfer coefficient which applies to the operation of the cell (see Fig. 20, section II/4.0). Figure 20 shows the expected increase in $(k'_R)_{11}$ at times close to the topping up of the cell.

[30]The evaluation given by NHE is considered further in section II/2.0 while section II/3.0 gives the application of the ICARUS methodology to this particular data set.

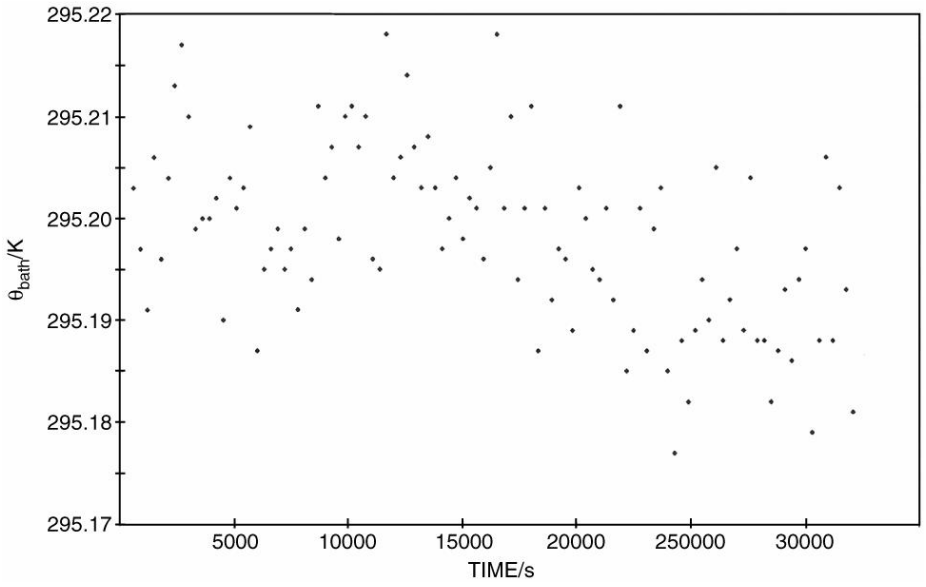

Fig. 6. The temperature of the water bath for the first 32400 s of the first measurement cycle (i.e., the period $0 < t < t_1$). Mean temperature: 295.198 K, $\sigma = 0.0088$ K.

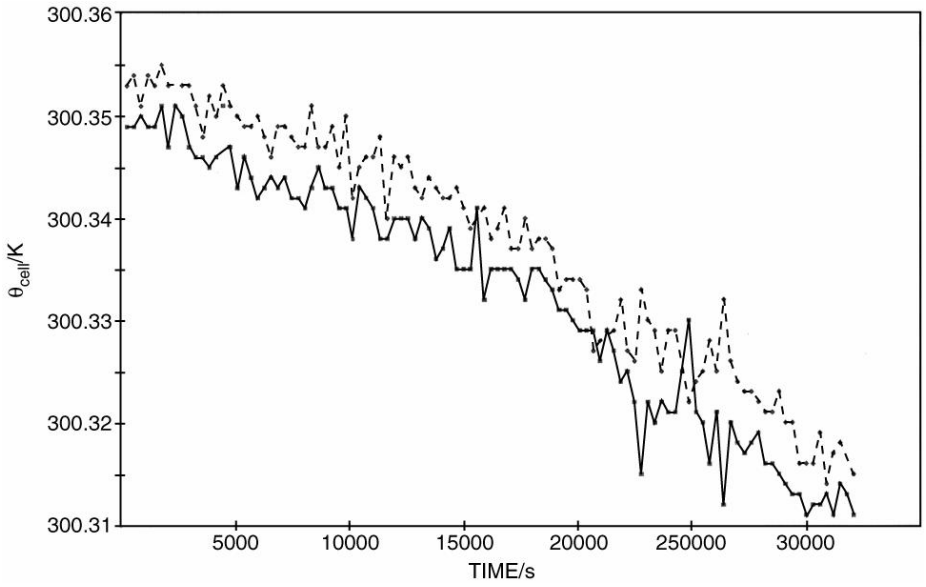

Fig. 7. The cell temperature at the two measurement locations for the first 32400 s of the first measurement cycle ($0 < t < t_1$). Mean temperature difference = 0.0045 K; $\sigma = 0.0027$ K.

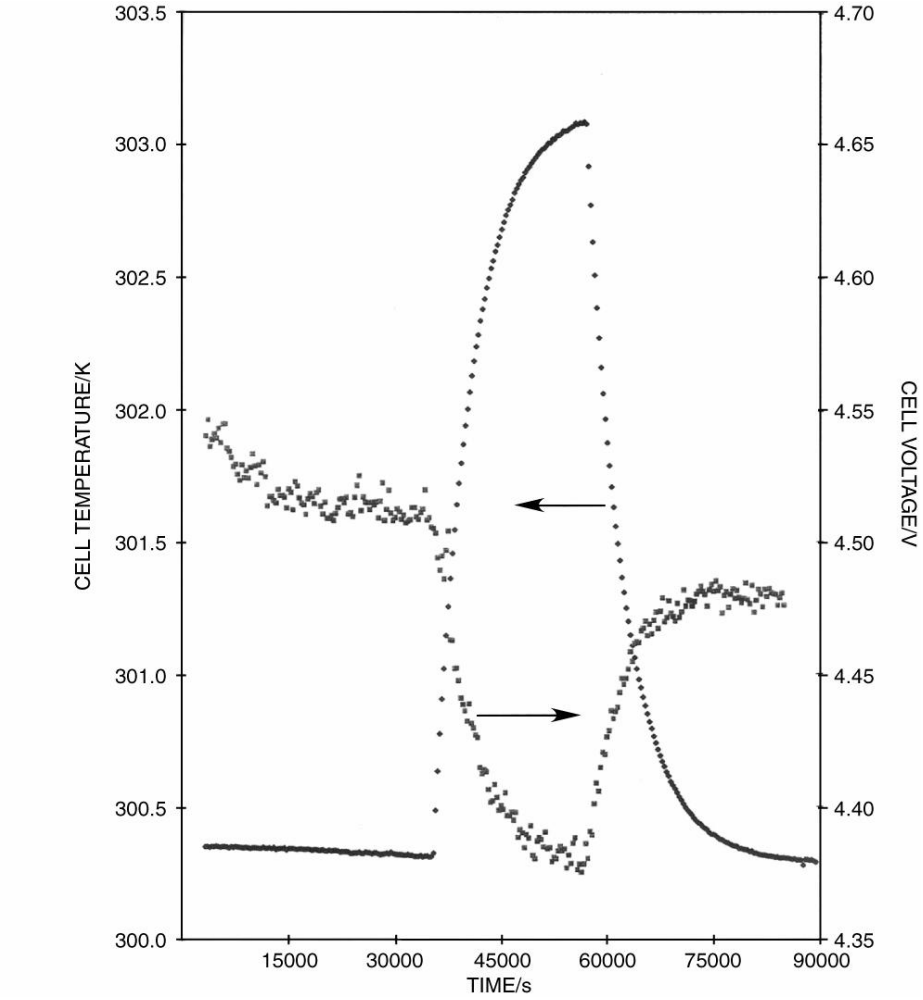

Fig. 8. The raw data – cell temperature and potential as a function of time – for the third measurement cycle.

We can see that we can immediately draw a number of important conclusions. Thus, Fig. 6 gives a plot of the temperature of the water bath versus time for the first 32,400s of the measurement cycle (the period $0 < t < t_1$ preceding the application of the heater calibration pulse) while Fig. 7 gives plots of the cell temperature versus time for the same period and for both positions in the cell where the temperature was measured, see Fig. 1.

It is evident that the noise level of the measurements in the water bath (σ = 0.0088 K, mean = 295.198 K) is much higher than that of the measurements of the cell temperature, Fig. 7. This difference is to be expected because the water bath is controlled by a single thermal impedance whereas the cell is controlled by two impedances in series. At the same time, the noise in the temperature of the water bath is much higher than that in our original measurements (σ = 0.003 K)[6] and, in our experience, such an increase is due to inadequate control of the room temperature.

It is evident that the noise in the measurements of the temperature of the water bath is one factor which limits the precision of the lower bound heat transfer coefficients, $(k'_R)_{11}$, via its effect on the temperature function, $f_1(\theta)$.[31]

It can be seen that the variation with time of the cell temperature measured at the two positions in the cell is systematic, Fig. 7. Moreover, it is clear that there is a systematic difference in temperature between the two positions which must be due to either one or two errors in the calibration.[32] For these measurements, we obtain mean $[\theta_1 - \theta_2]$ = 0.0045 K and $\sigma[\theta_1 - \theta_2]$ = 0.0027 K (subscripts 1 and 2 denote the short and long thermistors). The mean gives an indication of the accuracy in $(k'_R)_{11}$ which we can expect to achieve. The error *ca* 0.05% is somewhat above the target for the precision of the measurements, errors < 0.01%, which is hardly surprising. The standard deviation gives double the value of the expected standard deviation for the measurements with one thermistor. We can see that this value, *ca* 0.00135 K, will not affect the accuracy of the determination of any version of the true heat transfer coefficient. However, we should note that it is evidently desirable to calibrate the thermistors so that we can make the temperature measurements to within ±0.001 K.

[31]The value σ = 0.0088K is outside the range specified for the ICARUS–1 system if measurements are made at low cell temperatures. By contrast, the true heat transfer coefficients are not affected by such fluctuations because the temperature function $f_2(\theta)$ is determined by the cell temperature alone.

[32]Differences in temperature due to inadequate mixing have frequently been invoked in arguments about the performance of ICARUS calorimeters. However, inadequate mixing would not give rise to a systematic and time invariant difference in temperature between the two positions. Moreover, such differences in temperature would not be expected because the thermal relaxation time, $\tau = C_p M/4(k'_R)\theta^3$, is of the order 5000 s whereas the radial and axial mixing times are *ca* 3 and *ca* 20 as revealed by tracer experiments. Small differences in the cell temperature can only be observed in the vicinity of electrodes and calibration resistor, i.e., within the Prandtl boundary layers. However, their volumes are negligibly small compared to the electrolyte volume.

Differences in temperature between those given by the short thermistor and long thermistor will be considered further in section II/6.0 dealing with day 68 as the cell is being driven to dryness and in section II/8.0 dealing with "Heat-after-Death" on day 69. Finally we consider the plots of the raw data for day 3, Fig. 8. We can see immediately the inadequacy of restricting the calibration pulse to 6 hours because the temperature has not relaxed to equilibrium in this time period.[33] However, in this particular case, there is an evident complication because of the very early establishment of positive feedback. This effect can be seen most directly from the delayed relaxation of the temperature to the baseline following the cessation of the heater calibration pulse (the base line is given by the extrapolation of the $\theta - t$ series observed before the application of the calibration pulse). Evidently, the raising of the cell temperature by the calibration pulse has led to an increase in the thermal output from the cell which persists following the termination of the calibration, i.e., a form of positive feedback.[34] The calibration of such a system can obviously only be achieved with many restrictions and with great difficulty.[35]

The interpretation of Fig. 8 will be considered further in sections II/2.0 and II/3.0.

II/2.0 The NHE Interpretation of experiment Mc–21.

As has already been pointed out, the NHE interpretation of experiment Mc–21 rests on the determination of the true heat transfer coefficient on day 3 of the measurement cycles. Apart from the citation of the value of this coefficient (0.793504×10^{-9} WK^{-4}) in the header for the spreadsheet for day 1, the information given by N.H.E. is contained in a set of spreadsheets which appear to be related to the $(k'_R)_{11}$ spreadsheets of the ICARUS methodology for analyzing the data. We have to take note of the following observations:

(a) it is not clear how the value of the true heat transfer coefficient was determined nor which of the definitions of the heat transfer coefficients may have been used. However, it is likely that this was the coefficient $(k'_R)_{32}$ and it will be assumed here that this was the case, i.e., we will assume that the values of the excess enthalpies were based on calculations using the single value $(k'_R)_{32} = 0.793504 \times 10^{-9}$ WK^{-4}.

(b) it is also not clear to what extent the values of the true heat transfer coefficient and of the excess enthalpies may have been affected by the value $C_pM = 490$ JK^{-1} used in the calculations. Values as high as this applied to cells used

[33]With a thermal relaxation time of 5000 s, the temperature perturbation will only have reached 98.67% of its final value within the calibration period.

[34]Such effects can be seen in the raw data of some of the experiments carried out by the group at Harwell.

[35]This is a feature which will be common to all calorimetric systems used to investigate a thermal source subject to positive feedback. It is likely that the neglect of this fact is responsible for much of the confusion in the research on cold fusion.

prior to 1992 and the Handbooks for the ICARUS systems contained instructions for changing this (and other) parameter(s), depending on the value found using the methods of evaluation outlined in the Handbook [2, 2A]. It should be noted that the "guesstimate" of the water equivalent of the cell is: C_pM is approximately the sum of the contribution of D_2O in the electrolyte and of the glass in the inner cell wall = (422 + 31) JK^{-1} = 453 JK^{-1}. The remaining components of the cell (LiOD, metals, glass framing, heater, thermistor, a portion of the Kel–F plug) will contribute only a small additional term to C_pM. It follows, therefore, that observations of C_pM far above or below 453 JK^{-1} indicate malfunctions of the methods of data evaluation.

(c) as has been noted elsewhere (see section I/4.1), the values of the rates of evaporative cooling cannot be calculated using the instructions given in the handbooks for the ICARUS-1 and -2 systems [2, 2A]. The differences are not important at low temperatures (such as those which apply to day 3 of the measurement cycles) but become significant at temperatures close to the boiling point. However, at such elevated temperatures other factors neglected in the calculations carried out by NHE become even more important.

(d) it is apparent that the enthalpy inputs given in the NHE spreadsheets have been calculated using 1.54 V as the thermoneutral potential whereas most other authors have used the value 1.527 V. The circumstances leading to our choice of the value 1.54 V have been described elsewhere.[36]

(e) the most serious shortcoming of the NHE calculations is that the input due to the calibration heater has been entered as zero rather than the actual value given separately as 0.25000 W. In the procedure used by NHE [5] the lower bound heat transfer coefficient, $(k'_R)_{11}$, is calculated with this assumed zero enthalpy input and it is then assumed that the magnitude of the enthalpy input can be recovered together with any rate of excess enthalpy generation by using this derived lower bound heat transfer coefficient together with the true heat transfer coefficient, $(k'_R)_{32}$, and $f_1(\theta)$. Let us assume first of all that such a procedure is correct. Then we can see an immediate disadvantage as compared to the method outlined for the ICARUS systems in that we are unable to determine whether $(k'_R)_{11}$ during the period of the application of the calibration pulse in $t_1 < t < t_2$ is the same as for $t < t_1$, or $t > t_2$.[37] The data derived, e.g., see Fig. 9, are certainly further degraded by using incorrect values of C_pM. However, in actual fact, the procedure used by NHE is invalid as has been pointed out in a report and in subsequent correspondence.[38] It is difficult to see why the

[36] The water thermostats surrounding the cells were run at 30^0C in our early work. In 1988, we attempted to allow for this shift in the reference temperature as well as the fact that electrolysis takes place from 0.1 M LiOD in D_2O and not D_2O itself. While the thermoneutral potential is certainly not 1.527 V, it is closer to this value than to 1.54 V.

[37] More exactly, whether the value of $(k'_R)_{11}$ plotted versus time fall on a common staight line as shown in e.g. [6].

[38] The method proposed by NHE can only give the correct result provided there is a zero rate of excess enthalpy generation for the period $t < t_1$ before the application of the pulse

straightforward procedure outlined in the Handbooks for the ICARUS-1 system [2, 2A] was not followed.[39] We can only conclude from these data that the evaluations are incorrect based on the following evidence:

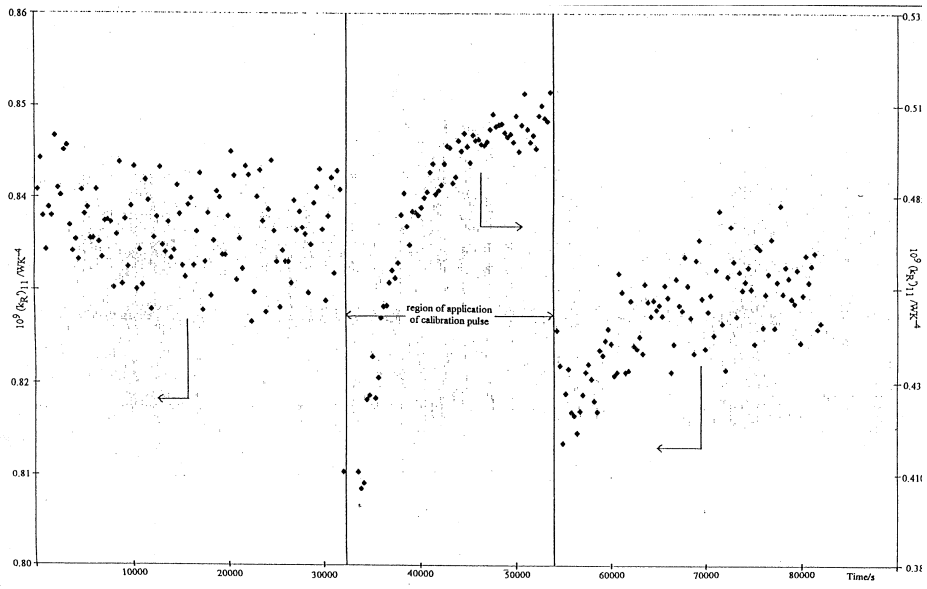

Fig. 9. The lower heat transfer coefficient, $(k'_R)_{11}$, as a function of time for the third measurement cycle as determined by the analysis provided by the NHE laboratories. The vertical lines delineate the period of application of the calibration pulse, $t_1 < t < t_2$. The amplitude of the calibration pulse, $\Delta Q = 0.2500$ W, has been excluded in the calculation of $(k'_R)_{11}$ during the period $t_1 < t < t_2$ and it has been assumed that $C_pM = 490$ WK^{-4}.

(f) it is impossible for the true heat transfer coefficient, $(k'_R)_{32}$, to be smaller than the lower bound heat transfer coefficient, $(k'_R)_{11}$, because the lower bound value is based on the assumption that there is a zero rate of excess enthalpy generation in the cell. The type of difference seen in Fig. 9 could only arise if the cell were endothermic and the endothermicity has already been fully taken into account using the thermoneutral potential. Any additional endothermicity therefore requires that the cell operates as a spontaneous refrigerator and this violates the second law of thermodynamics.

(as well as for $t > t_2$ following the termination of the pulse) while the calibration pulse itself (during $t_1 < t < t_2$) leads to the generation of excess enthalpy.

[39] In the method originally proposed by NHE the lower bound heat transfer coefficient determined before the application of the calibration pulse was used in attempts to derive the rate of excess enthalpy generation during the application of this pulse. It is not surprising that such a method can only give the correct result provided there is a zero rate of excess enthalpy generation for the period $t < t_1$ before the application of the pulse (as well as for $t > t_2$ following the termination of the pulse) while the calibration pulse itself (during $t_1 < t < t_2$) leads to the generation of excess enthalpy.

(g) the pronounced variation of the lower bound heat transfer coefficient, $(k'_R)_{11}$, with time following the application of the heater calibration pulse at $t = t_1$ and its cessation at $t = t_2$ implies at the very least that the raw data have been evaluated using an incorrect value of the water equivalent, C_pM of the cell.

(h) the excess enthalpy given by the NHE evaluation is apparently negative both for $t < t_1$ and $t > t_2$ which is further illustration of the apparent violation of the second law of thermodynamics.

(i) it has been maintained [5] that the NHE evaluation recovers the magnitude of the heater calibration pulse, ΔQ, during its period of application, $t_1 < t < t_2$, together with any rate of excess enthalpy generation.[40]

Figure 10 shows that this is incorrect: The values of the rates of enthalpy generation (which here include the enthalpy input to the calibration heater) are less than ΔQ in the period $t_1 < t < t_2$ if we take $Q_{excess} = 0$ as the base line. If we fix the baseline at the level of negative rate of excess enthalpy generation for $t < t_1$, then $Q_{excess} > \Delta Q$ during the period of the calibration pulse, $t_1 < t < t_2$. We conclude that the evaluation given by NHE is invalid and that it is likely that this evaluation is subject to several distinct errors.

II/3.0 The ICARUS type interpretation of experiment Mc–21.

As a first step, we correct the $(k'_R)_{11}$-spreadsheet by including the magnitude of the calibration pulse, ΔQ, in the definition of the lower bound heat transfer coefficient. The values of $10^9(k'_R)_{11}$ in the region $t_1 < t < t_2$ can now be shown together with those for $t < t_1$ and $t > t_2$ on a graph using a single scale for the ordinate, Fig. 11. While we cannot be certain whether or not an incorrect choice of C_pM can explain the fall of $(k'_R)_{11}$ in the region $t > t_1$ (but close to this time) or the rise for $t > t_2$ (but close to this time), it is clear that $(k'_R)_{11}$ drops markedly in the region $t_1 < t < t_2$ compared to the values for $t < t_1$ and $t > t_2$. Such a drop in $(k'_R)_{11}$ can only be due to the neglect of the build up of the rate of excess enthalpy generation during $t_1 < t < t_2$. It follows that the increase in temperature due to the calibration pulse increases the rate of excess enthalpy generation. In fact, experiment Mc–21 shows a very early establishment of positive feedback as is indeed evident from the plot of the raw data, Fig. 8. It is very important that the presence of positive feedback can be established by a simple examination of a $(k'_R)_{11}$–spreadsheet constructed according to the instructions in the ICARUS-1 Handbooks [2, 2A].

It should be noted that the amplitude of the calibration pulse would have had to be $\Delta Q = 0.2763$ W in order to bring the values of $(k'_R)_{11}$ in the region $t_1 < t < t_2$ to the level of the regression line which applies to the data for $t < t_1$ and $t > t_2$. Such a change in ΔQ is beyond all possibilities.

[40] It so happens that there is some validity to this conclusion due to the influence of positive feedback.

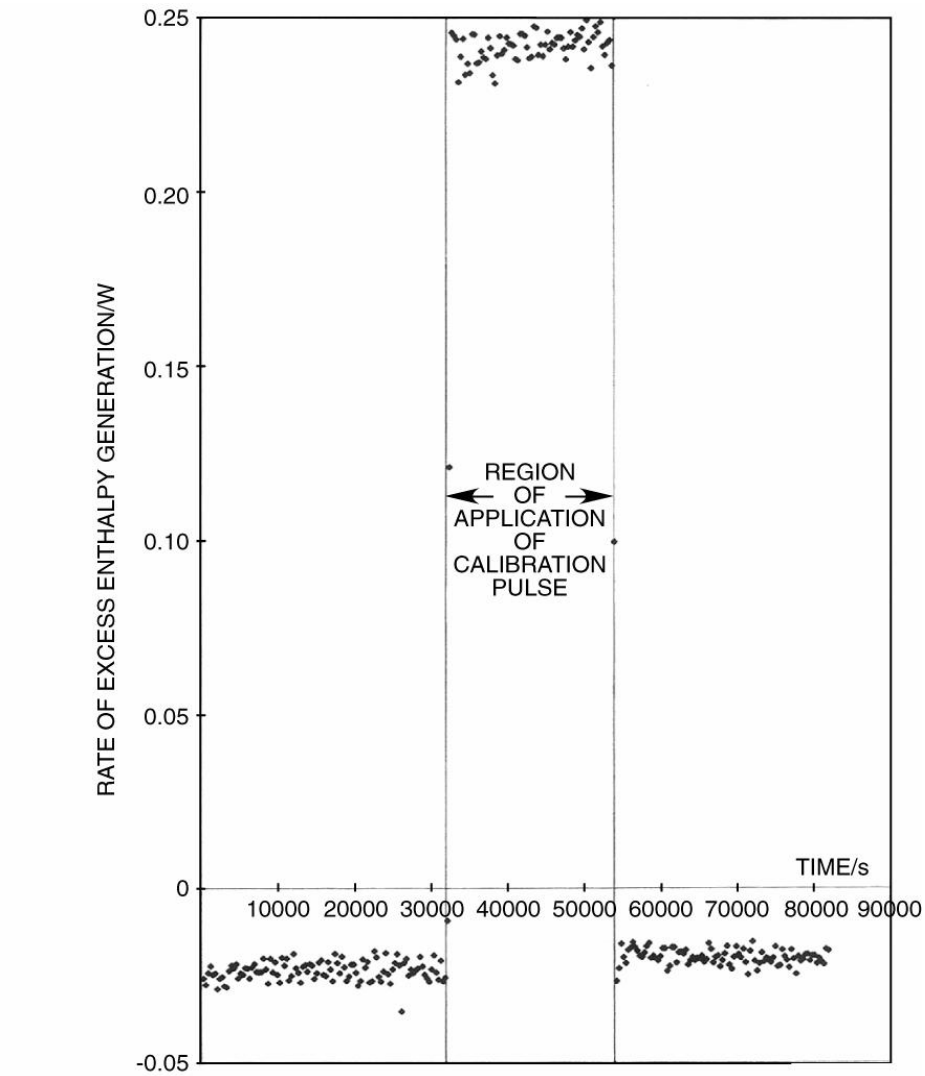

Fig. 10. The rate of excess enthalpy generation, Q_f W, as a function of time for the third measurement cycle as determined by the group at NHE laboratories.

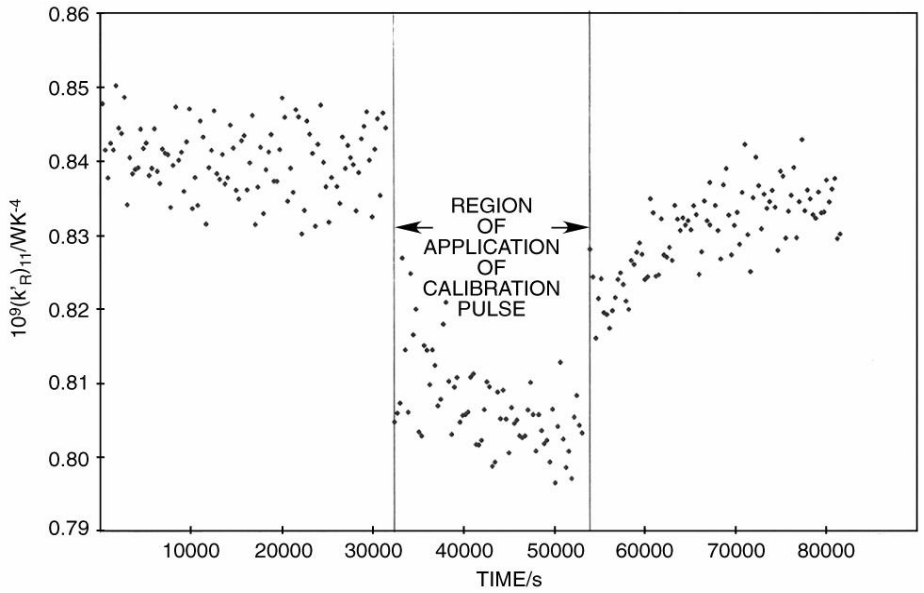

Fig.11. The lower bound heat transfer coefficient, $(k'_R)_{11}$, as a function time for the third measurement cycle as determined by the ICARUS systems procedure with the inclusion of the calibration pulse, ΔQ= 0.2500 W, in the calculation of $(k'_R)_{11}$ during the period $t_1 < t < t_2$. It has been assumed that C_pM = 490 JK^{-1}.

The next step is to prepare a modified $(k'_R)_{11}$– spreadsheet where we correct the enthalpy inputs (see (c), (d) and (e) in section II/2.0) and present the data in a form suitable for the application of Eq. (10). In view of the early intervention of positive feedback, we would only expect to be able to apply Eq. (10) at times close to t_1 where we see that the true heat transfer coefficient, $(k'_R)_{12}$ must be at least 0.83808 × 10^{-9} WK^{-4} while the water equivalent, C_pM is of the order of 454 JK^{-1} (in agreement with the "guesstimate," see section II/2.0 and the right hand part of Fig. 12).

The influence of positive feedback on the failure of simple methods for the evaluation of the lower bound and true heat transfer coefficients as well as of the water equivalent of the cell is also shown clearly by attempts to derive $(k'_R)_{181}$ (which rely on the combination of data for the time regions $t_1 < t < t_2$ and $t_2 < T$; see part I). This evaluation has been found to be especially useful in the analyses of data sets for blank experiments (e.g. see vol. II). Figure 11 illustrates that we are unable to obtain a satisfactory interpretation of such data for experiment Mc–21.

Figure 13 gives the plot of the data versus time and also shows the variation of $10^9(k'_R)_{11}$ with time predicted using the values for $t < t_1$ and the known

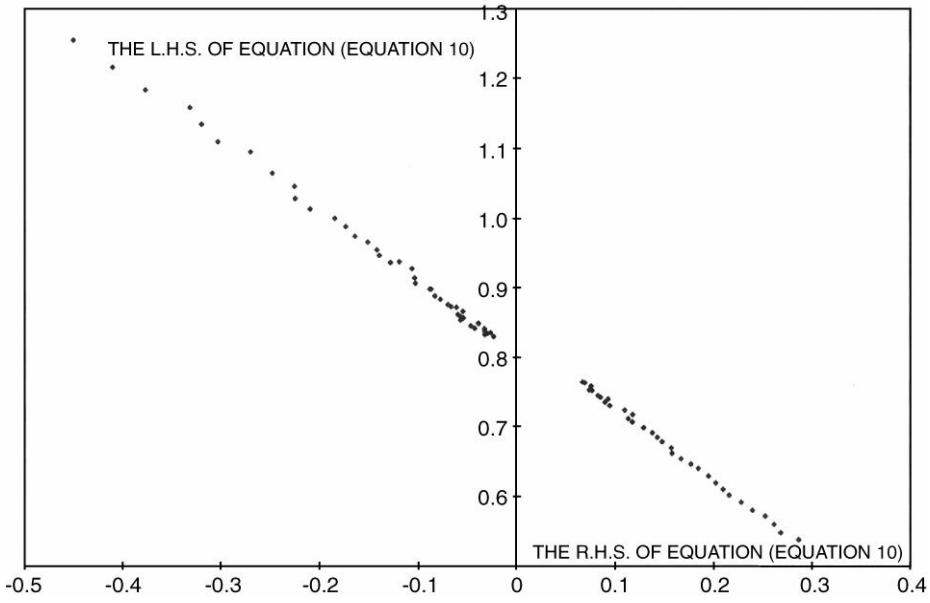

Fig.12. Evaluation of $(k'_R)_{1811}$ and C_pM according to Eq. (10).

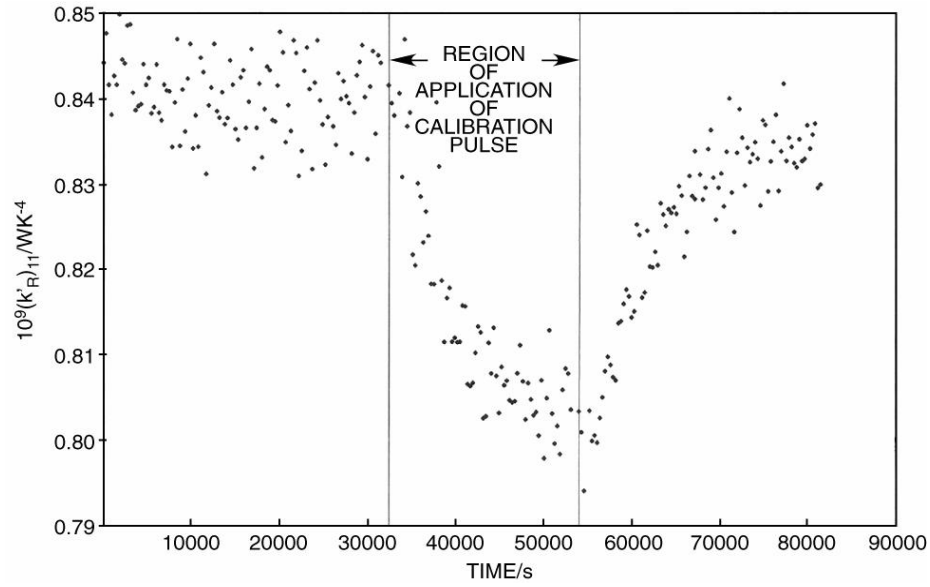

Fig. 13. The lower bound heat transfer coefficient, $(k'_R)_{11}$, as a function of time. Third measurement cycle; ΔQ= 0.2500W; C_pM = 450 JK^{-1}.

behavior established with appropriate blank experiments, e.g., [6]. As in the case of the data in Fig. 11, we can see that the temperature rise induced by the calibration pulse leads to a decrease in $(k'_R)_{11}$ while the cooling consequent on the termination of the pulse leads to an increase in $(k'_R)_{11}$. These changes can only be due respectively to an increase and decrease in the rate of excess enthalpy generation, which cannot be taken into account in deriving the values of $(k'_R)_{11}$, i.e., the effects of positive feedback.

Figure 13 shows that we still observe discontinuities in the lower bound heat transfer coefficient, $(k'_R)_{11}$ at t_1 and t_2. However, it is evident that there can be no mechanism, which could account for such changes which must therefore be due to an error in the analysis. The most obvious error is the use of an incorrect value of C_pM (see (b), II/ 2.0). The analysis of the time dependence according to Eq. (10) in the region $t > t_1$ (but adjacent to t_1) indicates that the correct value is 450 JK^{-1}. The heat transfer coefficients $10^9(k'_R)_{11}$ and $10^9(\overline{k'_R})_{11}$ are based on this value of C_pM. Figure 13 shows a plot of $(k'_R)_{11}$ values versus time and we can see that the discontinuities in the heat transfer coefficient at $t > t_1$ and $t > t_2$ (but adjacent to these times) are now eliminated. However, as expected, the effects due to positive feedback are maintained.

Figure 14 shows that there is indeed only a small rate of excess enthalpy generation for $t < t_1$ while the application of the calibration pulse leads to a build-up of this rate, which again decreases for $t > t_2$ (there is a small long-term increase in the rate of excess enthalpy generation for $t > t_2$). Figure 15 shows a similar calculation but using the NHE methodology (note the difference in scales of the y-axes in Figs. 14 and 15). We again see a near zero rate of excess enthalpy generation for $t < t_1$, while for $t > t_1$ but adjacent to t_1, we now see the step due to the calibration pulse, ΔQ= 0.2500 W. In the region $t_1 < t < t_2$, we then see the build-up in the rate of excess enthalpy generation due to positive feedback. At $t = t_2$ but adjacent to t_2, we again see a step in the total observed rate of excess enthalpy generation. As expected, this step again corresponds to the expected value ΔQ = 0.2500 W; at longer times, we see the gradual decrease of the rate of excess enthalpy generation due to the removal of the effects of positive feedback.

It can be seen that a comparison of the plots of $(k'_R)_{21}$ and $(k'_R)_{31}$ versus time, Fig. 16, with the corresponding plots for blank experiments, e.g., see [6], shows very clearly the intervention of positive feedback due to the superposition of the calibration pulse. If we focus attention first of all on the behavior of$(k'_R)_{31}$ for $t < t_1$, then we see the expected small decrease with increasing time.[41] For $t > t_1$ we see a more rapid decrease due to the onset of positive feedback. The effects of this positive feedback decrease for $t > t_2$ so that we observe a small increase of $(k'_R)_{31}$ with increasing time in this region.

[41]The values for the first 20 to 30 points must be excluded as the benefits of using the integral coefficients are only established with increasing time. Similarly, the first 20 to 30 points must be excluded if the interpretation is based on backward integration, i.e., if we consider $(k'_R)_{21}$.

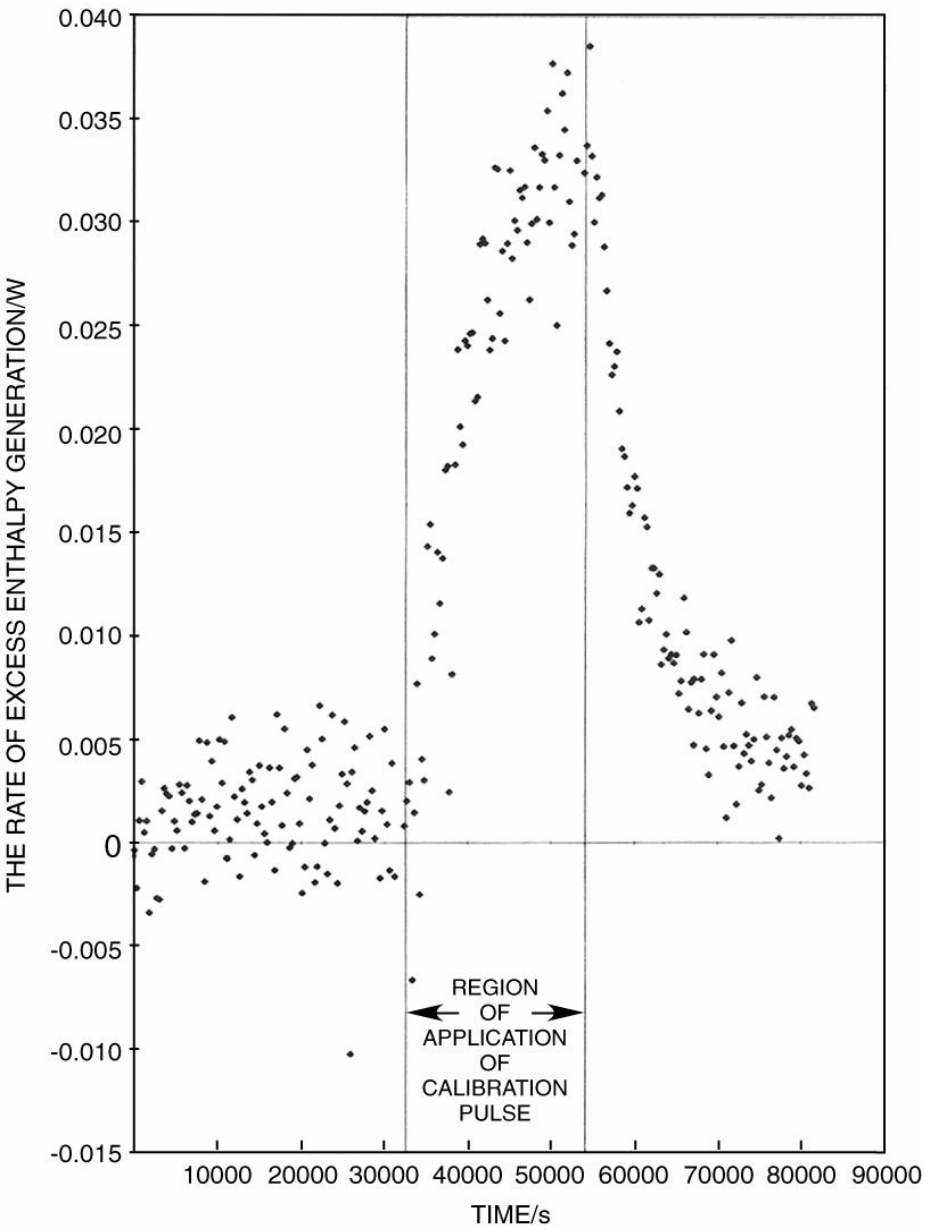

Fig. 14. The rate of excess enthalpy generation, Q, as a function of time for the third measurement cycle. $(k'_R)_{12} = 0.85065 \times 10^{-9}$ WK^{-4} and the values for the lower bound heat transfer coefficient shown in Fig. 12.

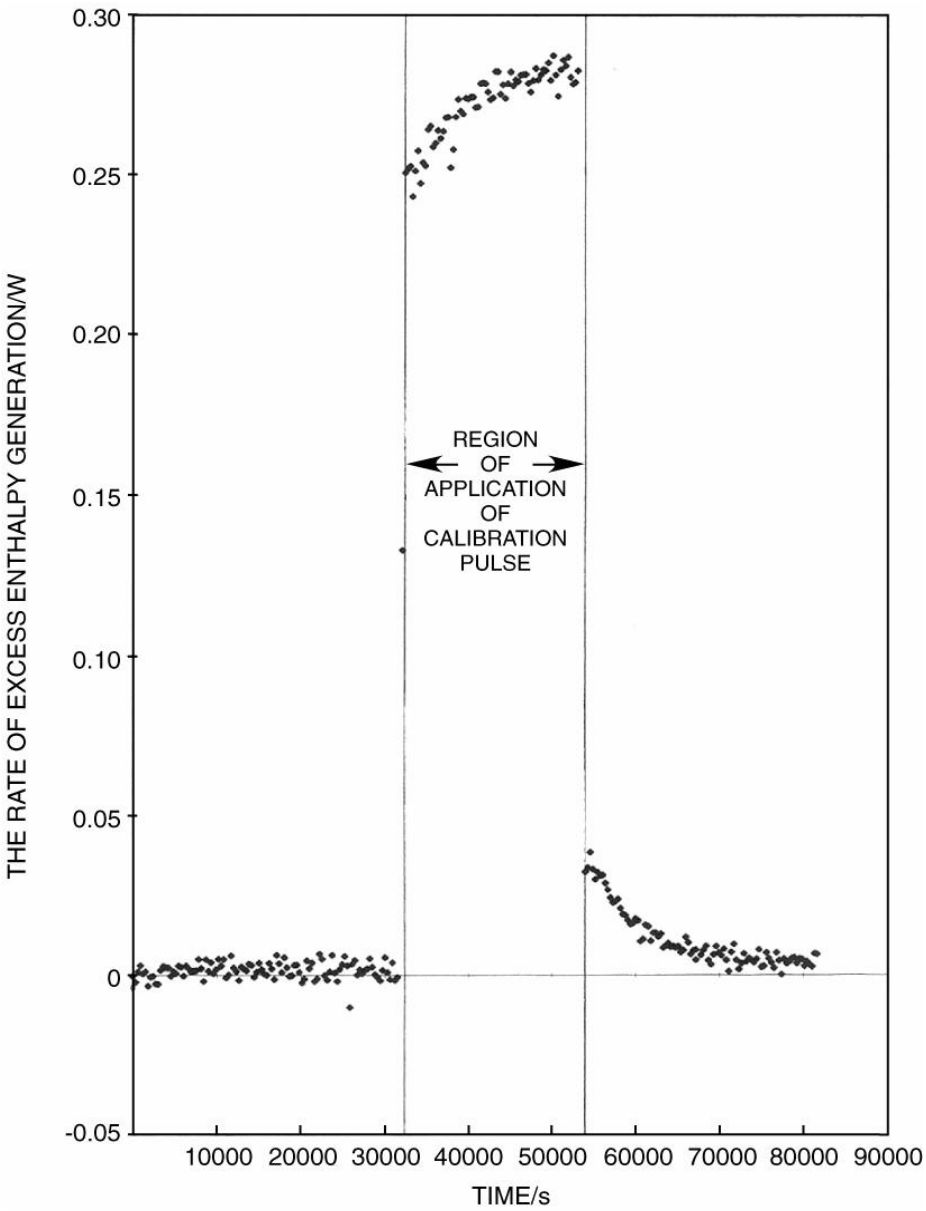

Fig.15. The rate of excess enthalpy generation as a function of time. Third measurement cycle; $(k'_R)_{12} = 0.85065 \times 10^{-9}$ WK^{-4}, $\Delta Q = 0.2500$ W

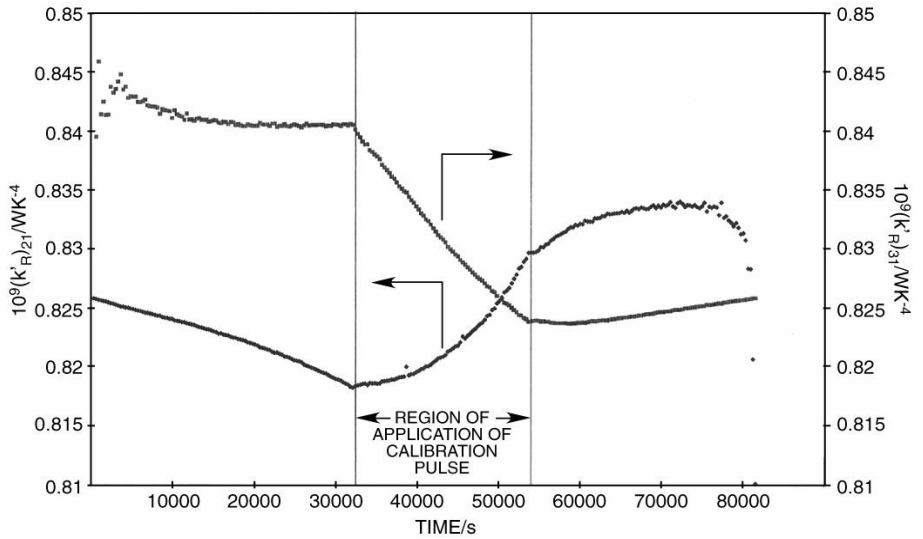

Fig. 16. The variation of $(k'_R)_{21}$ and $(k'_R)_{31}$ with time for the whole of the third measurement cycle.

The variation of $(k'_R)_{21}$ with time can be interpreted in a similar way provided one bears in mind that there is now no region in time in which the integrals used in the calculation of the heat transfer coefficient are independent of the effects of positive feedback. The influence of positive feedback on the integrals used in the evaluation of $(k'_R)_{21}$ explains why we cannot obtain a satisfactory evaluation of the target value of the lower bound heat transfer coefficient, $(k'_R)_{251}$. We would only expect to be able to apply the ICARUS methodology in a region of time where the influence of positive feedback can be expected to be adequately small, say, in the region 72,300 to 75,300 s of the measurement cycle. The estimates of the lower bound heat transfer coefficient, $(k'_R)_{261}$ and of C_pM, are 0.81821×10^{-9} WK^{-4} and 475.3 JK^{-1}.

The comments which have been made about the evaluation of the integral heat transfer coefficients using the whole measurement cycles apply equally to the evaluations according to the instructions and software in the ICARUS systems [2, 2A]. The precision of $(k'_R)_{31}$ and $(k'_R)_{351}$ is low because of the intervention of positive feedback and the consequent need to restrict attention to the region $t > t_1$ but close to t_1. This is equally true of the accuracy of $(k'_R)_{32}$ and $(k'_R)_{352}$.

However, the evaluations of these coefficients is instructive because it is virtually certain that the value of the true heat transfer coefficient quoted by NHE is either the value of $(k'_R)_{32}$ at a particular time or else $(k'_R)_{352}$ evaluated over a particular range of time. We therefore have to investigate whether we can modify the approach so as to allow the determination of this true heat transfer coefficient. We have to note that it is unlikely that we would be able to find a

generally valid procedure because it is in general not possible to calibrate closed loop systems subject to positive feedback. However, for the particular example of day 3 of experiment Mc–21, we can see that the effects of positive feedback are relatively small and, moreover, confined in the time-domain, Fig. 14. We can therefore include the observed values of the rates of excess enthalpy generation in the evaluation of the integral of the enthalpy input and use this modified integral to re-evaluate $(k'_R)_{22}$ and $(k'_R)_{252}$. Figure 17 illustrates this evaluation. It can be seen that we do indeed now obtain a satisfactory fit to Eq. (22) which explains the choice of $(k'_R)_{252} = 0.85065\times\ 10^{-9}$ WK^{-4} and $C_pM = 450$ JK^{-1} for the further evaluation of the data.

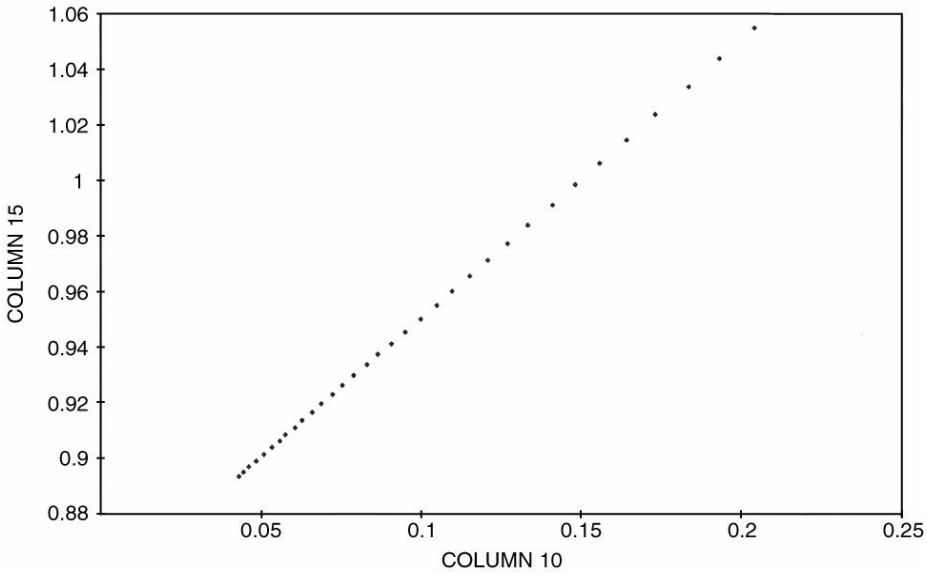

Fig. 17. Evaluation of the integral heat transfer coefficient $10^9(k'_R)_{252}/\mathrm{WK}^{-4}$, and water equivalent, C_pM/JK^{-1} for the third measurement cycle with correction for the effects of positive feedback (see Appendix).

In view of the fact that this evaluation of the true heat transfer coefficient, $(k'_R)_{252}$, requires the development of a special approach, it is necessary (and advisable) to investigate whether the value obtained can be confirmed by other means using different parts of the experiment (i.e., other measurement cycles). Such confirmations can be obtained using the measurements on day 61 and the first 57 hours of days 1 and 2. These confirmations are outlined in sections II/4.0 and II/5.0 respectively.

II/4.0 Application of the ICARUS Type Interpretation to the data for day 61.

The early intervention of positive feedback requires us to modify the ICARUS evaluation strategies in order to achieve the calibration of the system, i.e., to

determine the value of the true heat transfer coefficient. It is therefore important to find confirmatory evidence that this heat transfer coefficient is indeed *ca* $0.85065\times\ 10^{-9}$ WK^{-4} as given at the end of the previous section. Evidence pertinent to this conclusion is presented in the present section as well as section II/5.0.

We note in the first place the values of the total excess enthalpy for each day of operation calculated using the true heat transfer coefficient, $(k'_R)_{32} = 0.79350 \times 10^{-9}$ WK^{-4} as given by the NHE evaluation as well as those calculated with true heat transfer coefficient, $(k'_R)_{252} = 0.85065$ x $10^{-9}WK^{-4}$, as determined in section II/3.0 using the modified ICARUS methodology. These values are plotted in Figs. 18 and 19 respectively. We can see immediately that the evaluation given by NHE must be incorrect because we obtain negative excess enthalpies for some of these days which contravenes the second law of thermodynamics (cf. section II/2.0). On the other hand, the evaluation based on the heat transfer coefficient given by the modified ICARUS evaluation scheme only gives a very slightly negative excess enthalpy for day 61.

It is therefore reasonable to assume that the rate of excess enthalpy generation on day 61 is close to zero. The evaluation of the lower bound heat transfer coefficient, $(k'_R)_{11}$, must therefore be close to the values of the true heat transfer coefficient, $(k'_R)_{12}$. Figure 20 gives a plot of the relevant data compared to the plot which we predict using the value $(k'_R)_{12} = 0.85065 \times 10^{-9}$ WK^{-4} and the variation of $(k'_R)_{11}$ with time given by the relevant blank experiments [6 and vol. II]. It can be seen that the observed values of $(k'_R)_{11}$ are in close accord with those which we would predict on the assumption that there is only a low rate of excess enthalpy generation on that day.

It can be seen that there is only one region of time in which there is a marked deviation from the predicted behavior, namely, for $0 < t < 10,000$ s. In this region, $(k'_R)_{11}$ is markedly larger than the expected value and, moreover, decreases rapidly with time to these predicted values. It has already been noted in section II/1.3 that the cell was overfilled with D_2O at the start of this particular day (see Fig. 5) so that the level of electrolyte would have been expected to approach the base of the Kel-F plug sealing the top of the cell. Separate measurements have shown that the pseudo-radiative heat transfer coefficient increases by *ca* 5% over the expected value presumably because of an increase in the conductive contribution through the top of the cell. It is likely, therefore, that the deviation seen in this time range can be attributed to the overfilling of the cell.

II/5.0 A pre-ICARUS evaluation of the true heat transfer coefficient.

It is possible to find a further value of the true heat transfer coefficient $(k'_R)_{12}$ by applying a method used in 1992 [7, 8]. It was shown at that time that the lower bound heat transfer coefficient, $(k'_R)_{11}$, decreases markedly from the expected value during the initial stages of the measurement cycles. The full line in Fig.

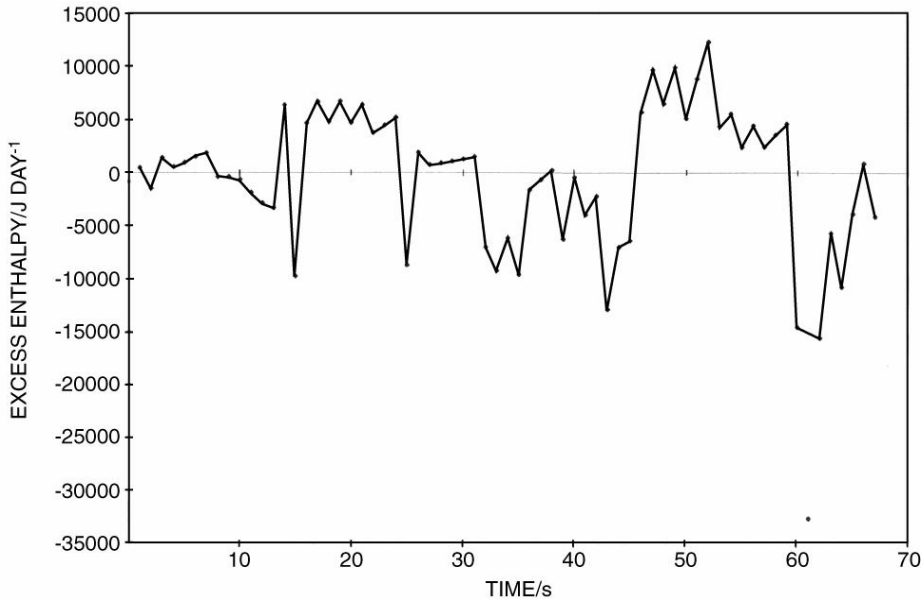

Fig. 18. The excess enthalpy as a function of time using true heat transfer coefficient, $(k'_R)_{12} = 0.79350 \times 10^{-9}$ WK^{-4} as given by the analysis of the group at NHE laboratories.

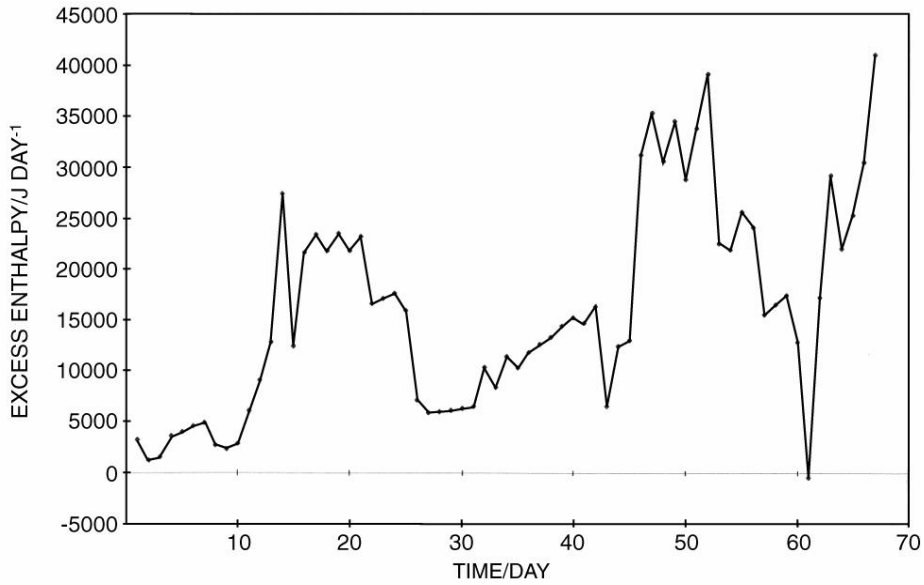

Fig. 19. Same as in Fig. 18 evaluated using $(k'_R)_{12} = 0.85065 \times 10^{-9}$ WK^{-4} as given by the ICARUS system analysis modified to account for positive feedback.

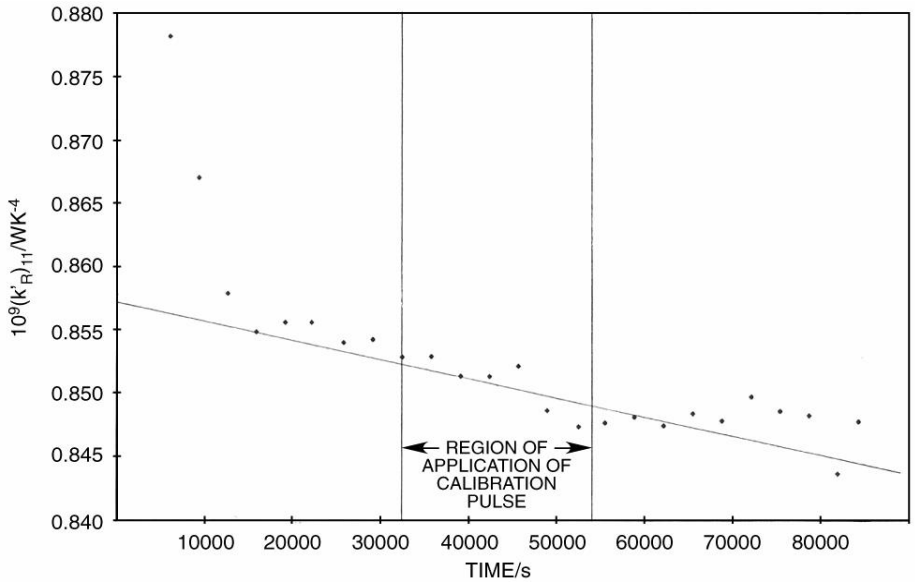

Fig. 20. The variation with time of the 11-point average of the lower bound heat transfer coefficient, $10^9(k'_R)_{11}$ for day 61. The full line gives the variation with time for the relevant blank experiments [6 and vol. II].

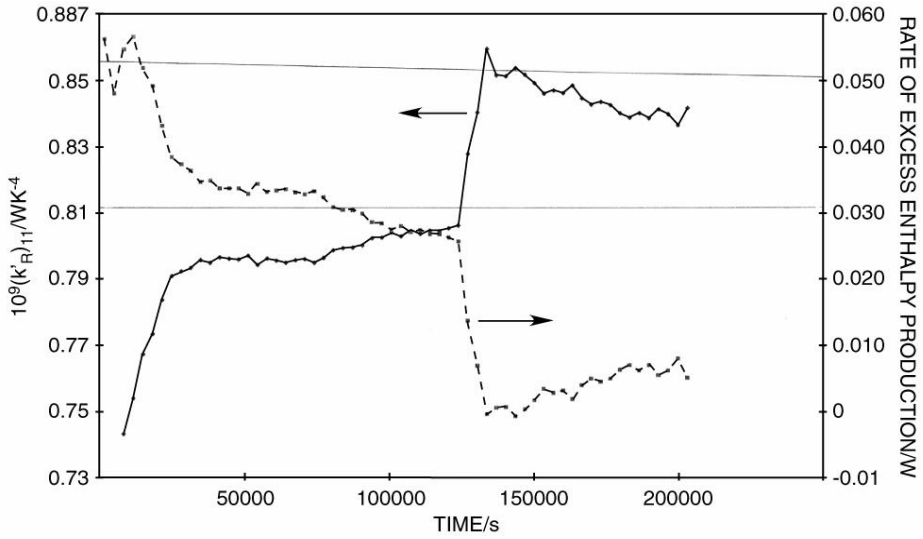

Fig. 21. The lower bound heat transfer coefficient, $(\overline{k'_R})_{11}$, and the rate of excess enthalpy generation, Q, for the first 57 hours of operation.

21 shows the expected variation with time for the present experiment. Values of Q are based on the assumption that $(k'_R)_{12}$ is given by the regression line. The horizontal line shows the value of Q based on the assumption that the current efficiency for the charging the electrode at t = 130500s is 100% and that the heat of absorption of deuterium in the lattice is 40 kJ/mole. In this case, the decrease, at t= 130500s, is due to the completion of the exothermic absorption of deuterium in the lattice. It would be expected, therefore, that the lower bound heat transfer coefficient, $(k'_R)_{11}$, would rise markedly to the expected true value as this process is completed with the proviso that we can observe a period of operation during which there is zero excess enthalpy generation. It follows that we can derive a value of the true heat transfer coefficient, $(k'_R)_{12}$, from the maximum of the lower bound heat transfer coefficient, $(k'_R)_{11}$, which is observed with increasing time. Figure 21 shows the relevant data for the first 57 hours of operation of experiment Mc–21 (i.e., up to the time of application of the heater calibration pulse on day 3). The full line shows the expected variation of $(k'_R)_{11}$ with time based on the value of $(k'_R)_{12}$ at $t = t_2$ on day 3, (i.e., $(k'_R)_{12} = 0.85065 \times 10^{-9}$ WK^{-4}, the assumption of zero excess enthalpy generation, (i.e., $(k'_R)_{11} = (k'_R)_{12}$) and the known variation of $(k'_R)_{11}$ with time established with blank experiments [6 and vol. II]. It can be seen that $(k'_R)_{11}$ does indeed rise to the predicted levels as the charging of the electrode is completed.

Figure 21 also shows the derived rates of excess enthalpy generation based on the experimental values of $(k'_R)_{11}$ and the assumption that the true heat transfer coefficient is given by the regression line. It can be seen that the experimental values are in reasonable accord with the assumption that the charging of the cathode is *ca* 100% efficient and that the heat of absorption is *ca* 40 kJMol^{-1}. Figure 21 furthermore shows that there is a small build-up of excess enthalpy generation on day 3 following the completion of the charging process (compare [7, 8]).

II/6.0 Day 68: the period $0 < t <$21,300 s during which the cell is driven to dryness.

We consider next the penultimate day of the investigation of experiment Mc–21; the cell is driven to dryness during the first part of this measurement cycle. We can draw a number of important conclusions from the raw data alone. We note in the first place that the temperature given by the long thermistor is now slightly higher than that given by the short thermistor whereas the opposite is true for measurements made at low temperatures. At first sight such a change might be attributed to a genuine effect, namely, the increase in the enthalpy input in the bottom part of the cell (containing the Pd-B cathode). However, such an interpretation is unlikely because the temperature difference between the two thermistors is essentially constant for, say, 20,000 s even though the enthalpy input increases by a factor of three. It is more likely therefore that this particular temperature difference is a further manifestation of errors in the calibration of the thermistors.

The temperature differences between the two thermistors are appreciably larger for the last four data acquisition points, and this difference is especially marked for the last point, 0.590 K. Such a difference is to be expected because the long thermistor is now in the relatively concentrated LiOD solution while the short thermistor is in the vapor phase. However, we also have to note that the temperature at both positions is above that of the boiling point of pure D_2O. Evidently, we have to take into account the increase of the boiling point with the electrolyte concentration as the D_2O is progressively evaporated (see section II/1.4). However, we also have to take note of the fact that the vapor phase can be superheated (albeit to only a limited extent).[42] If we do not take account of the increase of the boiling point with concentration, we arrive at the impossible result of negative enthalpies of evaporation with increasing temperature as shown by the NHE evaluation. We also have to use the correct atmospheric pressure in the calculation of the rate of evaporative cooling and we need to change the thermoneutral potential and the water equivalent of the cell in the NHE evaluation. As the water equivalent of the cell only leads to a significant term $C_pM(d\Delta\theta/dt)$ in the initial stages for day 68, it has been assumed that C_pM is unchanged throughout the stage leading to evaporation to dryness (however, see further comments in section II/7.0).

This calculation is similar to one which has been described previously (cf. vol. II) except that the published version included comments on the time dependence of the rate of excess enthalpy generation. It is quite obvious that the rate of excess enthalpy generation must increase with time because the initial rate on day 68 is less than 1 W. It is important therefore to try to establish the variation of the rate of excess enthalpy generation with time, if only to make a connection with the initial rate of "Heat after Death" observed after the cell has reached dryness (see section II/7.0). In order to derive this variation, we have to include an estimate of the rate of reflux in the cell and this part of the calculation will follow the scheme outlined in section I/4.0. We can see that the negative values of the enthalpies are now eliminated as the D_2O in the cell is maintained by the amount of reflux. The total amount evaporated is also in reasonable accord with the amount of D_2O initially in the cell. It is important to realize that we have assumed that the whole of the heat transfer from the cell in the region filled with vapor leads to recondensation, i.e., we have overestimated the reflux and underestimated the amount evaporated. We should also note that the calculation is improved somewhat if we allow for the fact that the boiling point reaches a limit due to the limited solubility of LiOD in D_2O at the boiling point (this aspect is not illustrated in this report).

Although the calculation as outlined gives a reasonable interpretation of the behavior of the cell as the contents are driven to dryness (elimination of negative

[42] Heat transfer to the walls of the Dewar cell is maintained by the vapor phase at the very least if this phase is filled with D_2O vapor at temperatures close to the boiling point of the electrolyte. The heat transfer coefficient for the cell filled with vapor will be *ca* 5% above the value 0.85065×10^{-9} WK^{-4}.

enthalpies of evaporation), we nevertheless still derive negative rates of excess enthalpy generation at long times. This is undoubtedly due to remaining inaccuracies in the calculation of the rates of evaporative cooling. At the present time it is best to restrict attention to the earlier part of the period leading to evaporation to dryness, say, to t <18,000s. The rate of excess enthalpy generation reaches *ca* 9.3 W at this time, or, say, 25 Wcm^{-3}. It is important to realize that similar orders of magnitude are obtained even with the interpretation given by NHE, i.e., the estimate is robust.

II/7.0 Day 68: The period 21,300s < t < 86,400 s following evaporation to dryness.

As has been noted in section II/1.2 one of the objectives of the present investigation has been the search for the presence (or absence) of the effects of "Heat after Death." The period following the evaporation to dryness on day 68 is an example of the protocol originally described as case **(ii)**[3, 4]
(ii) Cell empty: cell allowed to evaporate to dryness; cell then maintained at the rail voltage of the galvanostat with the exception that the cell did not reach boiling conditions during the period leading to dryness.

The original investigation was divided into two parts: (i) the investigation and interpretation of the cooling curves following evaporation to dryness; (ii) the evaluation of thermal balances in the corresponding period. Attention here will be confined to the second of these approaches.

The values of the rates of excess enthalpy generation have been based on true heat transfer coefficient, $(k'_R)_{12}$, observed for the cell filled with electrolyte, i.e., 0.85065×10^{-9} WK^{-4}, which will certainly apply to initial stage of the observation of "Heat after Death" when the cell is filled mainly with D_2O vapor. However, calibrations of cells filled with air [3, 4] have shown that the heat transfer coefficient falls to about 0.75 of the value for the cells filled with electrolyte. The values of the rates of excess enthalpy generation have therefore been calculated using $(k'_R)_{12} = 0.65 \times 10^{-9}$ WK^{-4}.

The initial rate of excess enthalpy generation is approximately the same as the rate reached during the period $0 < t < 21{,}300$ s as the cell is being driven to dryness, Fig. 22. Such a correspondence would, of course, be expected if excess enthalpy generation takes place in the bulk of the metal phase.

We note also that the rate of excess enthalpy generation is about 10 times that of the rate of enthalpy input during this period of "Heat after Death."

II/8.0 Day 69: The period 2400 s < t <32,400 s.

This period is of special interest in the operation of the cell because the cell was disconnected from the galvanostat at 2400 s so that the enthalpy input was

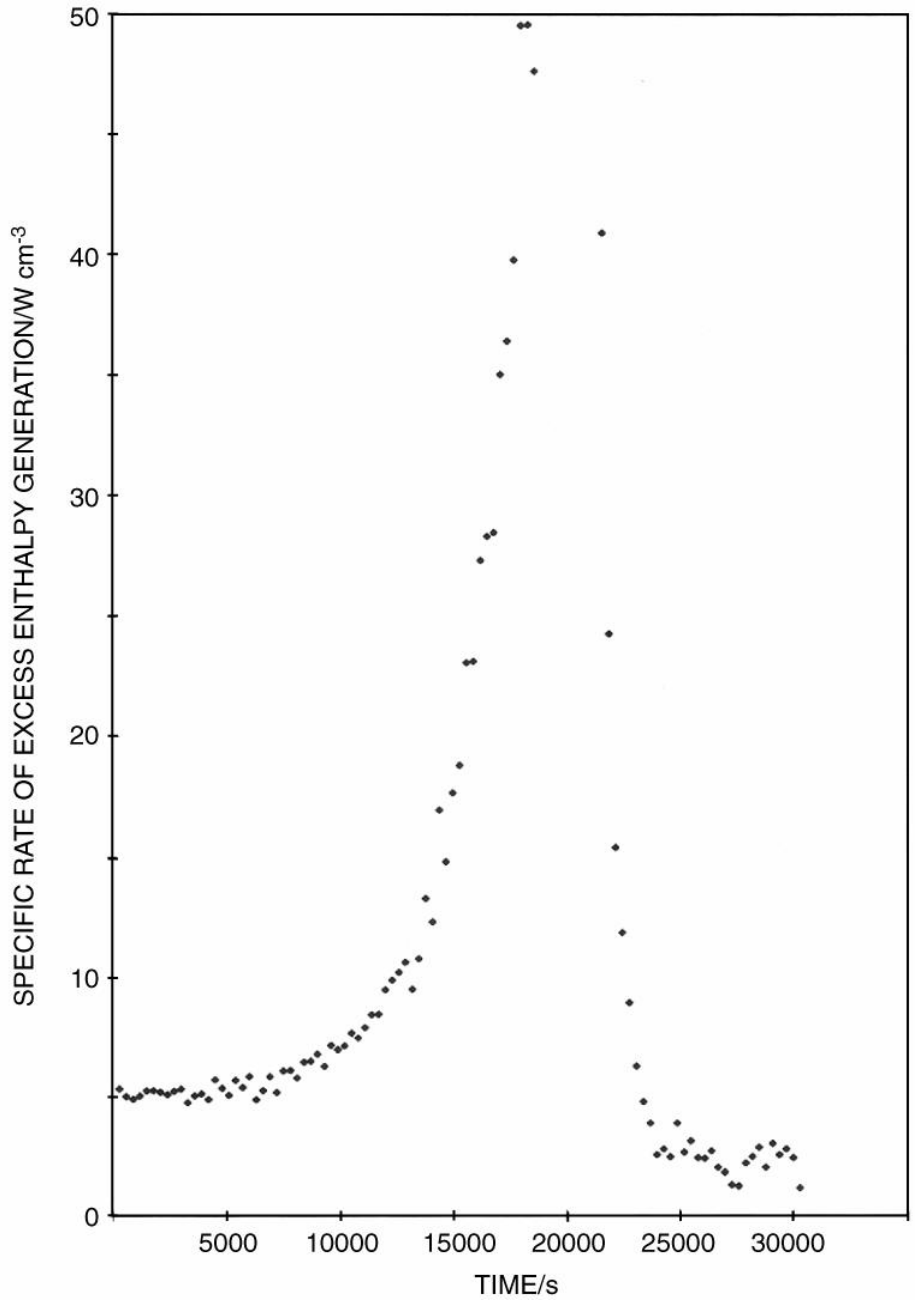

Fig. 22. Comparison of specific rates of excess enthalpy generation, Wcm^{-3}, on day 68 during the period $0 < t < 21{,}300$ s and the initial period 21,300 s$< t <$ 30,300 s of observation of "Heat after Death."

zero during the remaining period of operation. In any search for the effects of "Heat after Death," the protocol there should be described at case **(iii)**[3, 4] Cell empty: cell allowed to evaporate to dryness; cell disconnected from the galvanostat with the exceptions that the cell did not reach boiling conditions during the period leading to dryness and that the application of case **(iii)** was preceded by a period covered by case **(ii)** as described in section II/7.0.

The examination of the behavior of the cell has been restricted here to the time $t < 32{,}400$ s as the usual calibration pulse was applied at $t_1 = 32{,}400$ s. The Joule heat injected by the calibration system is developed in a small volume so that this calibration cannot be used to derive the true heat transfer coefficient of the cell for the particular operating conditions.[43] The cooling curve for this period of operation is plotted in Fig. 23. It can be seen that although the temperature differences between the cell and water bath are small, they are nevertheless significant.

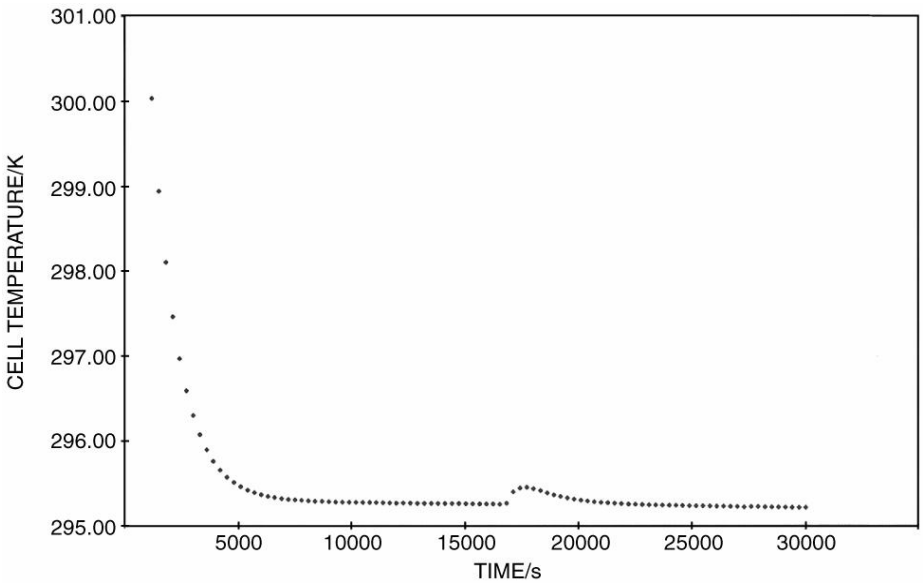

Fig. 23. The cooling curve on day 69 following the disconnection of the cell from the galvanostat.

Inspection of Fig. 23 shows that there must be a source of enthalpy in the system: firstly, because the rate of cooling at short times is too slow to be accounted for by the cooling of a calorimeter with a water equivalent of 28.3 JK^{-1} and any conceivable value of the heat transfer coefficient; secondly, because we can detect at least one period during which the cell contents are reheated.

[43] As has been noted, the calibration used in an earlier investigation were derived by using a heater spiral spanning the whole volume of the cell, i.e., heat was applied uniformly throughout this volume.

The analysis of the cooling curve according to the method originally outlined [3, 4] using the equation

$$ln[(1+y)/y(1+y_0)] + tan^{-1}(1+y) - tan^{-1}(1+y_0) = 4(k'_R)\theta_b^3 t/C_pM$$

where $y = (\Delta\theta/\theta)/\theta_b$; $y_0 = \Delta\theta_0/\theta_b$ and $\Delta\theta_0$ is the initial temperature difference. Figure 24 shows a plot of the experimental data; the full line shows the predicted behavior using $C_pM = 28.3$ JK^{-1} and $(k'_R) = 0.65$ x 10^{-9} WK^{-4}. The deviations from this plot due to enthalpy generation are similar to those previously observed [3, 4].

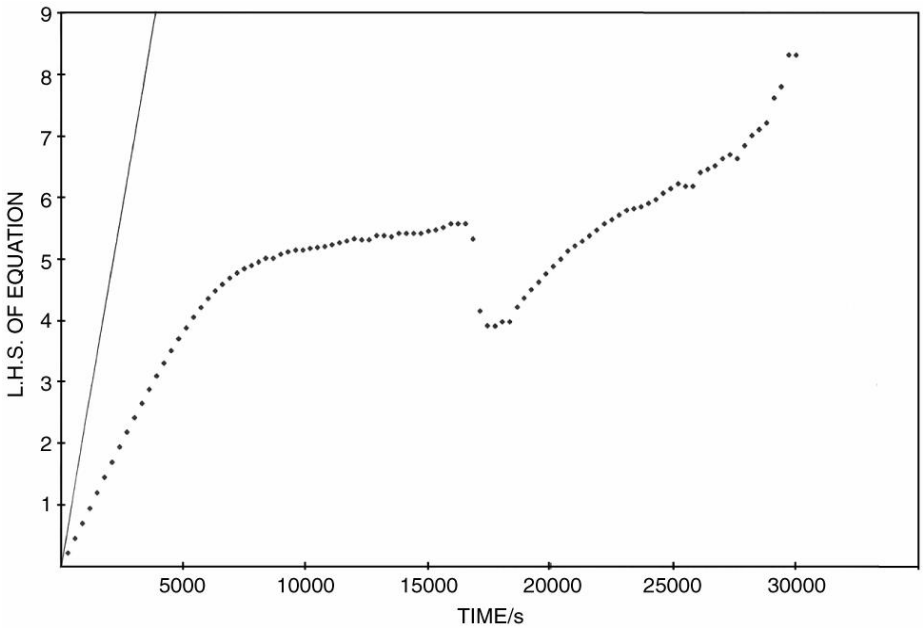

Fig. 24. The analysis of the initial portion of the cooling curve shown in Fig. 23. The full line shows the RHS of the equation plotted with $C_pM = 28.3$ JK^{-1}, $(k'_R)_{12} = 0.65\times\ 120^{-9}$ WK^{-4} and θ_b =295.204 K.

We can also make thermal balances at each point of the cooling curves using particular values of the water equivalent and true heat transfer coefficient. Those based on $C_pM = 28.3$ JK^{-1} and $(k'_R)_{12} = 0.65$ x 10^{-9} WK^{-4} give initial rates of enthalpy generation *ca* 0.5 W. Unfortunately, the thermal balances in the period preceding the disconnection of the cell from the galvanostat (i.e., the last part of case **(ii)**, section II/7.0) cannot be made with sufficient accuracy to allow a comparison of the rates of enthalpy generation at the end of the period following case **(ii)** and the beginning of the period following case **(iii)** (c.f. comparison of the rates at the end of the period leading to evaporation to dryness and the beginning of the period following case **(ii)**, sections II/6.0 and II/7.0).

II/9.0 Days 25 and 26: The period Day 25 + 76,300s $< t <$ Day 26 + 22,300 s.

As has already been noted in section II/1.2, there were frequent changes of current density in experiment Mc–21. Consideration of case **(i)** of the conditions likely to give demonstrations of the phenomenon of "Heat after Death" [3, 4]:
i) Cell full: cell operated at intermediate temperatures; cell current then reduced in stages shows that the change of current close to the start of day 26 of the measurement cycles is likely to provide the best example of this particular case, see Fig. 4.

There are two principal reasons that indicate this was the case. In the first place, the current density at the end of day 25 is above the threshold value required for the observation of the phenomenon [1] while on day 26 it is below this threshold value. Secondly, the cell temperature on day 25 is above that which has been observed to be important for the onset of positive feedback[7,8,11] whereas on day 26 it drops below this value. We would therefore expect to see a marked decrease of the rate of excess enthalpy generation at the start of day 26 from the value which applies at the end of day 25 to that which applies towards the end of day 26.[44]

The data covering measurements in the last stages of day 25 and the beginning of day 26 are used to define the lower bound heat transfer coefficient, $(k'_R)_{11}$. We note here that we have used the value $C_pM = 475$ JK^{-1} in view of the evident overfilling of the cell on day 25, see Fig.5. The rates of excess enthalpy generation derived are plotted in Fig. 25. We can see the well defined fall in the rate of excess enthalpy generation which, as in the other examples of "Heat after Death" discussed in this report, is consistent with a diffusional relaxation time. We can see from the plot in Fig. 25 that this evaluation predicts a negative rate of excess enthalpy generation on day 25.

As we have noted elsewhere in this report, such negative rates violate the second law of thermodynamics and are certainly due to the use of the incorrect value of the true heat transfer coefficient, $(k'_R)_{12}$, given by the NHE analysis. Nevertheless, we can see from Fig. 26 that we can detect the effects of "Heat after Death" on day 26 even when using this faulty analysis. Furthermore, the increasing values of the lower bound heat transfer coefficient $(k'_R)_{11}$ on that day demonstrate the presence of a rate of excess enthalpy generation which decreases with time.

If we use the value of $(k'_R)_{12}$ given by the correct ICARUS methodology, we obtain the rates of excess enthalpy generation shown in Fig. 26. It is important, however, to draw attention to a remaining difficulty in the interpretation,

[44]Excess of enthalpy generation was observed on day 3 of the measurement cycle at a current density below the threshold value while positive feedback was established at a temperature below this further threshold. We can, therefore, only regard the criteria used to search for category of the phenomenon of "heat after death" as rather "broad brush indicators."

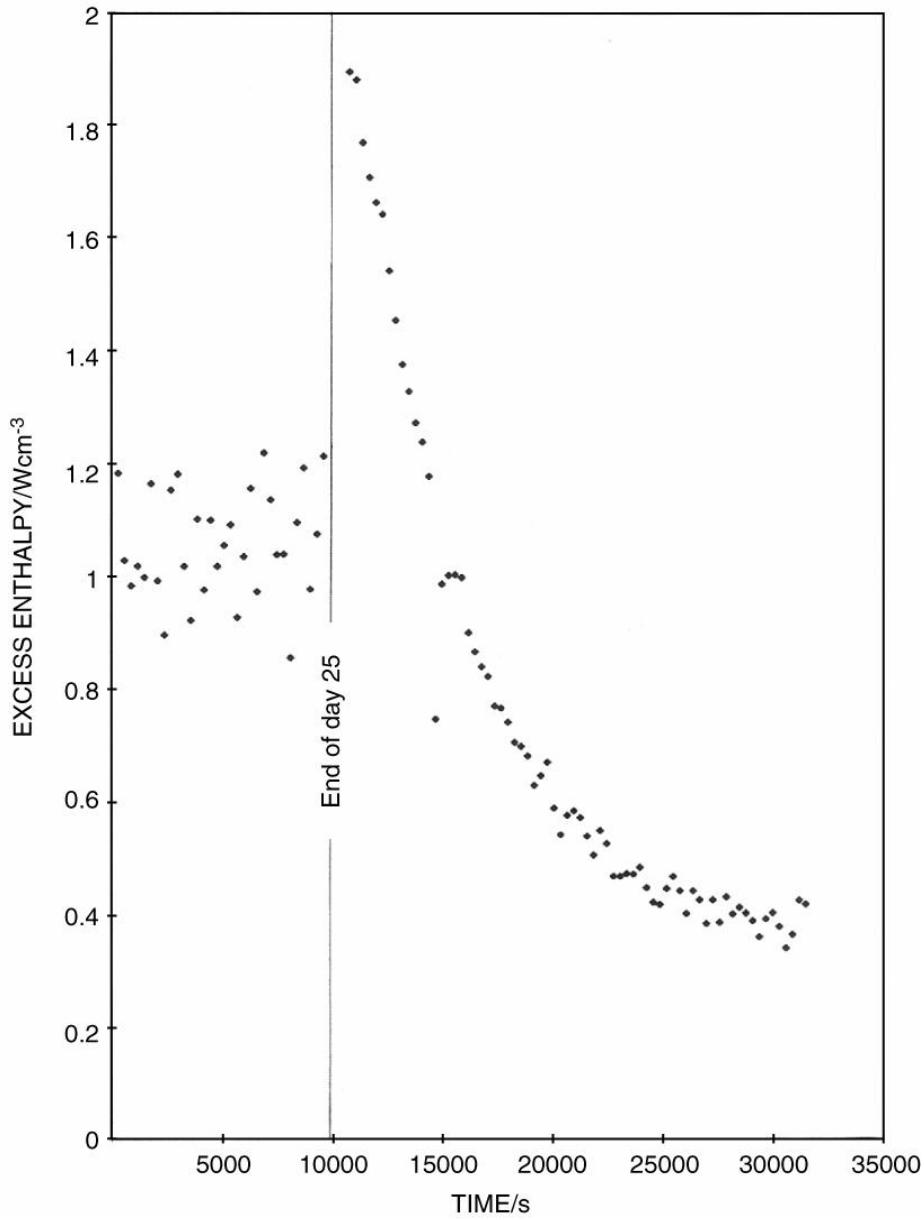

Fig. 25 The specific rate of excess enthalpy generation, Wcm^{-3}, for the last part of operation on day 25 and the first part on day 26.

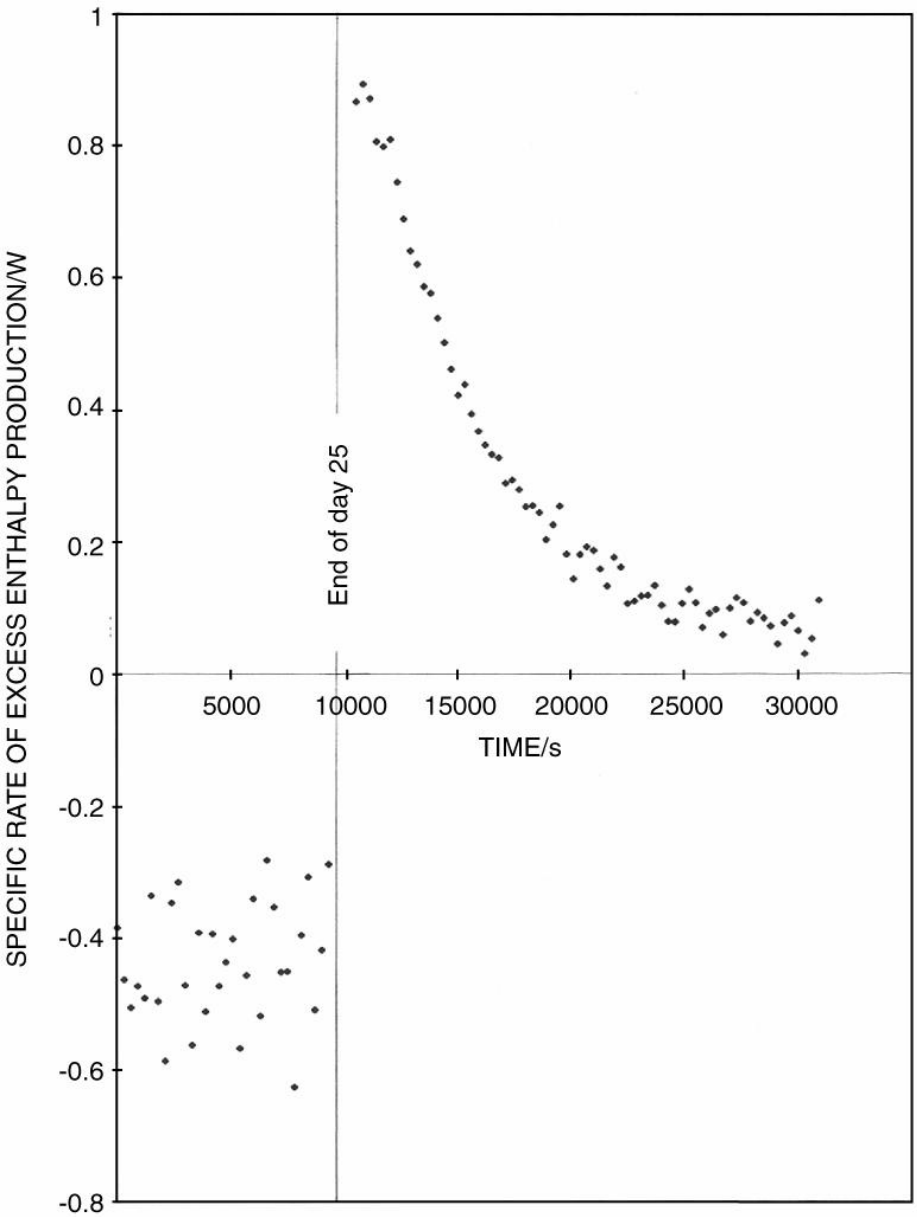

Fig. 26. The specific rate of excess enthalpy generation for the last part of operation on day 25 and the first part of operation on day 26. Evaluation given by the group at the NHE laboratories.

namely, that the initial rate of excess enthalpy generation on day 26 is larger than the final rate on day 25. The discrepancy would be diminished if the water equivalent were even higher than 475 JK^{-1} or if we increased $(k'_R)_{12}$ in view of the evident increase in the D_2O content of the cell, Fig. 5. It does not seem possible though to eliminate the effect completely by any sensible choice of the values of C_pM and $(k'_R)_{12}$ so that the effect may be real. If this is so, then the establishment of "Heat after Death" and/or positive feedback would be more complicated than is indicated by the state variables alone. For example, the time derivatives may also be involved [9, 10]. It is evident that much further work is required on these particular aspects. This work would be justified not only from the objective of clarifying the science involved, but, also, because the judicious use of positive feedback and "Heat after Death" offers us the prospect both of increasing the power density and, at the same time, of increasing the energy efficiency. It should be noted that if we exclude the enthalpy input due to the cooling of the cell, the rate of excess enthalpy generation in the initial stages of day 26 is approximately equal to the enthalpy input, i.e., a power gain of *ca* 100% whereas it approaches *ca* 1000% for the initial stages of "Heat after Death" according to case **(ii)**[3, 4], section II/7.0, and infinity for the example of case **(iii)**, section II/8.0. It appears that if the cooling of such cells is prevented (effectively by raising the temperature of the heat sink), then enthalpy generation may be maintained for long durations (*ca* 1 week) at very high energy efficiencies [13]. It is evident that this aspect of the work requires intensive further investigation, particularly with regard to attempts to raise the power density of such devices while maintaining the high energy efficiency.

II/10 Further Comments and Conclusions.

Experiment Mc–21 exhibits all the key features which have been found in earlier work. These are in the main:
(i) excess enthalpy generation in the early stages ($t < 2$ days) due to absorption of deuterium in the lattice followed by
(ii) a build up of the rate of excess enthalpy generation
(iii) the development of positive feedback, i.e., the increase in the rate of excess enthalpy generation with increase of temperature
(iv) a marked increase in the rate of excess enthalpy generation at temperatures close to the boiling point of the electrolyte
(v) a variety of examples of the phenomenon of "Heat after Death," i.e., a maintenance of elevated rates of excess enthalpy production following reduction of the current density which may be accompanied by the complete evaporation of the electrolyte.

At the same time there are some marked differences between experiment Mc–21 and the earlier investigations: the effects of some of these differences can be explained in terms of the earlier results while some of the results are surprising. The major difference is that the measurement cycles had to be carried out at rather low current densities (low for the observation of the phenomenon)

in view of the relatively high surface area of the electrode (it is necessary to limit the power input to the cell to satisfy the design criteria of the calorimeter). As the rate of excess enthalpy generation increases markedly with the current density [1], the values achieved in experiment Mc–21 were necessarily limited (the rates increased to *ca* 25 W cm^{-3} on day 68 prior to evaporation to dryness). A secondary consequence of the low current densities was that the electrode was polarized in the vicinity of the region for the onset of positive feedback for most of the experiment duration (see Fig. 3). The use of such conditions is known to limit the rates of excess enthalpy generation, and, in the limit, may destroy the phenomenon [9, 10]).[45].

The major unexpected difference has been the observation of the development of positive feedback at a very early stage of the experiments (day 3), at a low current density and at a low temperature. It is obviously very important to establish whether this early establishment of positive feedback is a property of Pd/B alloys (such as the electrode used in experiment Mc–21).

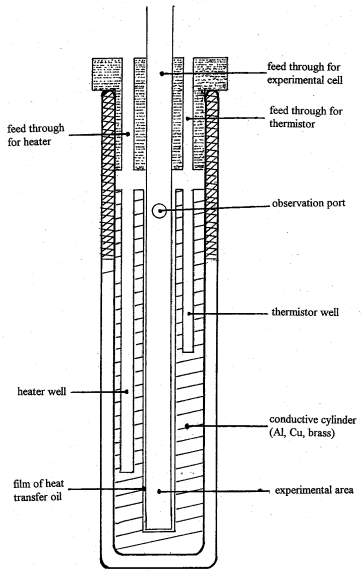

Fig. 27. The ICARUS–14 Calorimeter.

A major feature of the investigation of "Heat after Death" in experiment Mc–21 is the demonstration that the rates of excess enthalpy generation before and after the onset of the phenomenon are probably identical. Such an identity would be expected if excess enthalpy generation takes place in the bulk of the

[45]Possibly because of the cracking of the electrodes due to the repeated loading and deloading.

electrode, but these effects clearly require further investigation. It is also apparent that these processes relax with a diffusional relaxation time and prolonged maintenance of the effects evidently requires special conditions (increase of the temperature of the heat sinks) [13].

The investigation of experiment Mc–21 has demonstrated yet again that certain methods of data evaluation are unsound and/or inaccurate or imprecise (compare e.g., [6, 9, 10]). Furthermore, it is essential to avoid the effects of positive feedback as it is impossible in general to calibrate closed loop systems subject to such feedback. Calibrations can only be achieved if the effects are not too marked, as has been the case for day 3 of experiment Mc–21. Unfortunately, it is almost certain that the investigations carried out by NHE have relied precisely on such unsound and inaccurate methods of calibration and the effects of positive feedback have been ignored. However, this neglect is probably quite general and, no doubt, accounts for many of the contradictory results in this field of research. It should be noted that much of the pointless controversy in this field could have been avoided if it had been possible to replace the ICARUS-1 to -3 Calorimeters, Fig. 1, by the ICARUS-4 version,(later reclassified as the ICARUS-14 Calorimeter), Fig. 27. While it is not certain that this particular redesign would have eliminated the weak time dependence of the heat transfer coefficients observed with the ICARUS–1 Calorimeter, it is likely that this would have been true and that these systems could have been developed so that all measurements could have been evaluated with a single, predetermined value of the true heat transfer coefficient.

Finally, it is important to note that it has been possible to achieve:
(vi) a satisfactory interpretation of evaporation to dryness (day 68).

This interpretation has had to take into account: the actual barometric pressure, the change of the boiling point of the solution with increasing electrolyte concentration (saturation of the electrolyte – not discussed in the present report), and changes in the reflux ratio.[46] However, prolonged investigations of boiling conditions [7, 8] will clearly require the design and application of dual calorimeters such as the ICARUS-9 version [4, 8]. It is also important to determine whether the marked increase of the rates of excess enthalpy generation at temperatures near the boiling point are dependent on the establishment of boiling conditions or are simply due to the increase in temperature. While it is certainly desirable to develop pressurized systems to increase the boiling point, significant increases in the boiling point could also be achieved by using concentrated electrolyte solutions. The use of such electrolytes would allow the extension of the range of applicability of the ICARUS-1 calorimeters.

Finally, we can note that the interpretation of this experiment gives a good illustration of the need to evaluate all such measurements as individual case

[46]It is unlikely that the variation of the distillate with time (as determined in the NHE investigation) could be usefully interpreted.

histories: the state of development of research in this field in 1993 (when the first ICARUS system was constructed) was certainly not at the point at which such interpretations could be carried out as a matter of routine. Furthermore, the instrumentation also required a number of additional developments to facilitate any such attempts at routine evaluations. The ICARUS-14 system (then described with the label ICARUS-4) was to be the next step, but, as has already been noted, this modification could not be accomplished.

II/11.0 References.

1. M. Fleischmann, S. Pons, M. W. Anderson, L. J. Li and M. Hawkins, J. Electroanal. Chem., **287**, 293 (1990)
2. ICARUS–1, Document version 1.0 (Dec. 1993).
2A. ICARUS–2, Document version 2.0 (Feb. 1995)[47]
3. S. Pons and M. Fleischmann, ICCF–4, p. 8, 1994
4. S. Pons and M. Fleischmann, Trans. Fusion Technology, **26**, 87 (1994)
5. T. Saito, M. Sumi, N. Asami and H. Ikegami, ICCF–5 (1995)
6. M. Fleischmann, ICCF–7, p.119 (1998)
7. M. Fleischmann and S. Pons, ICCF–3, p.47 (1993)
8. M. Fleischmann and S. Pons, Physics Letters, **A 176**, 118 (1993)
9. M. Fleischmann, S. Pons, M. Le Roux and J. Roulette, ICCF–4. p. 1 (1994)
10. M. Fleischmann, S. Pons, M. Le Roux and J. Roulette, Trans. Fusion Technology, **26**, 323 (1994)
11. M. Fleischmann, ICCF–5, p. 140 (1995)
12. G. Mengoli, M. Bernardini, C. Maduchi and G. Zannoni, J. Electroanal. Chem., **444**, 155 (1998)
13. M. Fleischmann and S. Pons, unpublished, August 1994.
14. T. Roulette, J. J. Roulette and S. Pons, ICCF–6, p.85 (1996)

[47]Documents, ref. 2 and 2A are not available in open literature. Contact Dr. Miles for further information.

TABLE: Evaluation of heat transfer coefficients

The combined abridged $(k'_R)_{21}$ and $(k'_R)_{31}$– spreadsheets prepared according to the instructions in the ICARUS-systems Handbooks (restriction of the range of the integrations to the region of application of the calibration pulse $t_1 < t < t_2$). The third measurement cycle of experiment M–21. The evaluation of $(k'_R)_{31}$, $(k'_R)_{351}$, $(k'_R)_{32}$, $(k'_R)_{362}$, $(k'_R)_{22}$ and $(k'_R)_{262}$. Modification of the procedure for the evaluation of $(k'_R)_{22}$ and $(k'_R)_{262}$ to take account of the effects of "positive feedback" and evaluation of these coefficients.

Column 1: The elapsed times/s (from the start of the measurement cycle).

Column 2: $10^9 C_p M(\theta - \theta_0)/\int f(\theta)d\tau/$ WK^{-4}. Here, $\theta_0 = 300.3175K$, the average of the 11 measurements preceding the application of the calibration pulse.

Column 3: $10^9 \int (input)d\tau/\int f(\theta)d\tau/\mathrm{WK}^{-4}$

Column 4: $10^9(k'_R)_{31}/\mathrm{WK}^{-4}$.

Column 5: $10^9(k'_R)_{31}/\mathrm{WK}^{-4}$: correlation coefficient C_pM/JK^{-1}. The arrows indicate the range of the fitting procedure.

Column 6: $10^9 C_p M(\theta - \theta_0)/\Delta \int f(\theta)d\tau$ $/\mathrm{WK}^{-4}$ [evaluation of $(k'_R)_{32}$ and $(k'_R)_{352}$]

Column 7: $10^9 \Delta \int (input)d\tau/\Delta \int f(\theta)d\tau/\mathrm{WK}^{-4}$ [evaluation of $(k'_R)_{32}$ and $(k'_R)_{352}$].

Column 8: $10^9(k'_R)_{32}/\mathrm{WK}^{-4}$.

Column 9: $10^9(k'_R)_{352}/\mathrm{WK}^{-4}$; correlation coefficient C_pM/JK^{-1}. The arrows indicate the ranges of the fitting procedures.

Column 10: $10^9 C_p M(\theta - \theta_0)/\Delta \int f(\theta)d\tau/\mathrm{WK}^{-4}$ [evaluation of $(k'_R)_{22}$ and $(k'_R)_{252}$]. Here $\theta_0 = 303.074\mathrm{K}$, the average of the last 11 measurements during the application of the calibration pulse.

Column 11: $10^9 \Delta \int (input)d\tau/\Delta \int f(\theta)d\tau$ $/\mathrm{WK}-4$.

Column 12: $10^9(k'_R)_{22}$ $/\mathrm{WK}^{-4}$.

Column 13: $10^9(k'_R)_{252}/\mathrm{WK}^{-4}$: correlation coefficient C_pM/JK^{-1}. The arrows indicate the range of the fitting procedures.

Column 14: Modification of column 11 to take account the effects of "positive feedback".

Column 15: Values of $10^9(k'_R)_{22}$ taking into account the effects of "positive feedback".

Column 16: $10^9(k'_R)_{252}$ $/\mathrm{WK}^{-4}$; correlation coefficient taking into account the effects of "positive feedback C_pM/JK^{-1}.

1	2	3	4	5	6	7	8	9	10	11	12	13	14	15	16
32400									0.24271	0.99723	0.75452		1.09389	0.85118	
32700	0.46642	1.27671	0.81029		25.06(903)	24.33(815)	-0.731		0.22862	0.98311	0.75449		1.0798	0.85118	
33000	0.42785	1.25578	0.82793		12.747(14)	13.241(78)	0.494(64)		0.21588	0.97005	0.75417		1.06681	0.85093	
33300	0.40607	1.23659	0.83053		8.5514(0)	9.2018(3)	0.6504(3)		0.20383	0.95792	0.75409	0.7421	1.05478	0.85095	0.85065
33600	0.38577	1.21953	0.83375		6.40541	7.1495	0.7441		0.19286	0.94653	0.75367	477.1	1.04384	0.85098	449.5
33900	0.364	1.20417	0.84017		5.07334	5.92216	0.84882		0.18338	0.93579	0.75241	0.99997	1.03366	0.85028	0.99998
34200	0.35352	1.1896	0.83608		4.26961	5.06778	0.79817		0.17288	0.9257	0.75281		1.02378	0.8509	
34500	0.33827	1.17622	0.83795		3.62112	4.44399	0.82287		0.16413	0.91609	0.75197		1.0146	0.85047	
34800	0.32539	1.16323	0.83784		3.15141	3.97478	0.82337		0.15565	0.90713	0.75149		1.00624	0.85059	
35100	0.31191	1.15018	0.83828		2.76989	3.59848	0.82859		0.14816	0.89893	0.75076		0.99854	0.85038	
35400	0.29981	1.13779	0.83798	0.8354	2.46763	3.29456	0.82693		0.14104	0.89125	0.75021		0.99113	0.85009	
35700	0.29099	1.12608	0.83509	453.6	2.23996	3.04547	0.80551		0.13332	0.88404	0.75073		0.98387	0.85055	
36000	0.28023	1.11507	0.83484	0.99865	2.03271	2.83835	0.80565		0.12704	0.87724	0.7502		0.97724	0.8502	
36300	0.27048	1.10475	0.83427		1.86157	2.66515	0.80357		0.12099	0.87079	0.74981		0.97119	0.8502	
36600	0.26116	1.09493	0.83377		1.71403	2.51589	0.80186	0.82997	0.11535	0.86474	0.74939	0.74174	0.96543	0.85008	0.85145
36900	0.25283	1.08563	0.8328		1.58858	2.38598	0.7974	447.2	0.10976	0.859	0.74924	479.2	0.95999	0.85023	444.5
37200	0.24418	1.07686	0.83268	0.82059	1.47497	2.27325	0.79829	0.99966	0.10497	0.85353	0.74856	0.99985	0.9549	0.84993	0.99995
37500	0.23679	1.06864	0.83175	473.2	1.37989	2.1742	0.79431		0.09991	0.84836	0.74845		0.94993	0.85002	
37800	0.2298	1.06061	0.83081	0.99949	1.29538	2.08589	0.79051		0.09507	0.84345	0.74838		0.94514	0.85007	
38100	0.22279	1.05328	0.8305		1.21766	2.00793	0.79027		0.09076	0.83859	0.74784		0.94097	0.85022	
38400	0.21634	1.04647	0.83014		1.14887	1.93864	0.78976		0.08646	0.83378	0.74732		0.93727	0.85081	
38700	0.20943	1.03973	0.83029		1.0831	1.87497	0.79187		0.08312	0.8294	0.74628		0.93352	0.8504	
39000	0.20943	1.03309	0.82911		1.02949	1.81653	0.78704		0.07885	0.82544	0.74658		0.92966	0.85081	
39300	0.19822	1.02667	0.82844		0.97771	1.76266	0.78495		0.07535	0.82176	0.74641		0.92608	0.85073	
39600	0.19249	1.02061	0.82812		0.92928	1.71383	0.78455		0.07231	0.81817	0.74586		0.92279	0.85048	
39900	0.18757	1.01484	0.82727		0.88753	1.68916	0.78163	0.7952	0.06873	0.81472	0.74598	0.74364	0.91952	0.85079	0.85131
40200	0.18244	1.00923	0.82679	0.81535	0.8471	1.62754	0.78045	451	0.06586	0.81154	0.74569	464.2	0.91639	0.85053	445.4
40500	0.17786	1.00379	0.82593	480.7	0.81117	1.58878	0.7776	0.9999	0.06266	0.8066	0.74594	0.99924	0.91353	0.85087	0.9997
40800	0.17291	0.99855	0.82564	0.99985	0.77535	1.55266	0.77731		0.06044	0.80586	0.74542		0.91087	0.85043	
41100	0.16877	0.99363	0.82485		0.74495	1.51978	0.77484		0.05741	0.80311	0.74571		0.90837	0.85096	
41400	0.16414	0.98893	0.82479		0.71379	1.48932	0.77553		0.05563	0.80045	0.74483		0.90611	0.85048	
41700	0.16015	0.98436	0.82421		0.68662	1.46054	0.77392		0.05316	0.79802	0.74486		0.90382	0.85066	
42000	0.15643	0.97997	0.82355		0.66169	1.43369	0.772		0.0506	0.79569	0.7451		0.90134	0.85074	
42300	0.15281	0.97579	0.82298		0.63825	1.40873	0.77049		0.04819	0.79342	0.74523		0.89893	0.85074	
42600	0.14935	0.97168	0.82232		0.6163	1.3849	0.7686		0.04582	0.79145	0.74563		0.89697	0.85115	
42900	0.14574	0.96787	0.82214		0.59443	1.36309	0.76866		0.04417	0.78921	0.74503		0.89502	0.85085	
43200	0.14223	0.96413	0.82191		0.57377	1.34227	0.76851	0.78033	0.04274	0.78726	0.74452		0.89348	0.85074	
43500	0.13903	0.96055	0.82153		0.55506	1.32278	0.76772	459.9	0.04095	0.78535	0.7444		0.89158	0.85063	
43800	0.13633	0.95708	0.82075		0.53888	1.30424	0.76537	0.9999	0.03817	0.78357	0.7454		0.88944	0.85127	
44100	0.13325	0.95374	0.82049		0.5217	1.28674	0.76504		0.03678	0.78186	0.74508		0.88773	0.85095	
44400	0.13033	0.95052	0.82018		0.50567	1.2702	0.76453		0.03532	0.78022	0.7449		0.88633	0.85101	
44700	0.12757	0.94738	0.81981		0.49064	1.25441	0.76377		0.03378	0.77874	0.74496		0.88519	0.85141	

1	2	3	4	5	6	7	8	9	10	11	12	13	14	15	16
45000	0.12465	0.94437	0.81971		0.47544	1.23946	0.76402		0.03316	0.77729	0.74413		0.88411	0.85095	
45300	0.12231	0.94147	0.81916		0.46283	1.22536	0.76252		0.03094	0.77587	0.74493		0.8826	0.85166	
45600	0.1198	0.93866	0.81886		0.4499	1.21186	0.76197		0.02965	0.71456	0.74491		0.88128	0.85127	
45900	0.11727	0.93591	0.81864		0.43714	1.19887	0.76174		0.02884	0.7734	0.74456		0.88029	0.85145	
46200	0.115	0.93329	0.8183		0.42563	1.18663	0.761		0.0274	0.77219	0.74479		0.87919	0.85179	
46500	0.11274	0.93076	0.81802		0.41447	1.17498	0.76052		0.02625	0.77103	0.74479		0.87806	0.85181	
46800	0.11058	0.92829	0.81771		0.40392	1.1638	0.75988		0.02501	0.77003	0.74502		0.87699	0.85198	
47100	0.10854	0.92603	0.81749		0.39411	1.15369	0.75958		0.02365	0.76851	0.74486		0.87534	0.85169	
47400	0.10652	0.92376	0.81723		0.3845	1.14361	0.75911		0.02242	0.76735	0.74493		0.87428	0.85186	
47700	0.10452	0.92157	0.81705		0.37511	1.13404	0.75893		0.02155	0.76614	0.74459		0.87363	0.85206	
48000	0.10248	0.91943	0.81695		0.36575	1.12475	0.759		0.02136	0.76512	0.74377		0.87317	0.85181	
48300	0.10067	0.91734	0.81667		0.35737	1.11582	0.75845		0.0201	0.76416	0.74406		0.87222	0.85212	
48600	0.09901	0.91532	0.81631		0.35883	1.13635	0.75752		0.01815	0.76324	0.74508		0.8713	0.85315	
48900	0.09705	0.91336	0.8163		0.34102	1.099	0.75799		0.01891	0.76238	0.74347		0.87066	0.85175	
49200	0.09563	0.91145	0.81582		0.3344	1.09108	0.75668		0.01573	0.76158	0.74585		0.86978	0.85405	
49500	0.09378	0.90958	0.81581		0.32638	1.08341	0.75702		0.01676	0.76097	0.7442		0.86896	0.8522	
49800	0.09243	0.90776	0.81533		0.32024	1.07598	0.75574		0.01335	0.76049	0.74714		0.86803	0.85468	
50100	0.09074	0.90599	0.81525		0.31296	1.06882	0.75586		0.01399	0.7601	0.74611		0.86754	0.85355	
50400	0.08926	0.90428	0.81502		0.30657	1.06197	0.7554		0.01267	0.75964	0.74697		0.86667	0.854	
50700	0.08801	0.90264	0.81463		0.30102	1.05545	0.75544		0.00886	0.75903	0.75017		0.8653	0.85644	
51000	0.08642	0.90106	0.81465		0.29442	1.04925	0.75482		0.01024	0.7582	0.74197		0.86564	0.8554	
51300	0.08497	0.89952	0.81455		0.28841	1.04321	0.7548		0.01027	0.75759	0.74733		0.86619	0.85592	
51600	0.08373	0.898	0.81428		0.28314	1.03733	0.75419		0.00722	0.75725	0.75003		0.86504	0.85782	
51900	0.0825	0.89654	0.81405		0.27798	1.03169	0.75372		0.00402	0.75676	0.75274		0.86322	0.8592	
52200	0.08128	0.89514	0.81386		0.27293	1.02633	0.7534		0.00058	0.75579	0.75521		0.86019	0.85961	
52500	0.08027	0.89378	0.81351		0.26865	1.02116	0.75251		-0.01015	0.75445	0.7646		0.85718	0.86733	
52800	0.07883	0.89244	0.8136		0.26299	1.01608	0.75309		-0.00652	0.75358	0.7601		0.85731	0.86351	
53100	0.07775	0.89111	0.81336		0.25857	1.01111	0.75255		-0.01853	0.75349	0.77202		0.85985	0.87838	
53400	0.07649	0.86981	0.81332		0.25356	1.00626	0.7527		-0.0229	0.75471	0.77761		0.86311	0.88601	
53700	0.07547	0.88855	0.81308		0.24946	1.0016	0.75215		-0.07549	0.75743	0.83293		0.86599	0.94148	
54000	0.7409	0.88736	0.81327		0.24416	0.99723	0.75304								

CHAPTER 5: AN OVERVIEW OF COLD FUSION THEORY.

Scott Chubb

1.0 Introduction.

Naval Research Laboratory (NRL) involvement in cold fusion (CF) started when Talbot Chubb and Scott Chubb started to develop a theory of the anomalous heating effect [1]. The basis of this theory involves known phenomena (associated with wave-like behavior) that occur when hydrogen (H) and deuterium (D) interact with Pd (and other transition metal) lattices. In particular, at an early stage, Talbot and Scott Chubb observed that well known effects associated with H in metal systems, as well as the well documented literature concerning this area could imply that the hypotheses involving high energy, close proximity effects that were commonly thought to be relevant, at best, could be only tangentially related to the excess heat effect; at worst, these ideas could be largely irrelevant.

In most cases, the associated picture reflects an intuitive scenario that is based on conventional nuclear fusion, where a classical/semiclassical model applies, involving a collision between two, clearly distinguishable particles, at an isolated location in free space. Although this physical model is perfectly satisfactory for this kind of situation, it omits important details involving coherent effects in solids that are known to be especially important at low temperature.

This picture also implicitly requires that high momentum particles either be present or become involved in such a way that radiation, at copious levels, be released. Because, in fact, it is now known that appreciable levels of radiation are not involved, it is clear that this semiclassical picture at best is only tangentially involved. At worst, the associated picture oversimplifies the associated situation to such an extent, that it, in and of itself, can be viewed as providing

a hidden barrier for understanding the relevant physics. Because of the inherent limitations of such a barrier, it is convenient to view this conventional picture of existing physics as a box. Within this context, it is useful to examine precisely what is known about this box and how it relates in more general terms to less conventional pictures, which although consistent with conventional Physics, are viewed today as being outside the box.

With this in mind, in the next section, we re-examine the conventional picture of fusion, based on its pre-defined framework. (We refer to this framework as the box associated with conventional fusion, and to the underlying theory behind the framework as its organizing principles.) In the following section, inherent oversimplifications of these principles are identified. In the same section, through the conventional laws of physics, we explain how it is possible to move beyond the boundaries of the box, associated with these organizing principles. In the third section, we provide some history associated both with the identification of these boundaries and with attempts to overcome them. This provides a useful context for identifying well formulated theories, from those that must be viewed as being in a more primitive state. Specifically, although the associated phenomena have been illusive, with time not only have the most important effects been identified, three theories (by Chubb and Chubb [2], Hagelstein [3], and Kim [4]) provide a common theoretical framework, involving many-particle interactions (many-body physics), that are based on well formulated physical ideas that are consistent with known physical law, and these theories not only provide a useful framework for explaining many of these effects but for making new predictions concerning their behavior.

In particular, after presenting criteria for identifying the most useful theories, we examine three of the most well developed theories (which include [2–4], as well, as a fourth theory by Preparata [5]). Each of these theories is sufficiently well developed that it provides a procedure for constructing a realistic reaction rate expression that explicitly illustrates how reactions might occur, based on known physical effects, in such a way that excess heat could be produced through a fusion reaction, without neutrons, tritium, and radiation. Three of these theories [2 through 4] also make use of a basic, known idea, i.e., coherence, as it relates to many-body physics, to account for this. (Preparata's theory [5] involves coherence in a non-standard form, that might or might not be applicable to conventional many-body physics).

The three theories [2–4] also deal in fundamental ways, with the release of momentum, coherently from one location, to many locations, in a way that not only is consistent with the known laws of Quantum Mechanics, but that accounts for the reason that the standard, two-particle picture is deficient. Each of these theories has been formulated using a well formulated mathematical model. For this reason, each of these theories is known to apply when particular, well defined mathematically testable hypotheses, and limits hold. This is by no means true for many of the more speculative theories that have been presented previously.

Finally, the three theories [2 through 4] involve models that include coherent coupling to the solid that can be generalized, within the context of known physics, in such a way that they can be readily used to investigate other Low Energy Nuclear Phenomena. With this point in mind, in Section 5, additional information about the common features of the theories is discussed. The final section provides a series of conclusions about the existing state of affairs, and potential lessons that might be learned as a result of the adjudication process.

2.0 Inside and Outside the Box and the Organizing Principles of Conventional Fusion.

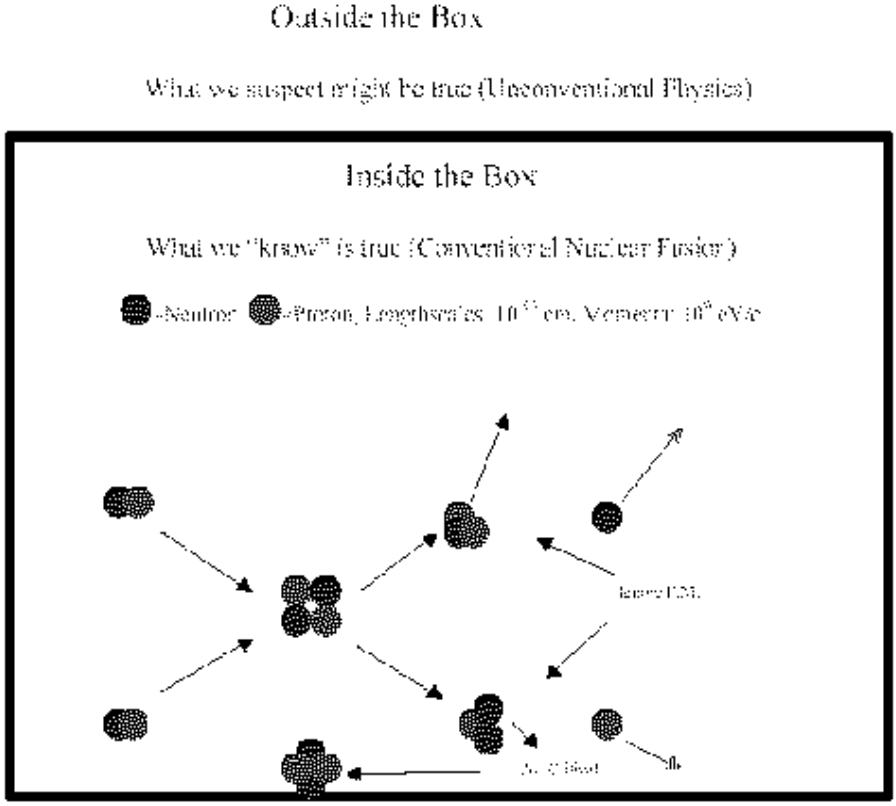

Logical thought requires rules. In physics, the logical rules follow from Newton's laws of motion, Maxwell's equations, quantum mechanics, and relativity. Because these rules provide a framework, often they can be self-limiting. For example, sometimes physicists misinterpret the rules, simply because they are conditioned to look at them in a particular way. They become used to a particular worldview. The worldview can be thought of as a kind of box that defines

a comfort zone. Often, the box is tied to the way we have learned a particular subject. Different people view the box in different ways. Kuhn [6] refers to it, abstractly, as it relates to science, as a paradigm. Others have not been as open minded [7].

Figure 1 shows a pictorial representation of conventional fusion reactions superposed on an idealized representation of the box, associated with what is commonly viewed as conventional (labeled inside the box) and unconventional (labeled outside the box) science. In this schematic, all reactions originate from a configuration in which two deuterons (shown as proton/neutron pairs) overlap with each other in a manner that forms a configuration (shown in the center of the plot) that resembles an excited state of a 4He nucleus. The two dominant reactions (D+D→3He+n, and D+D→3H+p) that occur in free space are essentially blind to the presence of the electromagnetic interaction (EMI). For this reason, it is possible to treat these reactions within a framework in which the dependence of the reaction on electromagnetic interactions is independent of its dependence on the nuclear (strong force) interaction. This means that in these reactions, the associated wave functions describing the initial and final states do not couple the nuclear and electromagnetic interactions. As a result, the general reaction rate expression effectively precludes the strong force from talking to the electromagnetic force, by construction. The figure schematically illustrates this point through the labels (ignore E. M.), next to the arrows that are shown in the right portion of the figure. Also shown is the remaining fusion reaction (D+D→4He). This reaction occurs rarely in conventional fusion. For this reason, in the figure it is shown as occurring at the boundary of the box. A second reason we have drawn it at the boundary is that it violates a paradigm that many nuclear physicists believe to be valid: in conventional fusion, the strong and electromagnetic interactions remain uncoupled. For this reason, it is widely believed that the final (D+D→4He) reaction should rarely occur and the two remaining reactions should occur with roughly the same probability. However, the D+D→4He reaction does occur, and the reason that it is not frequently observed is well understood: it violates energy and momentum conservation unless a high energy momentum $\gamma-$ ray is emitted, and the associated EMI involves a complicated (quadrupolar) coupling between nucleon spins (that occurs as a second order electromagnetic process). Two important points are as follows: (i) although this final reaction occurs infrequently relative to the others, when it occurs, the nuclear and electromagnetic interactions do talk to each other, and (ii) it occurs rarely because the associated processes involve overlap between two particles at a single location.

2.1 Motivational Physics for Getting Outside the Box.

Part of the confusion with the box associated with conventional nuclear physics involves the definition of momentum p: for a single charged particle, p does not equal mass (m) times velocity (v); the rules of the box are: for a particle possessing charge q, mv=p-q/c**A**, where **A** (the vector potential) is associated

with the electromagnetic interaction, and c is the speed of light. Although this rule is based on classical physics, how and where it applies seems to have been a source of confusion. The rule follows from the box defined by classical physics. (False assumptions about this rule not only appear to have led to confusion about Cold Fusion but to more serious problems.) An example of the importance of this distinction occurs in the p→0 limit, when many particles share a common density ρ_0. When this occurs, mv, which is proportional to the current J (provided ρ_0 is uniformly constant [8]), becomes proportional to **A**. But **A**, which is defined by the static wave equation ($-\nabla^2\mathbf{A} = 4\pi J/c$), then obeys a Helmholtz equation [8] ($-\nabla^2\mathbf{A} = -4\pi q^2\rho_0\mathbf{A}/mc^2$) that results in **A** asymptotically vanishing beyond a critical coherence length, where J approaches a constant value. This occurs even in the absence of an applied electromagnetic field (EMF). The resulting picture explains the phenomenon of superconductivity. It also explains how as p→0, superconductivity not only is present, but because the current vanishes at some boundary, surrounding the region where superconductivity occurs, the effects of boundaries may result in the expulsion of magnetic flux when p=0 (the Meissner effect) or flux quantization [8], when p does not vanish but takes on values that are consistent with the associated rules (defined by the box) associated with the requirements of quantum mechanics [8].

The basis of both phenomena is that p does not equal mv. In situations where the DeBroglie wavelengths of particles become sufficiently large, particles become wavelike. In this kind of situation, the average value of the gradient of the phase of the associated collection of waves (which is described by the many-body wave function) defines the momentum. The important point is that the phase of the many-body wave function, as opposed to a quantity related either directly to the current or to mass × velocity defines how the momentum behaves. When p→0, this quantity can be affected in ways that are non-local in character. This may occur because non-local changes in **A** can significantly alter the value of the phase. Because a priori, it is not possible to predict if a solid is at rest or in motion, for example, its center-of-mass wave function can be altered by an arbitrary complex number. This introduces the possibility of an arbitrary gauge transformation in the definition of the **A** that applies inside and outside a solid. Because in the p→0 limit, it becomes possible to determine if the solid is in motion or at rest, the associated arbitrariness in gauge is removed. Not only does this mean that the associated gauge symmetry becomes broken, but physical effects (for example, the expulsion of magnetic flux, or spontaneous lattice recoil [as in the Mossbauer effect]) can occur. The resulting coherence can be viewed in different ways, within the framework (the box) associated with a particular discipline.

In similar ways, effects of periodic order and other symmetries can become important in situations in which the wave-like character associated with large De-Broglie wavelengths becomes important. The important point is that because momentum is associated with wave-like behavior, it can change suddenly, in unexpected ways, on arbitrarily short time scales. These changes can result

in instantaneous changes in which large amounts of momentum coherently are shifted to many particles, and vice versa. How or if this occurs is dictated by the dynamics of the many-body system.

3.0 Some History of Theoretical Development and Some Useful Criteria

3.1 A Historical Development

In general terms, oversimplification has plagued CF and CF theory, both in the past, and at the present time. In particular, at a very early point in the adjudication process, the overly simplified picture of Fusion, associated with the box, described in section 2.0, undermined discussion of Cold Fusion (CF) claims to such an extent that the box, its products, and the associated context, obfuscated identification of the relevant products and process.

This created such confusion that the resulting uproar caused a serious breach in the conventional scientific process [9]. From this starting point, for quite a while, it became virtually impossible to obtain a reasonably unbiased assessment of the existing theoretical situation. This occurred not only in the conventional review process in mainstream scientific meetings (where discussions about CF and CF theories remained largely nonexistent until 1996), but also in less conventional settings (including the first five International Conferences on the subject).

It also affected not only how theories were adjudicated, but how various reviews of theories were prepared. In particular, because of lack of involvement of outside reviewers, theoretical ideas of marginal utility not only have been proposed, but published reviews of these ideas have appeared that neither have been objectively reviewed or assessed based on objective criteria. All of this has occurred primarily because of lack of funding and interest, and even rudimentary knowledge (in some cases [10]) of the relevant facts. Further aggravating the situation has been a language problem: the field, which was misnamed from the beginning, attracted many individuals with different backgrounds, areas of expertise, and even different intuitive notions about what constitutes a meaningful definition of theory.

A fundamental reason for this is that considerable attention was focused, from the beginning, on marginal effects (involving high energy nuclear products). As a result, many of the intuitive theoretical ideas associated with Nuclear and High Energy Physics were applied. Unfortunately, because the associated effects have proven to be marginal at best (if applicable, at all), the associated intuitive ideas have been a source of confusion.

For example, it was widely assumed that the seemingly obvious idea that high momentum particles are required by CF should be invoked. A less obvious intuitive notion that appears to have been a potentially more serious source of confusion is the opinion that one or several guiding principles, associated with

either one, or a small number of particular forms of particle/particle reaction, or particular forms of interaction, are responsible for all of the observed phenomena. In particular, initially, logic based on reduction (or reductionism) to a single form of reaction (or small set of reactions) led a number of theorists to speculate that some new form of particle (Rafelski [11], Teller [12]), or interaction (Mayer and Reitz [13], Vigier [14], Mills [15]) could be invoked. In subtler ways, this reductionist principle has persisted, even to the present time (Kozima [16]).

A theoretical construction involving this Reductionist philosophy can be appropriate and useful when it is possible to identify how momentum is distributed. It can (and probably does) cause confusion when many particles interact with low momentum. For this reason, the intuitive idea that such a construct should be applicable may obfuscate the relevant physics. Specifically, in situations where this philosophy has been used as a guiding principle, not only has confusion resulted, but, in a number of cases, arguments about terminology and meaning have resulted that have had a counterproductive effect on communication. Important reasons for the associated deterioration in dialogue partly reflect the very different perspectives between theoretical practices followed by High Energy and Nuclear Physicists, as opposed to those that are used by Chemists and Solid State Physicists.

An additional, potentially more significant reason for this deterioration, however, may reflect a more fundamental aspect of the problem: reliance on the Reductionist philosophy seems to be quite appropriate in the experiments involving collisions between particles possessing high momentum (HM), but probably does not apply in general. When HM particles are used, clearly defined experiments, involving well defined, controllable variables can be conducted. Reliance on this philosophy can become inappropriate in lower temperature environments, associated either with the ground state or near ground state configurations. This is because in these kinds of configurations, frequently, it is difficult to define either the experimental situation in precise terms or to identify precisely the variables that govern the underlying dynamics.

Another way of phrasing this potential problem is that because in the Reductionist philosophy an attempt is made to identify a particular form of interaction, it is possible to misidentify the relevant physics simply as a result of oversimplification. In particular, this kind of approach can simply fail to incorporate the effects of many-particle interactions that are known to occur at low/moderate momentum. The fact that it is entirely possible that these interactions are responsible for the complicated nature of the underlying phenomena suggests that a more useful approach involves a less restrictive set of assumptions than the ones that result from applying a Reductionist philosophy. For example, in invoking this Reductionism construct, Teller [12] pointed out that not only is it necessary that the associated theory be consistent with all known effects, but that insuring that this occurs is a difficult task.

The much simpler idea, that momenta could be shared by many particles, at once, in a well defined way in solids, or through related, coherent phenomena, involving many-body systems, not only is a considerably more workable hypothesis, but this idea was suggested early in the debate by Schwinger [17], and others [2]. The important point is that both the Reductionism approach and the appeal to the notion of coherence rely upon known strategies for overcoming seemingly impossible circumstances. Unfortunately, neither the idea of identifying a way to overcome existing theoretical limitations, or the underlying spirit that is responsible for adopting these kinds of strategies seems to have been fully appreciated. (In particular, Schwinger [17] was criticized [18, 1, 10], based on a detailed argument that focused on the particular mechanism that he proposed for coherence that assumed that the argument required that large changes in momentum occur at a particular point. Teller was criticized for his language. Neither criticisms paid attention to underlying motivation: a means of going outside the box, associated with conventional fusion.)

Despite these problems, both Schwinger [17] and Teller [12] recognized an important point. Conventional thinking about fusion has limitations. These were ideas. They were and remain important. But they are not theories. Ideas can lead to theories. Ideas, by themselves, are merely ideas. An unfortunate problem is that although well defined theories that are consistent with the known laws of physics do exist, the larger scientific community appears to be ignoring them. Partly because of this fact, even within the CF community, confusion [1, 10, 18, 19] exists about what constitutes (or should constitute) a theory.

3.2 Criteria for a Useful Theory

In 1990, Preparata [19] proposed a series of miracles that in his view any CF theory had to account for, in order to for it be considered "valid". Given the lack of communication that was present at the time, and the assumption that intuitive notions associated with high energy physics provided a useful starting point for understanding CF, this statement was useful. However, with hindsight, I would suggest this view reflected more a fundamental problem associated with the relevant perspective at the time than with the relevant physics. Specifically, Preparata defined the problems that *would be relevant provided CF mimics Hot Fusion.* In the context of Hot Fusion, overcoming these problems seemed to be miraculous because of a very basic assumption: *for CF to occur as it occurs in Hot Fusion, it is necessary for momentum from a small number of particles to be imparted, all at once, at a specific location.*

This is a perceived problem that *may be irrelevant, provided instantaneously, momentum is transferred* either from a small number of particles to many particles (as in the Mossbauer effect), or between many particles (as in a laser). In fact, both how Preparata identified and how he dealt with this problem, reflects a more general difficulty in the associated debate: a propensity for overreliance on specific, detailed views of the relevant theoretical framework, without identi-

fying a set of widely accepted organizing principles.

It can be argued that a more general principle probably applies: the possibility of coherent transfer between many particles of momentum to many locations, at once. Although in high energy physics this idea is foreign, (as illustrated by the examples mentioned in section 2.0), it is well known to occur in the low temperature (small momentum) limit in which the identities of individual particles can become lost.

Given the dynamics at the time, Preparata's efforts were admirable. In fact, he was quite correct in identifying a particular set of ideas that bother high energy physicists. He was also quite correct in identifying a particular concept that could eliminate the associated problem: coherent coupling between an electromagnetic field and a solid. In addition, he identified a particular form of coupling, involving the possibility of low momentum fluctuations that he suggested could provide such a coupling.

Although the idea of photon induced coherence involving low momentum fluctuations is a useful starting point for potentially describing the associated phenomena, there are two serious failings in his treatment: (i) he assumed an oversimplified (semiclassical) coupling between the photons and the solid, involving a picture in which discrete particles are involved in the interaction at isolated locations, and (ii) more importantly, he assumed that his very specific model would become widely accepted.

The reason for singling out this second problem is associated with what I would define as the most important goal of any theory:

1. For a theory to be useful, it must be accepted.

In order to satisfy this assumption, it follows that:

2. For a theory to be useful, it must be based on organizing principles that are consistent with the predominant language and theories that are present at the time the theory is formulated.

To insure that both of these assumptions are satisfied,

3. A theory must be reducible to mathematical expressions that are useful to experimenters and are based on known results, derived from the organizing principles associated with known theory, as accepted by the wider scientific community.

Although Preparata identified failures in the existing high energy physics paradigm associated with possible low energy nuclear reactions, he had difficulty having his theory accepted because it was not based on widely accepted organizing principles. In contrast to this problem, although Schwinger identified

widely accepted organizing principles, and used these principles to define a useful mathematical framework for analyzing the associated effects, his theory was not accepted by the high energy physics community (including Preparata) because this community found that his organizing principles were foreign. Unfortunately, because some of the mathematical details associated with his particular model could be questioned, even by solid state physicists, after his death, arguments were presented that questioned the validity of his theory, based on very specific aspects of his model [18, 1, 10]. In both cases, the theory failed to satisfy requirement 3. (Preparata failed because he based his theory on organizing principles that are not widely accepted. Schwinger failed because, although his organizing principles were sound, they were not recognized as being relevant and because a detailed analysis of the associated mathematical expressions could be questioned, based on known results.)

An additional reason both Preparata and Schwinger had difficulty in having their theories accepted is that the experimental situation was poorly defined initially. Since 1995, this situation has changed. In particular, it is now known that high energy particles essentially are not involved in the associated phenomena.

Although various low level byproducts are found to be produced, in the most well studied case (involving Pd/D), the dominant byproduct is Helium-4, which, in most cases, is released either in regions near the surfaces, interfaces, or cracks of the associated materials, or in the out-gases, located outside the materials. It also is now widely recognized that material preparation seems to be very important in initiating the effect, that Helium-3 also can be frequently produced (but that this is not the dominant byproduct), and that in cases involving anomalous heat in Ni-based systems, a very different form of reaction, initiated with significant amounts of H present, occurs.

These experimental results suggest three additional requirements for a valid CF theory involving Pd/D:

4. An appropriate Pd/D theory must explain why high momentum particles are virtually never emitted.

5. It must explain why coupling can be material specific.

An appropriate CF theory associated with Ni should

6. Either explain or provide a mechanism for explaining why the Ni environment potentially can result in forms of CF that are very different than in Pd/D.

In fact, in the context of many-body physics, based on a well defined reaction rate expression, it is possible to satisfy all six of these criteria, provided the associated theory addresses an additional requirement.

7. The theory should explain how nuclear dimension and atomic dimension pro-

cesses can be coupled without requiring the release of high momentum particles.

There are two additional criteria that obviously must be satisfied.

8. How to overcome the Coulomb barrier.

9. The theory should also provide a framework for understanding when high energy particles are released.

4.0 Useful Theories

In the last section, a set of criteria for identifying more mature theories from those that must be viewed as being incomplete has been provided. Given the limitations of what can be presented in an article of this scope, only those theories will be examined that satisfy these criteria. This does not mean that other creative ideas do not exist concerning the associated phenomena. (Literally hundreds of ideas about the subject have been suggested.) Information about the associated material can be obtained elsewhere (for example, in the review by Storms [20]).

To reiterate, for a theory to become acceptable (in a workable period of time), it must use existing physics, and the rules associated with explanations of existing phenomena. In this regard, it should be emphasized that beyond the well accepted rules of high energy physics, and conventional nuclear physics, there are additional constraints that are appropriate. For example, quantum mechanics (QM) is not a localized subject. The experimenter can affect outcomes, and because of this fact, certain premises based on assumptions about locality simply are inappropriate.

Finally, theories do have organizing principles; in particular, any viable theory must possess a limit where it is rigorously valid, i.e., provable by experiment. Given these assumptions, it simply is not true that criteria for assessing the validity of theories can be stated in terms of input and output information associated with predictions about experiments. It must have some tangible relationship with existing physical theory, and it must be relatable to experiments.

Serious implications follow from these assumptions. For example, it is simply incorrect to believe that a theory is credible that is not related to known phenomena. For this reason, the premise that theories that relate purely to Cold Fusion is not valid. Instead, a valid theory must be based on organizing principles that can be shown to have some validity outside Cold Fusion.

For this reason, a number of the more exotic theories (Mills, Matsumoto, etc, for example) do not have credibility. Furthermore, QM, and the well known rules for reactions associated with QM, should (and do) provide the guiding principles that should be used for assessing the validity of a proposed theory. Unfortunately, outside of efforts by a handful of persistent theorists, this kind

of approach has not been used.

These alternative efforts simply must be viewed as being incomplete. For this reason, theories that purport that they illustrate the phenomena as occurring (for example, by overcoming the Coulomb barrier) without showing how the results relate to reaction rates, or related quantities, simply must be viewed as being in a primitive state of development, and should not be taken as seriously as those that have done this.

As mentioned in section 2.0, an important source of confusion in CF has resulted from preconceived ideas about the possible interactions that may couple the different length scales associated with nuclear processes and atomic scale processes. In point of fact, although in most instances in conventional fusion, these scales remain so far apart that they effectively don't talk to each other before, during or after the associated process, because the electromagnetic interaction does penetrate to all length scales, it does provide a means for coupling to occur between the two sets of processes. Because the electromagnetic interaction is involved in a nonseparable way with the nuclear interaction in one form of reaction (D+D→4–He), experimental evidence exists that shows that the two forms of interaction can become coupled.

A number of individuals (Schwinger [17], Chubb and Chubb [2], Preparata [5, 19]) did recognize at an early stage that the two forms of interaction could be coupled, provided a form of coherence is involved. Schwinger and Chubb and Chubb recognized that the underlying rate expression could be significantly altered as a result of this. Preparata tried to work with the existing rate expression (in which the Gamow Factor is explicitly included) while modifying the underlying potential.

An important distinction evolved as a consequence. The underlying wave functions and wave function fields associated with the charged particles provided the vehicles for describing the associated processes in the theories by Schwinger and Chubb and Chubb; in the work by Preparata, greater emphasis was placed on the nature of coherence through processes that emphasize the behavior of photons and not on subtleties associated with the manner in which light can couple to charged particles coherently. (Specifically, for example, his theory does not include important effects that are present at low temperature and momentum associated with the manner in which charged particles, by themselves, can be coupled through effects associated with particle exchange.)

For the reasons outlined in section 2.0, at low energies (and momenta) these effects can be very important. Schwinger recognized this fact. Many of the textbooks on standard many-body physics, which are the basis of knowledge of many-body physics, for most physicists, are based on the Greens function ideas associated with statistical physics that came out of Schwinger's work. Preparata's approach is more closely related to formulations (associated with

higher energies) where these kinds of subtleties are not important.

Neither approach, a priori, should be viewed as being superior to the other. However, there is a very important distinction between the wave-like formulation (used by Chubb and Chubb and by Schwinger) and the one developed by Preparata. The field oriented picture includes the known, important, nonlocal effects, discussed in Section 2.0, that occur as the DeBroglie wavelengths of a large number of particles become large; in the picture proposed by Preparata, this physics is absent.

Preparata used an alternative organizing principle to introduce coherence: coherent fluctuations involving photons with charged matter. A distinguishing feature between the two approaches is that the wave picture is guaranteed to include well known effects (Meissner effect, superconductivity, etc.) through a well known language (QM/Many–body physics) in the limit of vanishing temperature, as a consequence. While the alternative (plasma) picture suggested by Preparata did require (and has required) that a new language be developed. As it has become apparent that in a large number of situations, there simply are no high energy particles, it has been clear that the kinds of forms of coherence associated with low momenta (large DeBroglie wavelengths) are probably involved.

In parallel to the developments associated with theories by Chubb and Chubb, and Preparata, Hagelstein developed a series of different theories. Each of these, in one way or another, invoked different forms of coherence. Initially, he felt that implicitly, in the evaluation of rate expressions, incorporation of Coulomb effects were such a serious impediment, that it was necessary to invoke a new form of interaction (involving neutral particles [neutron hopping], for example) to circumvent the associated difficulties. Note that in this context he did not rely (and has not relied) on a formulation in which the rate expression uses the Gamow factor, and thus (in common with Schwinger and Chubb and Chubb), has not constrained the strong and electromagnetic forces to be separable in the evaluation of rate expressions. (The Gamow theory assumes separability between electromagnetic and strong interactions.)

An important point is that in his present theory, he (Hagelstein) has included effects that implicitly involve coupling through the Coulomb interaction (through phonons). This has brought his theory more in line with some of the ideas suggested by Schwinger, and Chubb and Chubb. An important difference between the pictures, however, is that the effects of coherence, as manifested in the large DeBroglie wavelength limit phenomena (in which momentum $p \to 0$, for a large number of particles) are not directly included in his theory. Thus, as in Preparata's theory, he assumes the related $p \to 0$, coherent effects (such as superconductivity), associated with $T \to 0$, are not relevant. Also, at the present time, his theory does not incorporate boundary effects or finite crystal size effects.

From an early stage, the focus of Yeong Kim's work has been to develop a multi–nucleon theory that goes beyond the Gamow-like rate expression of conventional fusion. More recently, in examining problems that are involved in optically trapped (bosonic) atoms, it occurred to him that similar kinds of ideas could be used in the deuteron fusion problem in condensed matter. Because this framework is associated with coherence through effects that become important at large DeBroglie wavelengths, Kim does directly use the kinds of $p \rightarrow 0$ effects that Chubb and Chubb include, which are omitted by Hagelstein and Preparata and DelGuidice.

5.0 Common Features of Developed Theories.

Recently, a somewhat surprising development occurred. Three [2-4] of these four [2-5] theories adopted similar (many–body physics) formulations in which coherence follows either from a particular form of interaction (as in [4]) or from a combination of factors involving possible forms of many-body interaction, and particle indistinguishability (as in [2, 3]).

As a result, plausible explanations are beginning to emerge for a number of important phenomena. Specifically, consistent with the idea that for a theory to be believable it should relate to an existing theory (as outlined in Section 3.0), agreement between the theories appears to reflect: (i) use of a sufficiently sophisticated, and universally accepted form of mathematics that explains how nuclear scale and atomic scale processes can be related to each other without high momentum particles being released; (ii) use of reaction rate expressions that include coherent, nonlocal transfer of momentum, involving many particles; and (iii) reliance upon a formulation that includes a large number of charged, indistinguishable particles, expressed in terms of a standard, common, well accepted concept: the many-body wave function, associated with the QM of condensed matter physics. Chubb and Chubb have done this by explicitly illustrating how their atomic scale Ion Band State theory can be generalized to incorporate nuclear scale processes through a generalization of standard multiple scattering theory techniques [21, 22]. In the process, they explain how a non-separable coupling between nuclear dimension and atomic dimension scale can occur in the wave functions associated with nucleus/nucleus separation, in a non–local fashion.

By adopting an explicit form of representation for distinguishing between the coordinate dependencies involving the short ranged (nuclear) degrees of freedom and those that couple to the electromagnetic (longer ranged) force, Hagelstein [3] has developed a similar idea that generalizes the resonant group structure idea proposed by Wheeler [23] in the 1930s. In fact, a striking similarity, for the case associated with D-D fusion, occurs in Hagelstein's representation of the relevant wave function and the comparable choice used by Chubb and Chubb, once it is recognized that the correlation factors g(r1,r2) that are used by Chubb and Chubb to describe the dependence on the separation variable (r1-r2) between

deuterons located at r1 and r2, are equivalent to the channel factors Fj (in which the subscript "j" refers to r1-r2) defined by Hagelstein. From these observations, three distinguishing features between these two [2, 4] theories follow: 1. Chubb and Chubb point out that approximately discontinuous changes in the gradient of g(r1,r2) (that are not included explicitly included in Hagelstein's channel factors, Fj) illustrate the possible coupling (through the associated many-body problem) that allows for transfer of momentum to occur non-locally, even in the $T \rightarrow 0$ limit, 2. Chubb and Chubb illustrate, explicitly, the relationship between these discontinuities and coherent (lattice recoil effects) in which momentum can be transferred from a particular location, to many locations, instantaneously; and 3. although Hagelstein does not particularly identify this possibility, he points out that many nucleons can become coupled together, simply as a consequence of the existence of the associated relationship. Hagelstein, further, explores the implications of this coupling, explicitly, through coherent momentum transfer between nucleons to and from a coherent (or nearly coherent) set of optical phonons. He also uses the associated ideas to provide a possible explanation for the emission of high momenta particles from deuterated Ti films.

Kim [4] also adopted a picture, based on many-body physics. Beginning from the common starting point [2-4] (involving the complete many-body wave function), he has drawn this kind of connection by incorporating an approximate form for a potential many-body interaction involving bosons (borrowed from his optical atom trapping theory) so that it could be used in the Cold Fusion problem. An intriguing difference between Kim's approach and the approaches followed by Hagelstein and Chubb and Chubb is that he does not use the idea that deuterons (or other nuclei) are interacting with a well defined lattice. In place of this idea, he starts from the assumption that under suitable conditions, a collection of deuterons, interacting with a solid, might become effectively trapped in a manner that resembles the optical trapping of alkali atoms that forms the basis of atom Lasers, and the related forms of neutral atom Bose Einstein Condensates.

Although, superficially, this idea might seem somewhat foreign, in the limit of perfect periodic order, at sufficiently low temperature, the implications of this idea, and those associated with the ion band state theory proposed by Chubb and Chubb become identical. (Specifically, the D^+ ions that occupy ion band states in the Chubb and Chubb theory form a Bose Einstein condensate, at vanishing temperature.) A potentially important new idea, associated with Kim's work [4, 24] that he has applied to the CF problem, is the development of an effective two body Hamiltonian, from the exact many-body system, which can be used to determine a separable form for the ground state wave function of a many-body Bose system. Since the associated Hamiltonian is robust, the resulting expression for the wave function, may be applicable in many different situations. A second intriguing point is that both Kim and Chubb and Chubb, independently, have concluded that under suitable circumstances, coherence associated with the mechanism that is responsible for perfect Bose Einstein condensation (associated with the limit in which many particles, coherently, approach a state in which the

momentum of each particle approaches zero) provides a potentially important source for coherent, nonlocal momentum transfer that can be used to account for the lack of high momentum particles in CF reactions.

In summary, all three theories are now based on an organizing principle associated with condensed matter physics that explicitly includes a procedure for incorporating nuclear effects. And, although initially, two of the theories (Kim and Hagelstein) focused on nuclear scale phenomena, while the third (Chubb and Chubb) focused on atomic scale processes, all three now include effects that couple atomic and nuclear scale processes in a manner that is consistent with the criteria, outlined in Section 3.0.

Although the finer details associated with theoretical frameworks that have been used to couple the very different lengthscales are different, in each case, coherence that results through coupling to the electromagnetic field, provides the dominant form of interaction. The associated coupling is expressed in most general terms, using the multiple scattering theory [21, 22], discussed by Chubb and Chubb. In particular, within this framework, an exact rate expression is derived that relates all possible many-body collisions associated with a particular reaction to discontinuous changes in momentum. This expression illustrates explicitly how non-local momentum transfer can occur, coherently, instantaneously, in such a way that it becomes obvious how high momentum particles (through the accumulation of large amounts of momentum at isolated locations) can be avoided. The theory also can be readily generalized to incorporate arbitrary forms of interaction. Within the context of this theory [2], it is also possible to recover all of the previous results of the Chubb and Chubb theory [25].

In contrast to the work by Chubb and Chubb, which has focused primarily on D+D fusion, and issues associated with non-local momentum transfer, Hagelstein, on the other hand, has attempted to deal with a more general set of nuclear reactions. For this reason, while Chubb and Chubb have been concerned primarily with non-local forms of interaction, and questions related to materials properties, and solid state effects, Hagelstein has focused more closely on questions associated with the release of high energy particles, lattice imperfections, and the influences of injecting nuclei into the host. From this starting point, he has identified a number of potential, triggering phenomena associated with the emergence of fast particles and unconventional nuclear byproducts.

Although the recent focus of Kim's work has been on coherent deuteron fusion, from Bose condensed states, he has also investigated the possibility of novel, nuclear reactions. An important point about his most recent work is associated with the effects of finite size. In particular, he predicts optimal reaction rates, within a particular scenario, based on estimates of parameters that he infers from experiments.

Table 1 lists some of the organizing principles and common features of the three

theories described in this section, as well as the comparable features associated with Preparata's theory. In this table, under the label, organizing principle, by coherence, and the labels, Low P and High P, refer to the question of whether or not the theory applies in the low momentum (P) (Low P) limit, associated with low temperature, or in the high momentum (P) (High P) limit, or in both limits. Source refers to the effective form of interaction (or intermediate particle) that is responsible for the coherence. The designation Nuc/EM Separability in Rate Expression refers to the question of whether or not separability in the coordinate dependencies between nuclear (Nuc) and electromagnetic (EM) interactions is assumed in the associated wave functions and reaction rate expression, and to identify the organizing principle (for example, many-body physics) that treats the coupling between nuclear and electromagnetic interactions. The star in the final column refers to the idea that recoil momentum (associated with the possible nuclear reaction) can be incorporated directly through non-local transfer of momentum from the bulk to the surface region.

Table 1: Organizing principles/ideas in Cold Fusion theories

Theory	Coherence			Nuc/EM	Rate
	Low P	High P	Source	Separability	Expression
Chubb & Chubb	Yes	Yes	E.M. Interaction (all of it) / Particle Statistics	No	Many-Body Physics*
Hagelstein	No	Yes	Phonons	No	Many-Body Physics
Preparata	No	Yes	"Photons"	Yes	Semi-Classical (Gamow)$^{\star ?}$
Kim	Yes	Yes	E.M. Interaction (all of it) / Particle Statistics	No	Many-body Physics*

6.0 Suggestions for Testing Theories/Future Theoretical Work.

A number of predictions have come out of each of the three theories [2- 4] discussed in the last section. An important point to keep in mind is that, implicitly, these predictions, in most cases, seem to apply most rigorously within the context of a particular set of circumstances. For example, Chubb and Chubb suggested many years ago [25] that a bosons-in and bosons-out rule should apply, provided particular conditions are met. In the context of the multiple scattering theory presented in [2], the limitations of this rule were identified [26]: the rule applies rigorously in the low temperature limit, provided suitably large, ordered crystals

are used. Similarly, Hagelstein has identified limits in which optical phonons, vacancies, and other effects can significantly enhance fusion (or other nuclear process) rate. A potentially important point is that the well developed theories [2–4] have evolved to the point that they include well defined mathematical expressions that relate particular reaction rates, rigorously, to known situations that apply under specific conditions. The significance of this point is that in each case where a reaction rate expression has been derived, given the uncertainties of existing experiments, it is probably important to attempt to match a particular experimental study so that it mimics the conditions associated with the particular expression.

For example, Chubb and Chubb predicted optimal crystal sizes (with characteristic linear dimensions of approximately 0.1 μm^3) for producing large amounts of excess heat at elevated temperatures. The motivating argument associated with this estimate was the requirement that crystalline order be maintained and the helium byproduct be expelled. At reduced temperatures (for example, below 200 degrees K), the arguments associated with these predictions do not hold. This is because as the temperature is reduced and crystalline order is increased, other factors associated with surface preparation, periodic order, and loading, become more important.

The important point is that under certain circumstances, one theoretical prediction probably will be more useful than another. Confirmation of this point is important, in my opinion, because if it is confirmed that different theories are valid in different situations, the speculation that a single mechanism is responsible for all CF phenomena is probably without merit. With this point in mind, it seems appropriate to emphasize an obvious lesson that has come out of the last decade of theoretical work: in order for theorists to formulate a meaningful theory, they require detailed information about material preparation and related factors (crystalline quality, and size, as well as temperature, and loading, for example). In the future, theorists certainly would benefit from measurements associated with these kinds of factors, as well as through additional information documenting correlations between these kinds of variables and potential triggering phenomena.

Finally, it is useful to identify a number of Lessons Learned associated with the interplay between theory and experiment. In this context, we would like to note in passing three apparent success stories that have occurred: (i) Independent predictions by Chubb and Chubb (C&C) and Preparata (P) that high loading is beneficial in deuterium fusion in Pd/D (observed in various places), (ii) comparable predictions by C&C and P that He-4 should be the predominant byproduct (observed by Miles et al., and Bush et al.), and (iii) the suggestion by Bhakta Rath (based on the idea put forth by Chubb and Chubb that small crystals in a porous medium could be beneficial) that Pd/B could potentially provide a useful composite material for producing excess heat (which has been verified by Imam and Miles, as documented in this report, cf chapter 3). An important lesson,

to date, however, is that although theory predicted these successes prior to the actual experiments, theory has been largely ignored. In particular, only in the third example (involving PdB) was theory actually used to guide the associated experiment. Given the apparent lack of consensus about theory that has existed in the past, it is plausible that a degree of skepticism about theoretical predictions has been warranted. However, the situation has evolved considerably since the initial days of CF. In the future, one would hope that experimenters would more closely monitor and test the predictions of the more mature theories.

There is a final, more general lesson, associated with the manner in which CF has been judged by the scientific community and with the potential role of theory in this process. In particular, an extremely naive, overly simplified picture of the relevant physical situation was adopted by most physicists, based on an idea (associated with conventional nuclear physics) that was doomed to fail, from the outset. When most experimenters failed to reproduce the effect, this extremely naive picture not only was used as formal justification for assuming the phenomenon did not exist, but to preclude the notion that a different, more sophisticated theory might be more appropriate. On the other hand, although most physicists followed this route, a few more creative physicists thought of alternative ideas, which not only were discarded by most physicists, but, in some cases, were outwardly scorned. It seems appropriate, given the fact that not only did the field not die, but that viable theoretical explanations for what is involved have evolved, to ask a fundamental question about the impact of naive skepticism on the adjudication process. In particular, it is clear that in some cases, creative ideas about CF were stifled to such a degree that nonexperts [7, 10, 27] not only have been allowed to openly ridicule and attack them, but to do so without allowing the responsible parties to respond. Rhetorically, one might ask, Isn't it always useful to look at a creative idea with an open mind, especially when an undercurrent of skepticism is present? More poignantly, one might ask, How can similar failures be avoided in the future?

At this time, it is clear that creative theories, based on mainstream thinking do exist. In particular, three have been identified that should be tested and applied. Despite the fact that these theories have been developed, only limited work in this area is going on at the present time. This situation must and should change. Hopefully, this article will have a positive impact in changing this situation.

References.

1. T. A. Chubb and S. R. Chubb, Fusion Technology, **17**, 710 (1990)
2. S. R. Chubb and T. A. Chubb, *Theoretical Framework for Anomalous Heat and 4–He in Transition Metal Systems,* Proc. ICCF8.
3.Y. E. Kim and A. L. Zubarev, *Ultra Low–Energy Nuclear Fusion of Bose Nuclei in Nano–Scale Ion Traps*, Proc. ICCF8.
4. P. L. Hagelstein, *A Unified Model for Anomalies in Metal Deuterides,* Proc. ICCF8.

5. G. Preparata, Trans Fusion Technol., **26**, 397 (1994); *QED Coherence in Matter*, World Scientific Publishing Co., Singapore; chap. 8, pp. 153–178 (1995).
6. T. S. Kuhn, *The Structure of Scientific Revolutions*, Univ. of Chicago Press, Chicago, (1962).
7. R. L. Park, *Voodoo Science: The Road from Foolishness to Fraud*, Oxford University Press, Oxford, 2000.
8. R.P. Feynman, R.B. Leighton and M. Sands, *The Feynman Lectures on Physics*, Addison Wesley Publishing, Inc., New York, 1965.
9. S. R. Chubb, Accountability in Research, **8**, (2000).
(http://www.gbhap us.com/journals/149/149-top.htm). C. Beaudette, *Excess Heat: Why Cold Fusion Research Prevailed*, Oak Grove Press, LLC, ME, 2000. available through
http://www.infinite-energy.com
10. D. R. O. Morrison, Physics Today **50**,14 (1997).
11. J. Rafelski, M. Sawicki, M. Gajda and D. Harley, Fusion Technol., **18**, 136 (1990).
12. E. Teller, in Proc EPRI-NSF Workshop, Ed. Schneider, Electric Power Research Institute, Palo Alto, CA, pp. 1-2 (1989).
13. F. J. Mayer and J. R. Reitz, Fusion Technol. **19**, 552 (1991); ibid. **20**, 367 (1991).
14. J. P. Vigier, Proc. ICCF 3.
15. R. Mills, *The Grand Unified Theory of Classical Quantum Mechanics*, BlackLightPower, Inc., Princeton, N.J.
16. H. Kozima, *Discovery of the Cold Fusion Phenomenon: Development of Solid State Nuclear Physics and the Energy Crisis in the 21st Century*, Ohtake Shuppan Inc., Tokyo, 1998.
17. J. Schwinger, J., Nuclear Energy in an Atomic Lattice, in Proc. First Annual Conference on Cold Fusion (ed. Will, (ICCF–1) Salt Lake City, UT, 1990); Z. Phys. D: At., Mol. Clusters, **15**, 221 (1990); Z. Naturforsch., **45A**, 756 (1990); Prog. Theor. Phys., **85**, 711 (1991); Springer Proc. in Physics **57** (Evolutionary Trends in the Physical Sciences; Eds: M. Suzuki, R. Kubo, 1991), 171.
18. M. Rabinowitz, Y.E. Kim, V.A. Chechin and V.A. Tsarev, Trans Fusion Technol., **26**, 3 (1994).
19. G. Preparata, Fusion Technology, **20**, 82 (1991).
20. E. Storms, Infinite Energy, **6**, 54 (2000).
21. A. Gonis and W.H. Butler, *Multiple Scattering in Solids*. Springer Verlag, N.Y. 2000).
22. J. Korringa, Physica, **13**, 392 (1947);. W. Kohn and N. Rostoker, Phys. Rev., **94**, 1111 (1954).
23. J. A. Wheeler, Phys. Rev., **52**, 1107 (1937).
24. Y. E. Kim and A. L. Zubarev, J. Phys. B: At. Mol. Opt. Phys., **33**, 1 (2000).
25. S.R. Chubb and T.A. Chubb, AIP Conference Proc. **228**, 691 (1991) (eds. S. E. Jones, F. Scaramuzzi and D. Worledge), Amer. Inst. Phys. (New York); T.A. Chubb and S.R. Chubb , Fusion Technology, **20**, 93, (1991); S.R. Chubb

and T. A. Chubb, Distributed Bosonic States and Condensed Matter Fusion, NRL Memorandum Report 6600 (Documents, Code 2627, Naval Research Laboratory, Washington, DC, 20375-5321, 1990); T. A. Chubb and S. R. Chubb, Nuclear Fusion in a Solid via a Bose Bloch Condensate, NRL Memorandum Report 6617 (Documents, Code 2627, Naval Research Laboratory, Washington, DC, 20375-5321, 1990).
26. S. R. Chubb and T. A. Chubb, Theoretical Framework for Anomalous Heat Without High Energy Particles from Deuteron Fusion in Deuterium/Transition Metal Systems, talk presented at Winter 2000 American Nuclear Society meeting, 8 Nov. 2000, Washington, DC.; S. R. Chubb and T. A. Chubb, 2000 Trans. Amer. Nuc. Soc., **83**, 362 (2000).
27. D. Lindley, Nature, **344**, 375 (1990); Minutes of the 189th Meeting of Washington Philosophical Society, (Washington Philosophical Society, Washington, D.C.), 31 Jan. 1992.

APPENDIX: LISTING OF PUBLICATIONS/PRESENTATIONS RELATED TO COLD FUSION

This listing is limited to the contributions from the U.S. Navy Laboratories. It contains publications, theoretical and experimental, covering topics directed toward better understanding of the Fleischmann–Pons effect and reflecting scientific interests of their authors.

Contributions from the Space and Naval Warfare Systems Center, San Diego, San Diego, CA 92152–5001 (formerly: Naval Command, Control and Ocean Surveillance Center, RDT&E Div., San Diego, CA)

Journal publications

1. S. Szpak, P. A. Mosier–Boss and J. J. Smith, On the behavior of Pd deposited in the presence of evolving deuterium, J. Electroanal. Chem., **302**, 255 (1991)
2. S. Szpak, C. J. Gabriel, J.J. Smith and R.J. Nowak, Electrochemical charging of Pd rods, J. Electroanal. Chem., **309**, 273 (1991)
3. S. Szpak, P. A. Mosier–Boss, S. R. Scharber and J.J. Smith, Charging of the Pd/^{n}H system: role of the interphase, J. Electroanal. Chem., **337**, 147 (1992)
4. S. Szpak, P. A. Mosier–Boss, C. J. Gabriel and J.J. Smith, Absorption of deuterium in palladium rods: model vs. experiment, J. Electroanal. Chem., **365**, 275 (1994)
5. S. Szpak, P. A. Mosier–Boss, R. D. Boss and J. J. Smith, Comments on the analysis of tritium content in electrochemical cells, J. Electroanal. Chem., **373**, 1 (1994)
6. S. Szpak, P. A. Mosier–Boss and J.J. Smith, Deuterium uptake during Pd–D codeposition, J, Electroanal. Chem., **379**, 121 (1994)
7. S. Szpak, P. A. Mosier–Boss, S. R. Scharber and J.J. Smith, Cyclic voltammetry of Pd+D codeposition, J. Electroanal. Chem., **380**,1 (1995)

8. S. Szpak, P. A. Mosier–Boss and J. J. Smith, On the behavior of the cathodically polarized Pd/D system: Search for the emanating radiation, Physics Letters A, **210**, 382 (1996)
9. S. Szpak and P. A. Mosier–Boss, On the behavior of the cathodically polarized Pd/D system: a response to Vigier's comments, Physics Letters A, **221**, 141 (1996)
10. S. Szpak, P. A. Mosier–Boss, R.D. Boss and J.J. Smith, On the behavior of the Pd/D system: Evidence for tritium production, Fusion Technology, **33**, 38 (1998)
11. S. Szpak and P. A. Mosier–Boss, On the release of $^{n}_{1}$H from cathodically polarized palladium electrodes, Fusion Technology, **34**, 273 (1998)
12. P. A, Mosier–Boss and S. Szpak, The Pd/^{n}H system: Transport processes and development of instabilities, Il Nuovo Cimento, **112 A**,577 (1999)

Proceedings of ICCF

1. S. Szpak, P. A. Mosier–Boss and J. J. Smith, Reliable procedure for the initiation of the Fleischmann–Pons effect, Proc. ICCF – 2 (1991)
2. S. Szpak, P. A. Mosier–Boss, Comments on the Methodology of Excess Tritium Determination, Proc. ICCF – 3 (1992)

Contributions from the Naval Air Warfare Center Weapons Division, China Lake, CA

Journal publications

1. M. H. Miles and R. E. Miles, Theoretical Neutron Flux Levels, Dose Rates, and Metal Foil Activation, J. Electroanal. Chem., **295**, 409 (1990)
2. M. H. Miles, K. H. Park and D. E. Stilwell, Electrochemical Calorimetric Evidence for Cold Fusion in the Palladium–Deuterium System, J. Electroanal. Chem., **296**, 409 (1990)
3. B. F. Bush, J. J. Lagowski, M. H. Miles and G. S. Ostrom, Helium Production During the Electrolysis of D_2O in Cold Fusion Experiments, J. Electroanal. Chem., **304**, 271 (1991)
4. M. H. Miles, R. A. Hollins, B. F. Bush, J. J. Lagowski and R.E. Miles, Correlation of Excess Enthalpy and Helium Production During D_2O and H_2O Electrolysis, J. Electroanal. Chem., **346**, 99 (1993)
5. M. H. Miles, B. F. Bush and D. E. Stilwell, Calorimetric Principles and Problems in Measurements of Excess Power During Pd–D_2O Electrolysis, **98**, 1948 (1994)
6. M. H. Miles, B. F. Bush and J. J. Lagowski, Anomalous Effects Involving Excess Power, Radiation and Helium Production Using Palladium Cathodes, Fusion Technology, **25**, 478 (12994)
7. M. H. Miles and B. F. Bush, Heat and Helium Measurements in Deuterated Palladium, Trans. Fusion Technology **26**, 156 (1994)

8. M. H. Miles, Reply to "Examination of Claims of Miles et al. in Pons–Fleischmann Type Cold Fusion Experiments, J. Phys. Chem. **B 102**,3642 (1998)
9. M. H. Miles, Calorimetric Studies of Pd/D_2O + LiOD Electrolysis Cells, J. Electroanal. Chem., **482**, 56 (2000)
10. M. H. Miles and K. B. Johnson, Electrochemical Insertion of Hydrogen into Metals and Alloys, J. New Energy, in press

Proceedings of ICCF

1. M. H. Miles, K. H. Park and D. E. Stilwell, Electrochemical Calorimetric Studies of the Cold Fusion Effect, Proc. ICCF – 1 (1990)
2. M. H. Miles, G.S. Ostrom, B.F. Bush and J.J. Lagowski, Heat and Helium Production in Cold Fusion Experiments, Proc. ICCF – 2 (1991)
3. M. H. Miles and B. F. Bush, Search for Anomalous Effects Involving Excess Power, Helium and Tritium During D_2O Electrolyses Using Palladium Cathodes, Proc. ICCF – 3 (1993)
4. M. H. Miles and B. F. Bush, Calorimetric Principles and Problems in D_2O Electrolysis, Proc. ICCF–3 (1993)
5. M. H. Miles, The Extraction of Information from an Integrating Open Calorimeter in Fleischmann–Pons Effect Experiments, Proc. ICCF – 5 (1995)
6. M. H. Miles and B. F. Bush, Radiation Measurements at China Lake: Real ODR Artifacts, Proc. ICCF – 7 (1998)
7. M. H. Miles, Calorimetric Studies of Palladium Cathodes Using Fleischmann–Pons Dewar Type Cells, Proc. ICCF – 8 (2000)

Contributions from the Naval Research Laboratory, Washington, DC.

Journal publications

1. T. A. Chubb and S. R. Chubb, Bloch—Symmetric Fusion in PdD_x, Fusion Technology, **17**, 710 (1990)
2. T. A. Chubb and S. R. Chubb, Cold Fusion as an Interaction between Ion Band States, Fusion Technology, **20**, 93 (1991)
3. S. R. Chubb and T. A. Chubb, Ion Band State Fusion: Reactions, Power Density and the Quantum Reality Question, Fusion Technology, **24**, 403 (1993)
4. S. R. Chubb and T. A. Chubb, The Role of Hydrogen Ion Band States in Cold Fusion, **26**, 414 (1994)
5. S. R. Chubb and T. A. Chubb, Theoretical Framework for Anomalous Heat without High Energy Particles from Deuteron Fusion in Deuterium–Transition Metal Systems, Trans. Am. Nuc. Soc. **83**,362 (2000)
6. S. R. Chubb, Review of "Excess Heat: Why Cold Fusion Research Prevailed",

Fusion Technology, **39**,288 (2001)
7. P. L. Hagans, D. D. Dominguez and M. A. Imam, Surface Composition of Pd Cathodes, *Progress in New Hydrogen Energy*, vol. 1 p. 249 (1996)

Proceedings of ICCF

1. S. R. Chubb and T. A. Chubb, Quantum Mechanics of "Cold" and "Not–So–Cold" Fusion, Proc. ICCF–1,119 (1990)
2. S. R. Chubb and T. A. Chubb, An Explanation of Cold Fusion and Cold Fusion By–Products, Based on Lattice-Induced Nuclear Chemistry, Proc. ICCF – 2 (1991)
3. S. R. Chubb and T. A. Chubb, Ion Band State Fusion, Proc. ICCF – 3 (1992)
4. T. A. Chubb and S. R. Chubb, The Ion Band State Theory, Proc. ICCF – 5 (1995)
5. S. R. Chubb and T. A. Chubb, Hidden Results of the Ion Band State Theory, Proc. ICCF – 6, Proc. ICCF – 6 (1996)
6. T. A. Chubb and S. R. Chubb, Radiationless Cold Fusion: Why Small Crystals are Better, N_{cell} Requirement and Energy Transfer to Lattice, Proc. ICCF – 6 (1996)
7. S. R. Chubb and T. A. Chubb, Periodic Order, Symmetry and Coherence in Cold Fusion, Proc. ICCF – 7 (1998)
8. S. R. Chubb and T. A. Chubb, Really Cold, Cold Fusion, Proc. ICCF – 7 (1998)
9. T. A. Chubb and S. R. Chubb, Deuteride Induced Strong Force Reactions, Proc. ICCF – 7 (1998)

Initial distribution list

Spawar Systems Center San Diego, San Diego

Naval Air Warfare Center, China Lake

Dr. Melvin H. Miles(10). Code 4T4220D
Dr. Robin A. Nissan, Code 4T4200D
Dr. Geoffrey A. Lindsay, Code 4T42200D
Dr. Jeffrey J. Davis, Code 4T4330D
Office of General Counsel, Patent Office, Code 772000D
Technical Library, Code 4TL000D

Naval Research Laboratory, Washington DC

Dr. Timothy Coffey, Code 1001
Dr. Bhakta Rath, Code 6000
Dr. Scott R. Chubb (10), Code 7252
Dr. Ashraf Imam, Code 6320

Office of Naval Research

Dr. Fred E. Saalfeld, Technical Director

Defense Technical Information Center
Alexandria, VA 22304–6145

Navy Acquisition, Research and Development Information Center (NARDIC)
Arlington, VA 22244–5114

Professor J. O'M. Bockris
4973 Afton Oaks Drive
College Station, TX 77845

Dr. Talbot A. Chubb
Research Systems, Inc.
5023 North 38–th Street
Arlington, VA 22207

Professor John Dash
Physics Department
Portland State University
P. O. Box 751
Portland, OR 972078–0751

Professor Peter L. Hagelstein
Massachusetts Institute of Technology
Dept. of Electrical Engineering and Computer Science
Room 36–225
77 Massachusetts Ave
Cambridge, MA 02139

Dr. Eugene Mallove
New Energy Research Laboratory
P. O. Box 2816
Concord, NH 03302–2816

Dr. Michael McKubre
SRI International
333 Ravenswood Ave
Menlo Park, CA 94025

Dr. Michael Melich
Naval Postgraduate School
1224 Meigs Drive
Niceville, FL 32578–3018

Professor George H. Miley
Fusion Studies Laboratory
University of Illinois
103 S. Goodwin Ave
Urbana, IL 61801

Dr. David J. Nagel
The George Washington University
2933 K Street, Suite 340J
Washington, DC 20052

Dr. Robert J. Nowak
DARPA
3701 N. Fairfax Drive
Arlington, VA 22203

Professor Richard A. Oriani
112 Amundson Hall
University of Minnesota
421 Washington Ave SE
Minneapolis, MN 55455

Dr. Jerry J. Smith
U. S. Department of Energy
Code SC–13/GTN
19901 Germantown Road
Germantown, MD 20874–1290

Professor Louis D. Smullin
Massachusetts Institute of Technology
Cambridge, MA 02139

Dr. Lowell Wood
Hoover Institution HT – 1004
Stanford University
Stanford, CA 94305–6010

INITIAL DISTRIBUTION

Defense Technical Information Center
Fort Belvoir, VA 22060–6218 (4)

SSC San Diego Liaison Office
C/O PEO-SCS
Arlington, VA 22202–4804

Center for Naval Analyses
Alexandria, VA 22302–0268

Office of Naval Research
ATTN: NARDIC (Code 362)
Arlington, VA 22217–5660

Government-Industry Data Exchange
Program Operations Center
Corona, CA 91718–8000

Naval Air Warfare Center,
Weapons Division
China Lake, CA 93555–6001 (15)

Naval Research Laboratory
Washington, DC 20375–5320 (13)

Office of Naval Research
Arlington, VA 22217–5660

Professor J. O'M. Bockris
College Station, TX 77845

Research Systems, Inc.
Arlington, VA 22207

Portland State University
Portland, OR 97207–0751

Massachusetts Institute of Technology
Cambridge, MA 02139

New Energy Research Laboratory
Concord, NH 03302–2816

SRI International
Menlo Park, CA 94025

Dr. Michael Melich
Niceville, FL 32578–3018

University of Illinois
Urbana, IL 61801

The George Washington University
Washington, DC 20052

Defense Advanced Research Projects Agency
Arlington, VA 22203–1714

University of Minnesota
Minneapolis, MN 55455

U.S. Department of Energy
Germantown, MD 20874–1290

Massachusetts Institute of Technology
Cambridge, MA 02139

Stanford University
Stanford, CA 94305–6010